

AD-758 691

PROJECT BAND (BOTTOM AMBIENT NOISE  
DIRECTIVITY). PHASE I. DESIGN AND PRELIM-  
INARY FEASIBILITY TESTS

R. M. Robertson, et al

General Motors Corporation

Prepared for:

Office of Naval Research

February 1973

DISTRIBUTED BY:

**NTIS**

National Technical Information Service  
U. S. DEPARTMENT OF COMMERCE  
5285 Port Royal Road, Springfield Va. 22151

TR73-15  
FEBRUARY 1973

FINAL REPORT

AD 758691

**Project BAND (Bottom Ambient Noise Directivity)**

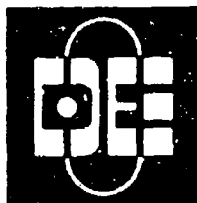
**Phase i Design and  
Preliminary Feasibility Tests**

Prepared by  
R.M. Robertson and R.F. Podlesny

Prepared for  
DEPARTMENT OF THE NAVY  
Office of Naval Research  
Arlington, VA 22217

Under  
Contract No. N00014-73-C-0137

*Sea Operations Department*



**Delco Electronics**

*General Motors Corporation  
- Santa Barbara Operations  
Santa Barbara, California*

124

TR73-15  
FEBRUARY 1973

COPY NO. 10

FINAL REPORT

**Project BAND (Bottom Ambient Noise Directivity)**

**Phase I Design and  
Preliminary Feasibility Tests**

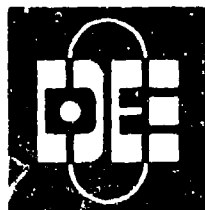
Prepared by  
R.M. Robertson and R.F. Podlesny

Prepared for  
DEPARTMENT OF THE NAVY  
Office of Naval Research  
Arlington, VA 22217

Under  
Contract No. N00014-73-C-0137



*Sea Operations Department*



**Delco Electronics**

*General Motors Corporation  
- Santa Barbara Operations  
Santa Barbara, California*

1

CONTENTS

<u>Section</u>		<u>Page</u>
I	Introduction and Summary	1
	Introduction	1
	Summary	1
II	System Considerations	3
III	Electronics	14
	Signal Conditioning	14
	Band Processors	17
	Array	19
	Signal Conditioning	21
	Discrete Fourier Processor	29
	Frequency Beamformer	30
	Digital Resolver	38
	Post Integrator	38
	Incremental Tape Recorder	38
	Input Simulator	42
	Readout System	42
IV	Major Structural Components of the System	46
	The Anchor/Buoy Assembly	46
	Electronic Pressure Vessel	48
	The Acoustic Array	52
V	Tests	55
	Deployment Systems	55
	Cable Array Disconnect Tests	61
	Recorder Tests	61
VI	Implantment and Recovery	64
	The Implantment System	64
	Recovery System	67
VII	Phase II Requirements and Schedules	70
	Appendix: Power Beam Patterns	A-1

ILLUSTRATIONS

<u>Figure</u>	<u>Title</u>	<u>Page</u>
1	Wenz's Curves	4
2	15 Element Arrays	6
3	Beam Width at 1/2 Power	7
4	Beamwidth vs Normalized Frequency (15 Element Array Spatial Shading $d_n = 1.1 d_{n-1}$ )	8
5	Beamwidth vs Normalized Frequency, 15 Elements, Equally Spaced Amplitude Shading (-15 dB)	9
6	Comparison of 60° Beams	10
7	Steering Angle vs Frequency 10 dB Max. Back Lobe	12
8	3-Array Network	13
9	Beam Crossovers, 16 Elements Equally Spaced	16
10	Band Processor	18
11	Signal Conditioning	22
12	Preamp Topology	23
13	Noise Data Equalized by Second-Order Zero at 60 Hz	24
14	Preamplifier Gain vs Frequency	26
15	Filter Topology	27
16	Multiplexer	28
17	Discrete Fourier Transform Processor	31
18	DFT Reference Generator	32
19	Frequency Beamformer	33
20	Beam Directions	35
21	Phase Angle Generator	36
22	Digital Resolver	39
23	Post Integrator	40
24	Recorder	41
25	Simulator	43
26	Readout System	44
27	Tape Recorder	45
28	Anchor/Buoy Assembly	47
29	Pressure Vessel	49
30	Electronics Package	50
31	Digital Electronics	51
32	Cable Configuration	53
33	Clamp-on Assembly	54
34	BAND Swing-In System	56
35	BAND Vertical Implantation	57
36	Summary Plot of XY Position During Swing-Away BAND Experiment, 1 Nov 1972	59
37	Summary Plot of Pull-Over BAND Emplantment, 1 November 1972	60
38	Test Fixture	62
39	Test Fixture	63
40	Anchor/Buoy Assembly	65
41	Implantment and Recovery System	66
42	Recovery Sequence	68
43	Timer	69
44	Phase II Schedules	71

SECTION I  
INTRODUCTION AND SUMMARY

INTRODUCTION

The performance of a passive sonar is dependent upon the noise environment. Almost all available noise data are limited to statistical percentiles of noise levels measured with single omnidirectional hydrophones. Performance of an array system could be considerably affected, however, by a predominant directional nature of the noise field. This noise field can be expected to be geographical and temporal dependent and can be measured only with an array of sufficient aperture and directivity in the frequency band of interest. Such measurements that exist have been made after a system has been designed, constructed, and installed. The need exists then for a survey or research tool that: (1) can statistically sample noise anisotropy; (2) can be deployed and retrieved economically; (3) can be reusable; and (4) will be independent of the surface during its data logging period.

A recent development in digital electronic circuitry and components has made possible a small, low-power, in situ processor for the beamforming, filtering and logging functions for such a device.

This report describes the conceptual design studies and preliminary subsystem component tests in the lab and tests of installation ideas at sea that were made to determine basic feasibility. The work was accomplished under contract N00014-73-C-0137 with Code 1020S ONR (LRAPP) during the period Oct 1972 to Feb 1973.

The acronym BAND (Bottom Ambient Noise Directivity) was used to identify the system.

SUMMARY

This report describes the design of a recoverable acoustic array which measures the anisotropy of the ambient noise in the deep ocean. The system consists of a straight line array of 29 hydrophones, an electronic processing and recording system, and a submerged recovery buoy with acoustic command recall.

The 29 hydrophones form three linear arrays of 15 elements. Each array operates in a different frequency band. The frequency spectrum covered is from 20 Hz to 160 Hz.

The electronic processor synthesizes eight narrow band filters with a bandwidth of 2 Hz. The center frequency of each filter can be arbitrarily placed in any of three frequency bands.

Twenty-nine beams are formed within  $\pm 60^\circ$  sectors from broadside. The beam spacing provides equal power levels at cross-over angles of adjacent beams.

The output dynamic range of the system is 96 dB and it can operate at depths to 18,000 ft for 20 days, with data being processed for one minute followed by a seven minute quiescent state. The beam output levels are recorded on an incremental tape recorder.

The system is small and light and can be launched from small vessels. The total in-water system will weigh less than 1500 lb in air, including the throw-away anchor. All of the components of the system are recoverable except the simple, cheap clump anchor.

Details of the components and assemblies are described as well as tests of some major components and critical areas. Feasibility tests of the implantment and of the recovery of the system are discussed. Requirements and schedules for Phase II (construction, test and sea installation of an operational unit) of the project are included.

Results of the study indicate that the concept is basically feasible in all respects and that there are no critical or high risk problem areas. It is recognized, of course, that for a system designed for installation in the real ocean and expected to survive 20 days and then be retrieved, the ultimate feasibility necessitates construction and sea tests of a complete operational system. This has not yet been accomplished and awaits Phase II of the BAND development.

## SECTION II SYSTEM CONSIDERATIONS

The purpose of the BAND (Bottom Ambient Noise Direction) system is to measure the anisotropy of the ambient noise in the deep ocean. The system analyzes three fundamental noise parameters: detection, identification, and localization. From an array of sensors, a receiving beam is formed which accepts energy emanating from a particular direction while simultaneously rejecting, to some degree, energy emanating from all other directions. The power content of this beam provides for detection and its spectral content provides for identification or classification. The direction of the beam provides the information pertinent to the area of localization. To accomplish the measurements, a processing system that performs both spatial and spectral filtering is suggested. The functional components of the system will include an array of sensing elements, a signal conditioning unit, a processing unit, and a recording medium.

Before a reasonable system can be developed to make the measurements, bounds must be placed on the characteristics of the ambient noise. The power level will be limited to a 42 dB dynamic range in which the lower limit is taken from Wenz's curves at 50 Hz (see Figure 1). This places the higher limit at -13 dB re  $\mu$ bar. The spectrum of interest is from 20 Hz to 150 Hz. It would be uneconomical to cover this entire band; however, the system will be capable of interrogating eight 2-Hz wide windows. These windows may be centered anywhere within the 130 Hz bandwidth in 1/2 Hz steps. There are no directional limitations except those which may later be imposed by either hardware or array configurations.

The shape of the array is fixed by practical considerations. A circular array provides the best beam patterns but deployment of a large circular array in deep water is difficult. For this reason, a linear array is chosen, even though ambiguous beams exist. The widths of beams developed at end fire of the array are quite large. However, this need not be a problem if we limit the bearing coverage to  $\pm 60^\circ$  around broadside.

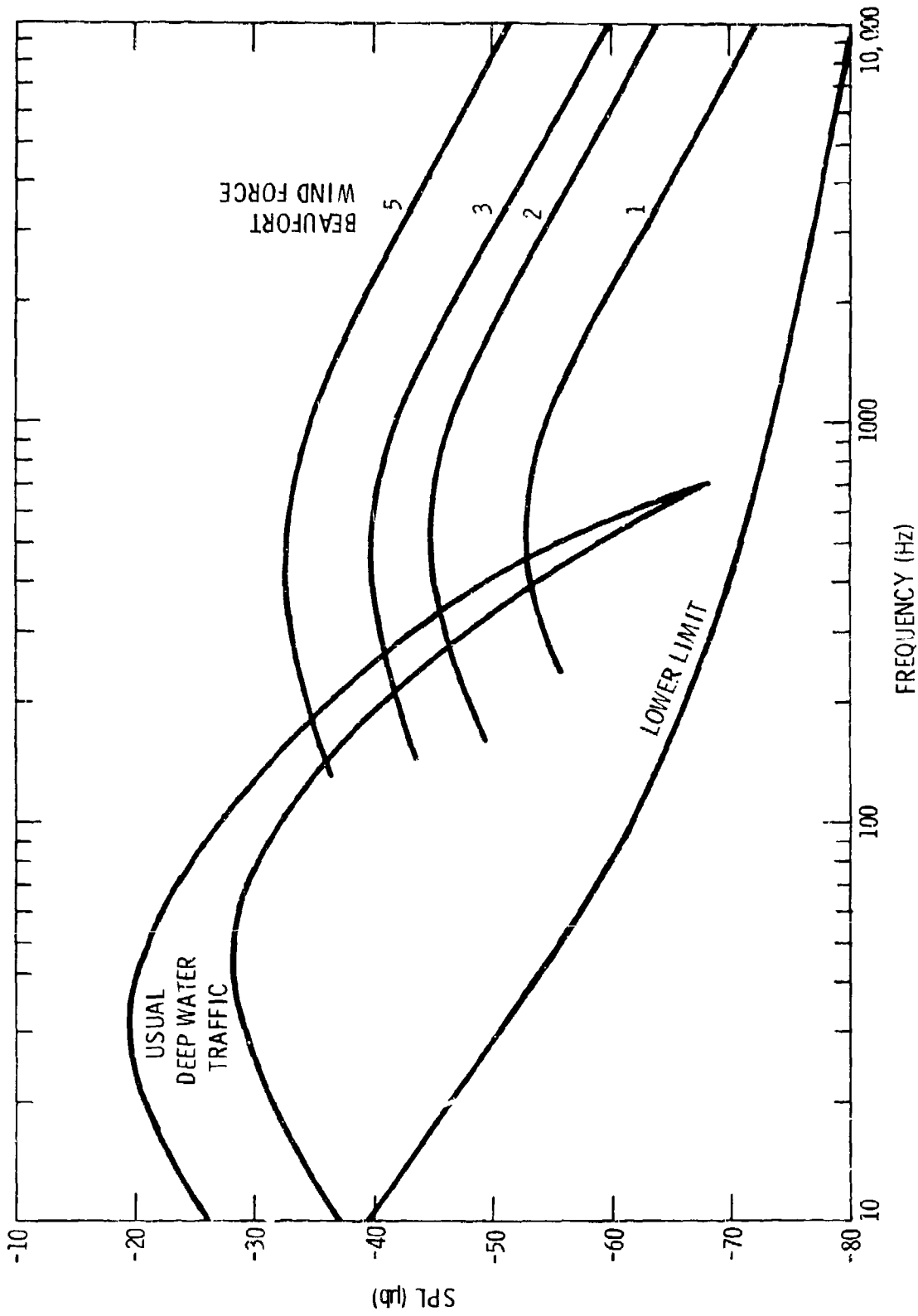


Figure 1. Wenz's Curves

Considering the spread of the frequencies it is unreasonable to have a single array to cover this bandwidth. At the high frequency end of the band, huge side lobes will appear or at the low frequency end the beams will be too wide, with a corresponding loss of directivity. These requirements dictate a series of arrays to cover the band.

Another consideration is the number of elements in each array. Since array directivity is a function of the number of elements, a large quantity is desirable. On the other hand a longer array (because of the large number of elements) causes problems in deployment. From a processor point of view, it is desirable to set the number of elements equal to or less than some power of two. Since processors operate on binary numbers, some simplification of hardware will result. The latter consideration suggests element numbers such as 7, 8, 15, 16, 31, or 32.

The smaller numbers of the set generate beam widths too broad to be practical. At the high end, the array length becomes too cumbersome to deploy in deep water. Fifteen or sixteen elements is a good choice. From a performance standpoint, there is little difference between either 15 or 16 elements. In either case, the processor is designed to operate as though there were 16 inputs. However, if only 15 inputs were used, the processor could use the idle time to do resets of other control functions. Hence, fifteen hydrophones are the choice.

With the number of elements selected, the problem of hydrophone spacing and the number of arrays was analyzed. The solution was a cut and try process. The results are shown in Figure 2. Three arrays are required. The heavy vertical lines represent the half wavelength frequencies. These bands were selected to optimize the arrays at the frequencies of greatest "operational" importance.

Amplitude or spatial shading was analyzed. Figures 3, 4, and 5 show the relationships of beamwidth vs normalized frequency for equally spaced elements, spatial shading, and equally spaced elements with amplitude shading. In all cases, the frequency was normalized to the half wavelength frequency. The band of interest ranges from 0.75 to 1.3 times the half wavelength frequency. Below this band, the beams are too broad and above the band side lobes are a problem. Figure 6 compares the  $60^{\circ}$  beams for the three cases. For spatial shading, the beam width was greater than the equally spaced array by about two degrees.

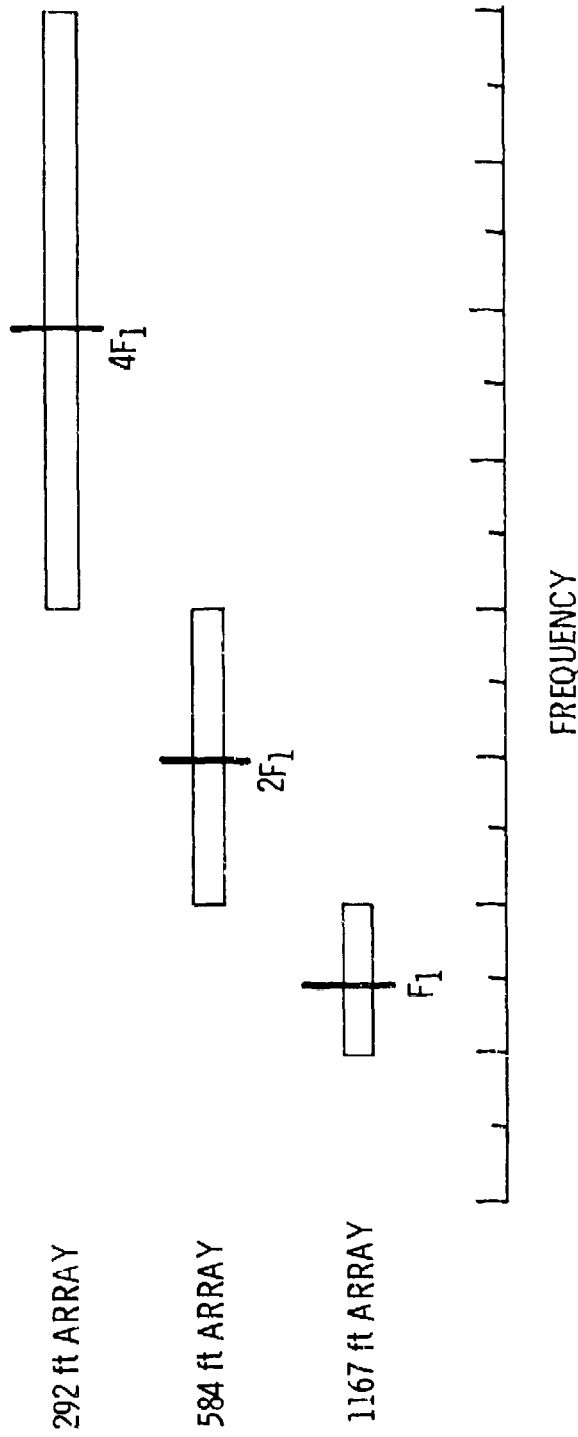


Figure 2. 15 Element Arrays

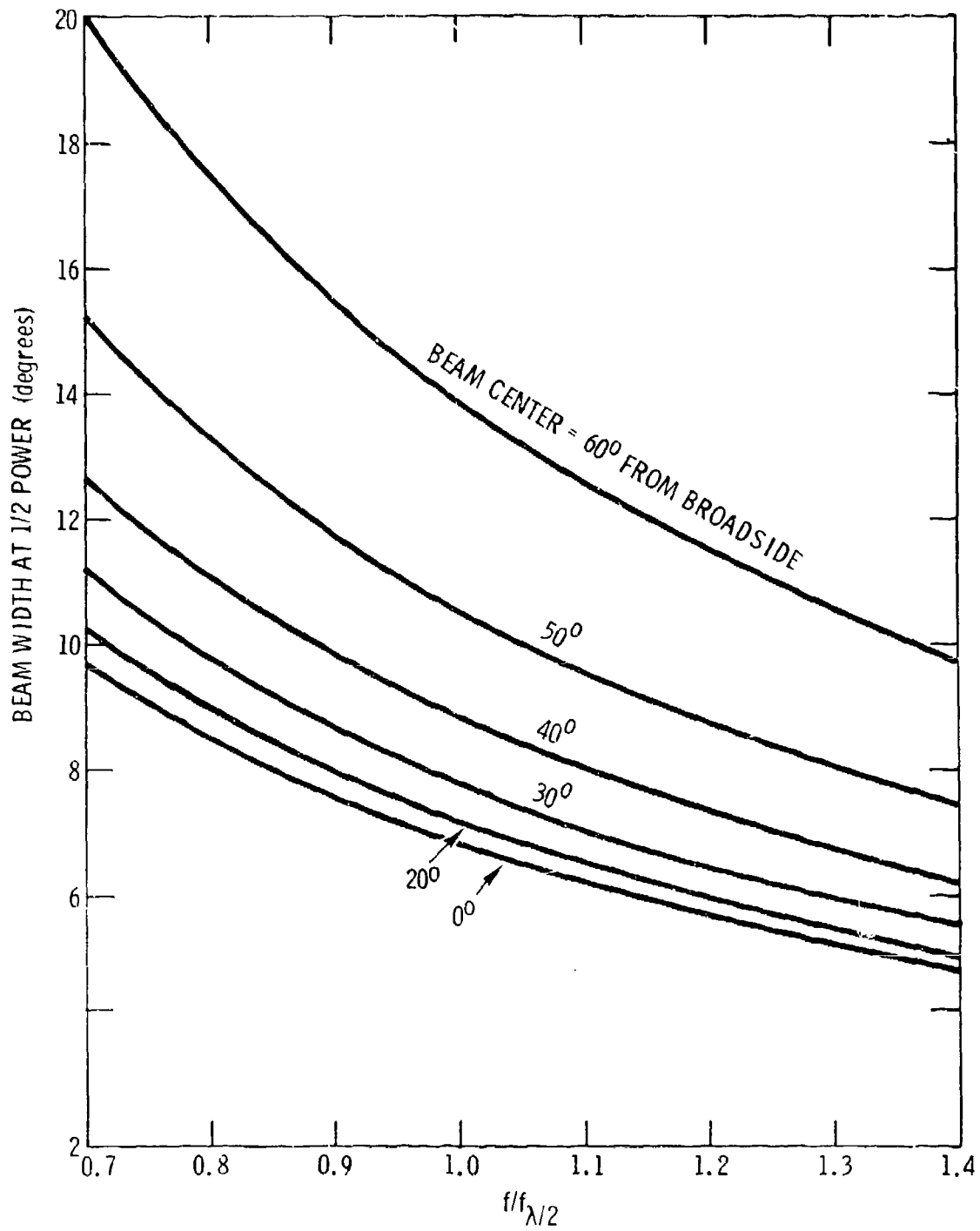


Figure 3. Beam Width at 1/2 Power

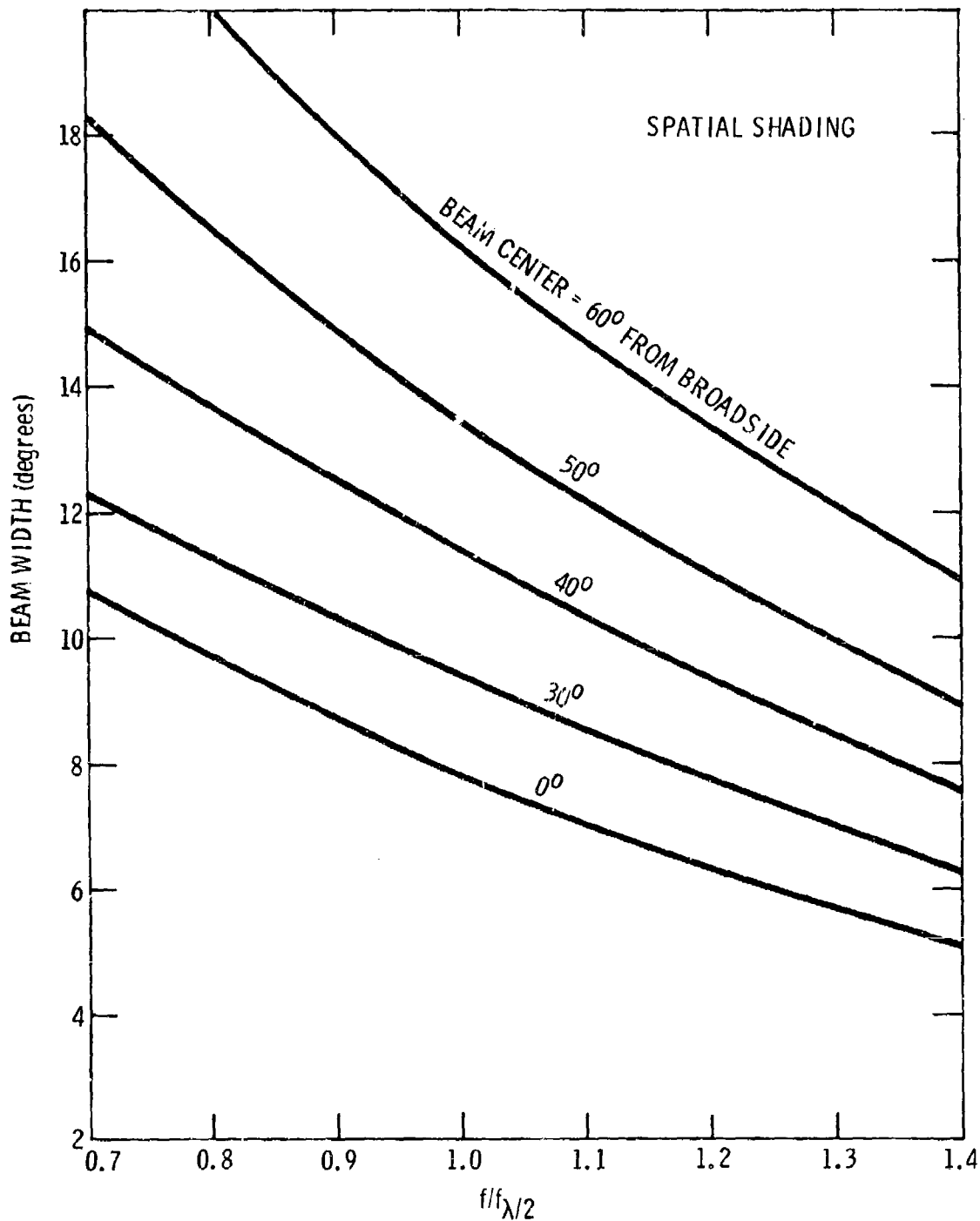


Figure 4 Beamwidth vs. Normalized Frequency (15 Element Array Spatial Shading  $d_n = 1.1 d_{n-1}$ )

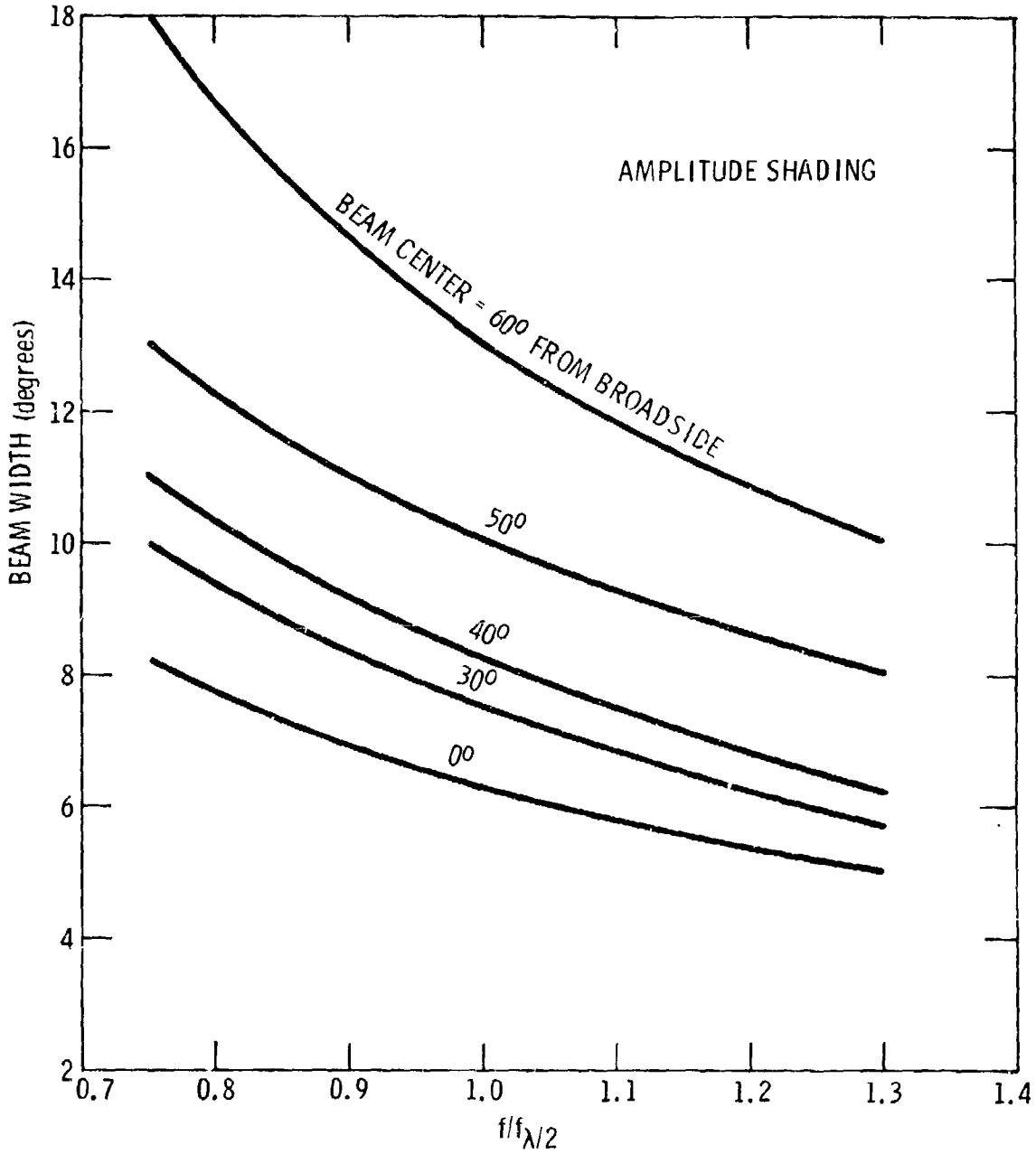


Figure 5 Beamwidth vs Normalized Frequency, 15 Elements, Equally Spaced Amplitude Shading (-13db)

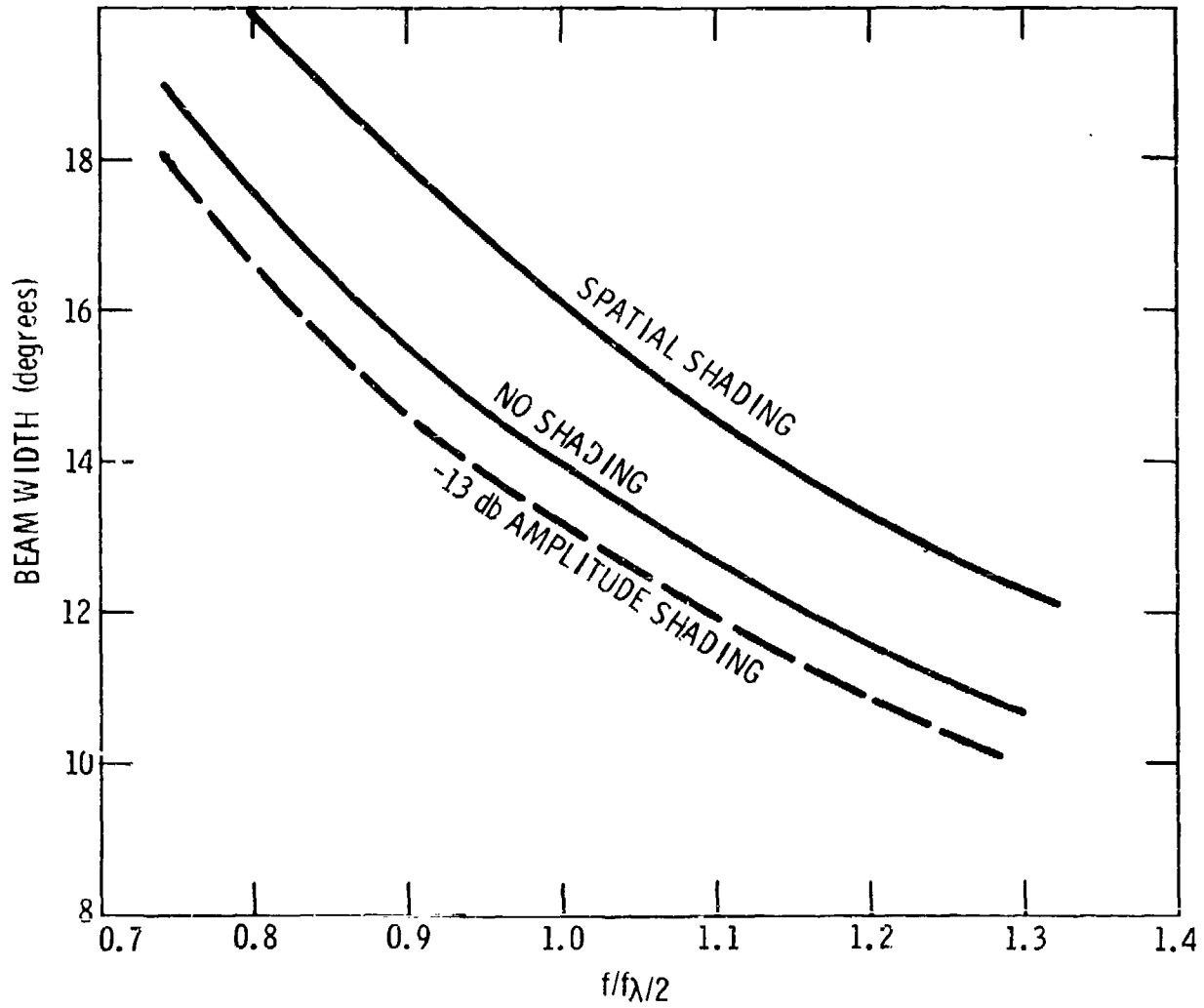


Figure 6 Comparison of 60° Beams

This is not desirable. In the case of amplitude shading, however, the beam width actually decreased by one degree. This is unusual since a wider beam width is usually expected when side lobes are reduced. It can, however, be explained.

The technique of amplitude shading is to multiply the output of each sensor by a real constant before summing in the beamformer operation. In the particular case of a linear, uniformly spaced array, the amplitude response can be made to correspond to a Tchebyscheff polynomial, the result being an array with uniform side lobes level. By using this technique, any side lobe level can be specified and no side lobe will exceed this level. Specifying the side lobe level also determines the main lobe beam width, however, and there is the usual reciprocal relationship between the two, i. e., reducing the side lobe level increases main lobe beam width and vice versus. We specified the side lobe level to be -13 dB down from the main lobe. However, most of the side lobes were already considerably lower than this level; hence, the side lobes were raised with a corresponding decrease in main lobe beam width. This would not have been the case had we specified the side lobe level to be -26 dB.

Spatial shading is a method sometimes considered for improving the beam characteristics of an array. The method used is to space the elements according to a prescribed mathematical relationship. This, however, decreases performance at any one frequency. We investigated a spatial shading utilizing a factor of 1.1, where the distance between the pair of elements was 1.1 times the adjacent spacing. It was determined that the technique improves only the broad band characteristics and we are interested in discrete frequencies in a broad range, so the technique was discarded.

Figure 7 shows the relationship between steering angle and normalized frequency for -10 dB maximum back lobe. In the case of the equally spaced array, no back lobe is greater than -10 dB for all steering angles within  $\pm 60^\circ$  sector at a normalized frequency of 1.05 or lower. Above this value the back lobe is troublesome. In the cases of the spatial and amplitude shading, the results are different but not necessarily better. For this reason, it would be best to use a linear spaced array with no shading, since there will be no back lobe within  $\pm 60^\circ$  for frequencies 1.05 times the half wavelength frequency and no back lobe within  $\pm 30^\circ$  between 1.05 and 1.3.

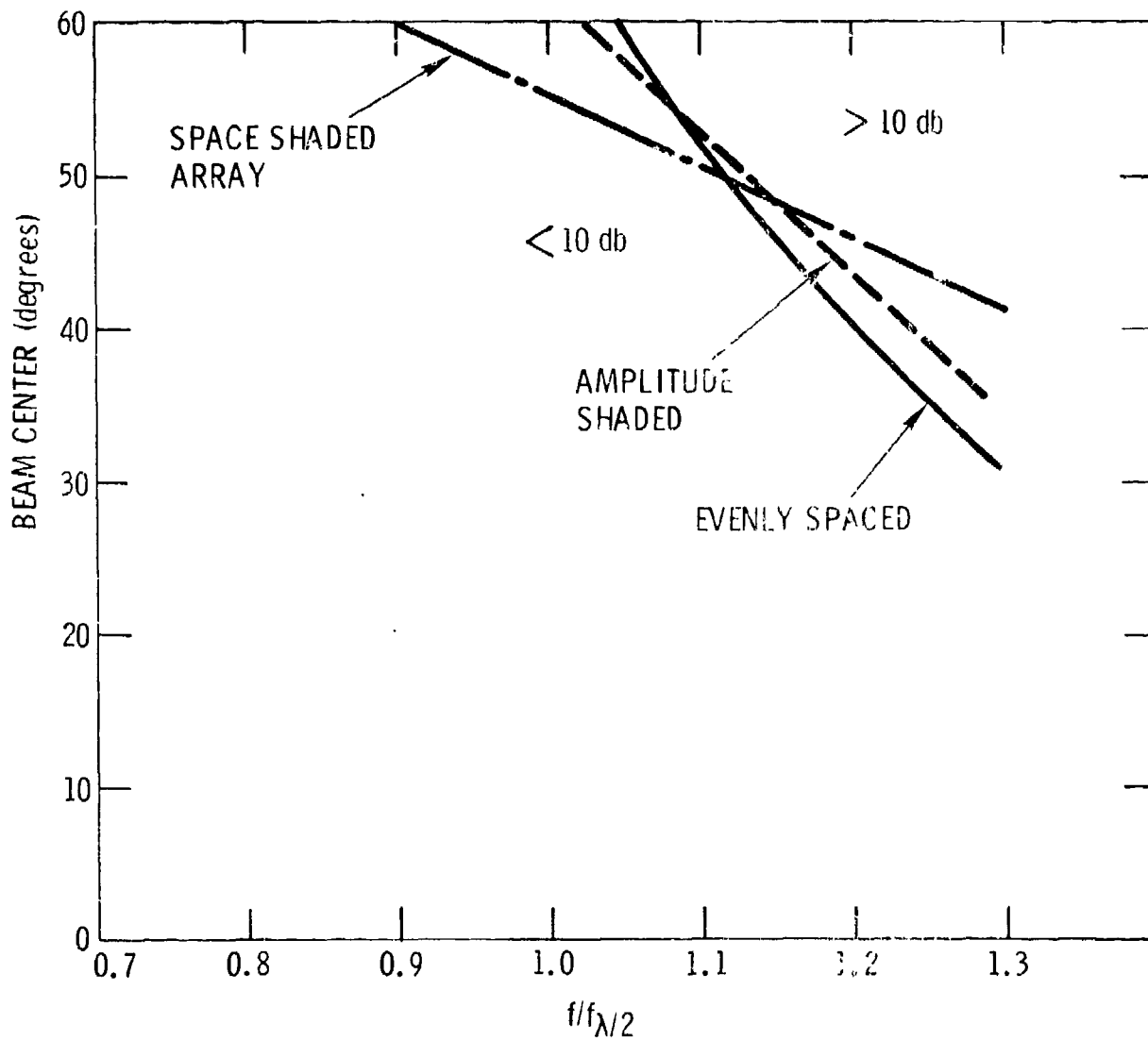


Figure 7. Steering Angle vs Frequency 10 dB max back lobe

In conclusion, three linear arrays are necessary to cover the frequency band. The elements are equally spaced and only 29 elements are required (see Figure 8).

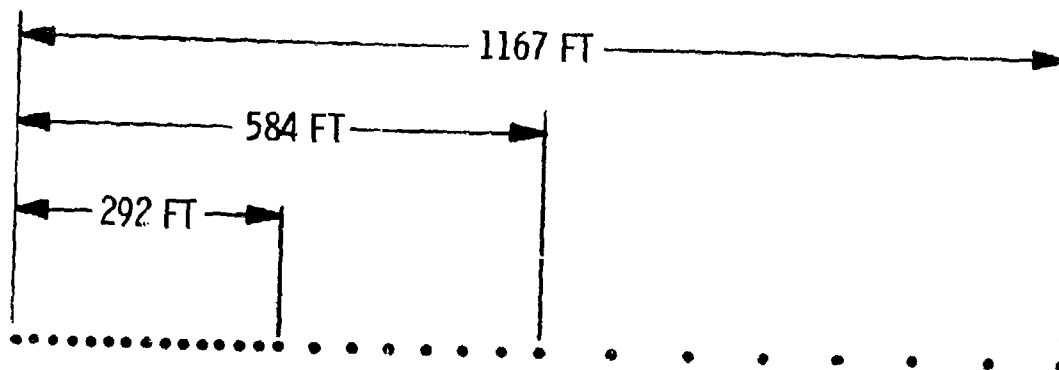


Figure 8. 3-Array Network

### SECTION III ELECTRONICS

#### SIGNAL CONDITIONING

The signal conditioning equipment consists of the hydrophone, preamplifiers, filters and analog-to-digital converters. The hydrophones selected for the BAND processor are International Transducer Corp., Model ITC-1051. The performance characteristics of these devices are as follows:

- Frequency range: 10 Hz to 3 kHz
- Open circuit voltage: -90 dB re 1 volt/ $\mu$ bar
- Capacitance: 16,000 picofarads
- Operating depth: unlimited

The preamplifiers will be designed to operate in a 42 dB dynamic range. The lower limit of this range is the lower limit of Wenz's curves at 50 Hz.

Three sets of low pass filters are required. The cutoff frequency will be determined by the actual frequencies selected. The pass band ripple will be limited to  $\pm 1/2$  dB or greater. The rejection band is defined as twice the cutoff frequency and greater. The analog-to-digital converter will be capable of operating as the output of the filter and will have an 8-bit output.

#### PROCESSOR

With respect to the processor, the points considered during the study were the number of beams to be formed, the configuration of the processor, and the type of data to be recorded. The purpose of an on-line processor, in any application, is to reduce data before it is recorded or stored. For this reason, performing a complete spectral analysis is not reasonable. Spectral analysis is a process of transforming information from the time domain to the frequency domain and does not reduce data. If this was to be performed, merely recording the time samples and conducting the spectral analysis on shore would be better, but the storage requirements would be immense. The process of post integration is, however, a data reducer. It furnishes answers that are the average of many time samples. The processor, then, consists of limited spectral analysis, beamforming, and post integration.

The number of beams to be formed was determined by the beam power output at beam crossover. The beam crossover angle is the angle at which two adjacent beams have the same power output. For convenience of the processor, beam numbers such as 16 and 32 were considered. The power outputs at crossover are shown in Figure 9. Thirty-two beams is the better choice, since the degradation at crossover is almost uniform for all frequencies. The beam spacing varies as the arcsine  $c/k/16$  where  $k$  is an integer. For reference purposes the appendix contains beam patterns for various frequencies.

With respect to the configuration of the processor, a system employing a spectral beamformer was selected over a system employing a time domain beamformer. In the latter, a delay and sum beamformer is used at the front end and Discrete Fourier analyzers are used at the rear, operating upon the beam outputs. In the former case, the Discrete Fourier analyzers operate at the hydrophone outputs with beamforming accomplished by a phase and sum operation on the Fourier coefficients. Since the system was designed to form 32 beams from the information of 15 hydrophones, the complexity of the Discrete Fourier analyzer is considerably reduced, since it uses 15 input channels rather than 32. In either case, the complexity of the beamformer is about the same. For these reasons, a system containing spectral beamforming was selected.

Although 32 beams will be processed during a sample interval, only the outputs from 29 will be recorded (stored in memory). This permits three memory bins to be used as follows:

- The averaged filtered output from a single hydrophone will be recorded. After deployment of the array, an acoustic projector will be used to transmit all of the preselected frequencies at different levels of attenuation on a given direction. Using the results of the single hydrophone and the beam outputs, a calculation of array gain can be made.
- The outputs of two adjacent hydrophones will be added and recorded. These data and the single hydrophone output will be used to measure worst-case noise incoherence. The projector will not be used for these data.
- The outputs of the two terminal hydrophones will be added and recorded. These data and the single hydrophone output will be used to measure signal coherence. The projector will be used for these data.

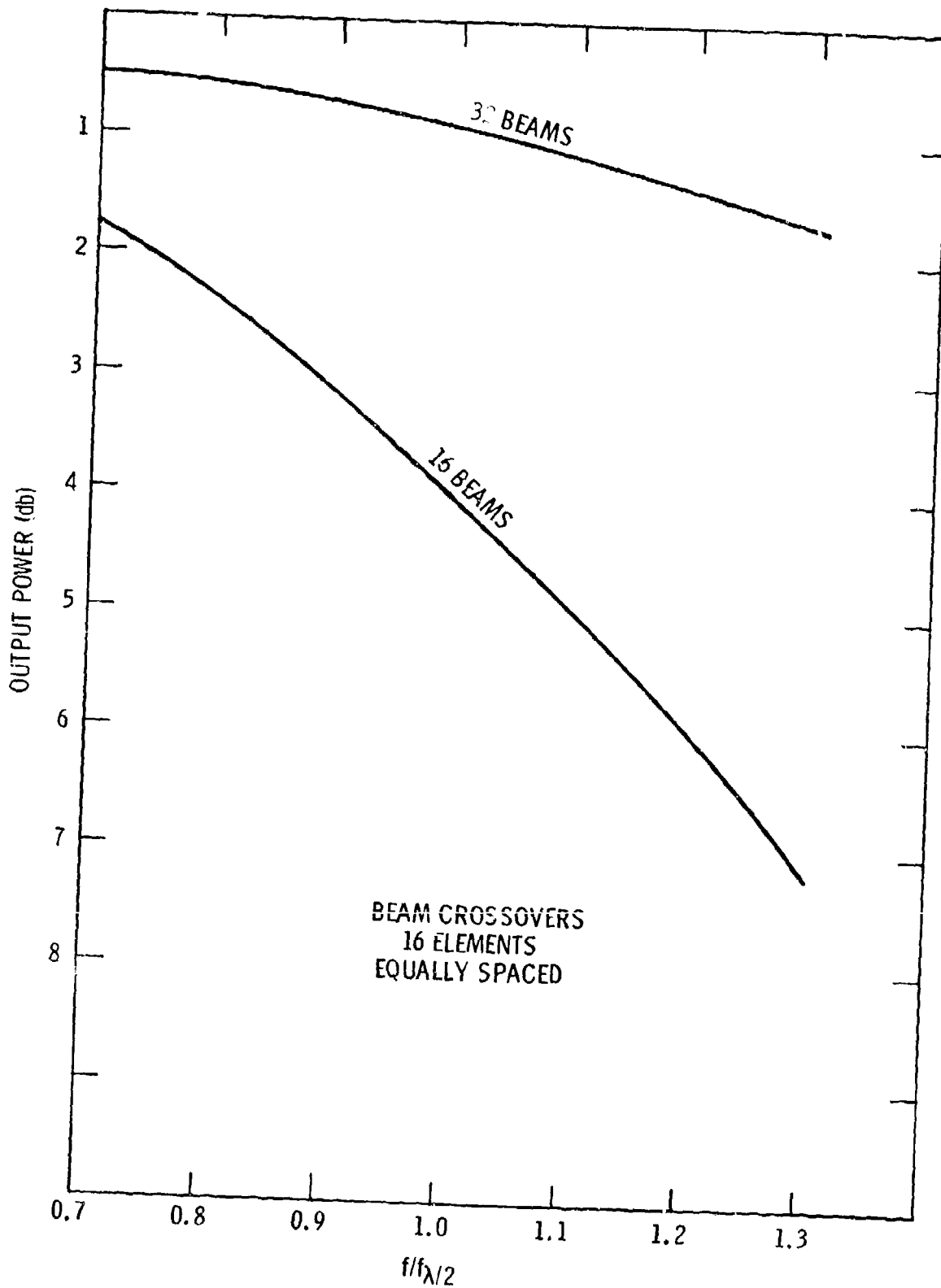


Figure 9. Beam Crossovers, 16 Elements Equally Spaced

### Recorder

The storage medium is a digital, incremental-recorder with a storage capacity of 2.2 million bits. This will permit the storage of the data from 3600 sample periods. If the sample period is 8 minutes long, a total storage time of 20 days is indicated.

### BAND PROCESSORS

The BAND processor system is shown in Figure 10. The signal conditioning section consists of a 29-element array, preamps, filters, and selection logic on an 8-bit analog-to-digital converter. The processing section consists of a Discrete Fourier Processor and a frequency beamformer. The absolute magnitude of the beamformer is smoothed by the post integrator and then recorded on an incremental tape recorder.

In operation, the BAND processor forms a 2 Hz filter centered on the selected frequency. Only one frequency is selected during an eight minute processing period, but up to eight different frequencies may be processed. During an eight digital minute (512 sec) interval, actual processing is conducted in the first digital minute (64 sec). During the remaining interval, nothing occurs. Operation begins when the processor recognizes which frequency is to be processed. After this is done, the appropriate group of 15 hydrophones are selected. Signals from these hydrophones are passed through preamplifiers and filtered, multiplexed, and converted into an eight bit two's complement binary number. The sampling rate for each of the 15 inputs is exactly four times the center frequency of the filter being formed.

The Discrete Fourier Processor, operating upon these 15 independent time series, computes the real and imaginary coefficients for the discrete Fourier Transform. A new set of coefficients is formed every 1/2 second. This 1/2 second integration period permits a 2 Hz wide filter to be formed on each of the input channels. The response characteristics of these filters is a  $\frac{\sin X}{X}$  curve, since no input weighting is performed.

Principle of operation of the frequency beamformer is based upon phasing and summing instead of delaying the summing as in a time domain beamformer (DIMUS) type. The phasing operation is performed by passing the Fourier coefficients from the Discrete Fourier Processor through a series of vector rotators. Each of these vector rotators rotates the input vector through a fixed angle. These angles are  $90^\circ$  for the first vector

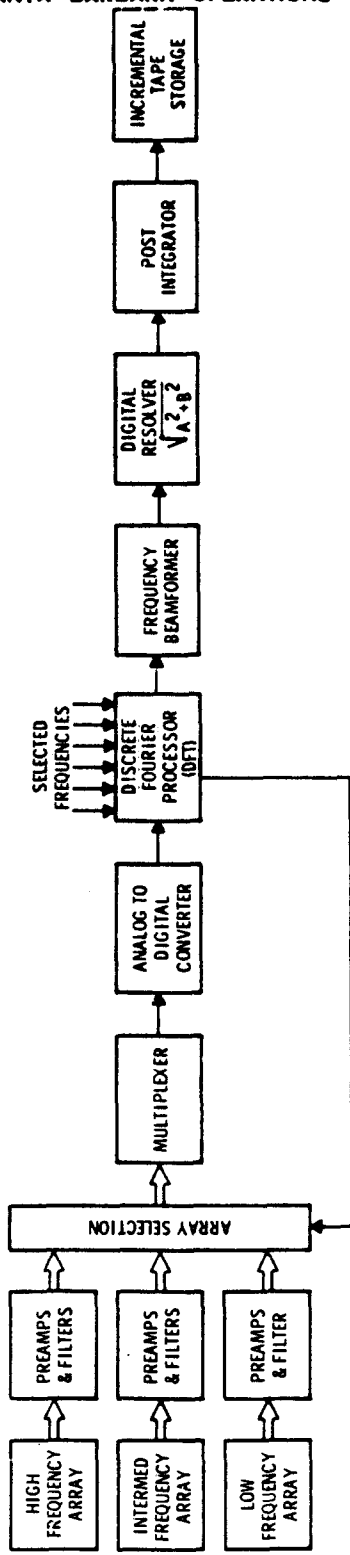


Figure 10. Band Processor

rotator,  $45^{\circ}$  for the second unit, and in decreasing angles down to  $3.6^{\circ}$  for the last vector rotator. Each vector rotator always displaces the input vector by the same angle. Only the direction (plus or minus) is changed. This is controlled by the phase angle generator. By rotating the input vectors in this manner, each set of coefficient is phased through an angle corresponding to the DIMUS delay value for the frequency being formed. The final process of the frequency beamformer is to sum the phased vectors across the number of elements. This operation is the same as in a time domain beamformer.

The absolute magnitude is performed by taking the square root of the sum of the squares of the real and imaginary output from the beamformer. To accomplish this, a unique algorithm is used, similar to the vector rotator operation performed in the beamformer. That is, the input vector is rotated until it lies entirely within the real axis. When this is accomplished, the imaginary component is reduced to zero and what is now the real component is the desired square root of the sum of the squares of the real and imaginary part.

The post integrator performs the function of temporal smoothing on each of the 29 beams. The time of smoothing is one minute and is performed by adding each new beam output into the appropriate one of 29 bins. The averager starts at zero during each integration period and accumulation is performed for one minute. At the end of this time, the results are recorded on the incremental tape recorder and the processor then becomes quiescent for the next seven minutes.

#### ARRAY

The array is a linear array of 29 elements with a total length of 1167 feet. The displacement of each of the 29 elements is shown in Table I. For any given frequency, only the appropriate 15 elements are chosen for processing. These characteristics are also shown in the table. If a high frequency line is to be processed, the first 15 elements are chosen. If an intermediate frequency is to be processed, every other element of the first 15 and the next seven are selected. In the case of the low frequency array, every other one from the intermediate group and the final seven are selected. In each case, a linear array of 15 equally spaced elements is selected for processing.

Element No.	Nominal Displacement	Low Frequency Array Channel No.	Intermediate Frequency Array Channel No.	High Frequency Array Channel No.
0	0	0	0	0
1	20.8			1
2	41.7		1	2
3	62.5			3
4	83.4	1	2	4
5	104.2			5
6	125.0		3	6
7	145.9			7
8	166.7	2	4	8
9	187.6			9
10	208.4		5	10
11	229.2			11
12	250.1	3	6	12
13	271.0			13
14	292.0		7	14
15	333.0	4	8	
16	375.1		9	
17	416.5	5	10	
18	458.5		11	
19	500.1	6	12	
20	541.8		13	
21	583.5	7	14	
22	666.9	8		
23	750.2	9		
24	833.6	10		
25	916.9	11		
26	1,000.3	12		
27	1,083.7	13		
28	1,167.0	14		

Table I. Array Characteristics

SIGNAL CONDITIONING

Figure 11 is a block diagram of the BAND Signal Conditioning Subsystem. Each of the 29 hydrophones in the array is followed by a low noise FET input preamplifier whose topology is shown in Figure 12. These 29 preamps are followed by three sets of 15 low pass filters. Each set of filters connects to a different set of 15 hydrophones in order to form the array corresponding to the desired frequency band. The 45 outputs from the filters connect to a 45 input multiplexer-selector and then to the analog-to-digital converter.

Because of the requirement for low power consumption, only those sets of 15 analog elements that are required for a particular band are supplied with power. This function is provided by the array select and power control block. The multiplexer only scans 15 channels at a time, depending upon the selected frequency band.

The preamplifier is designed to have a voltage gain that rises with frequency to cause the noise spectrum to be flattened (whitened). The particular frequency shaping that was chosen to achieve the pre-whitening function is a double zero at 60 Hz, which results in a noise spectrum as shown in Figure 13. A computer program was written to calculate the Wenz usual deep water traffic, upper-limit noise, in a band of frequencies corresponding to the low pass filter cutoff frequencies. Table II is the computer printout. If  $N(f)$  is the pre-whitened noise spectrum level at a frequency  $f$ , then the RMS noise in a band of frequencies between  $f_1$  and  $f_2$  is

$$N_{RMS} = \text{SQRT} \left( \int_{f_1}^{f_2} N^2(\epsilon) df \right).$$

This figure is shown in the column "Integrated Noise." The column "dB Correlation" shows the preamp gain increase caused by the double zero at 60 Hz. The column "Wenz' Corrected Upper Limit" lists the noise spectrum level after frequency shaping.

Figure 13 shows the topology of the preamplifier. The FET is a low noise device from the Siliconix 2N4867A family. This particular topology has been used very successfully in past programs where a stable gain, low noise preamp is required. The transfer function of this preamp is  $H(s) = 10^4 s (1 + 2.65 \times 10^{-3} s)^2 / (1 + 7.95 \times 10^{-3} s) (1 + 5.3051 \times 10^{-5} s)^2$ , which places the lower -3dB point at 20 Hz and the double zero at 60 Hz. This transfer function is plotted in Figure 14.

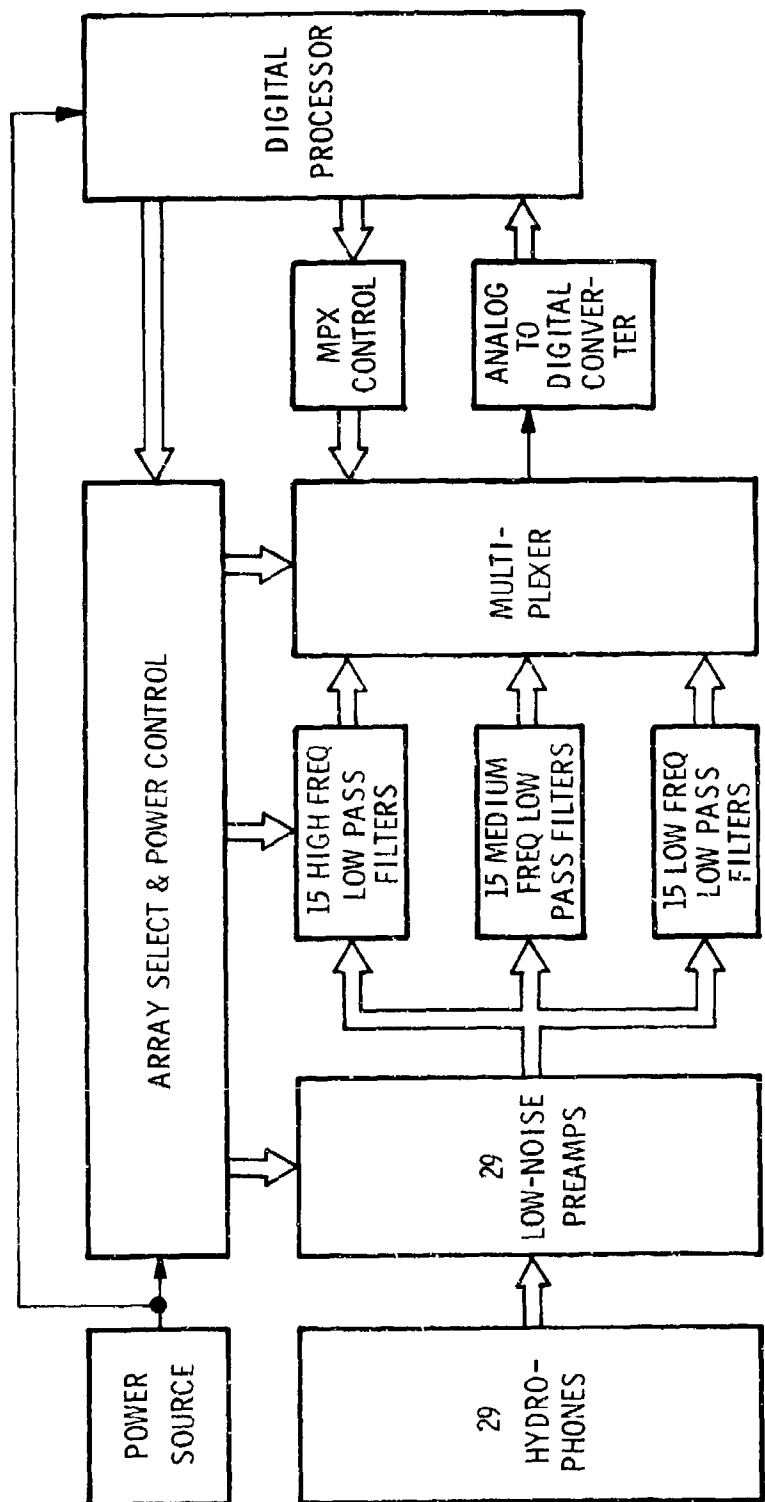


Figure 11. Signal Conditioning

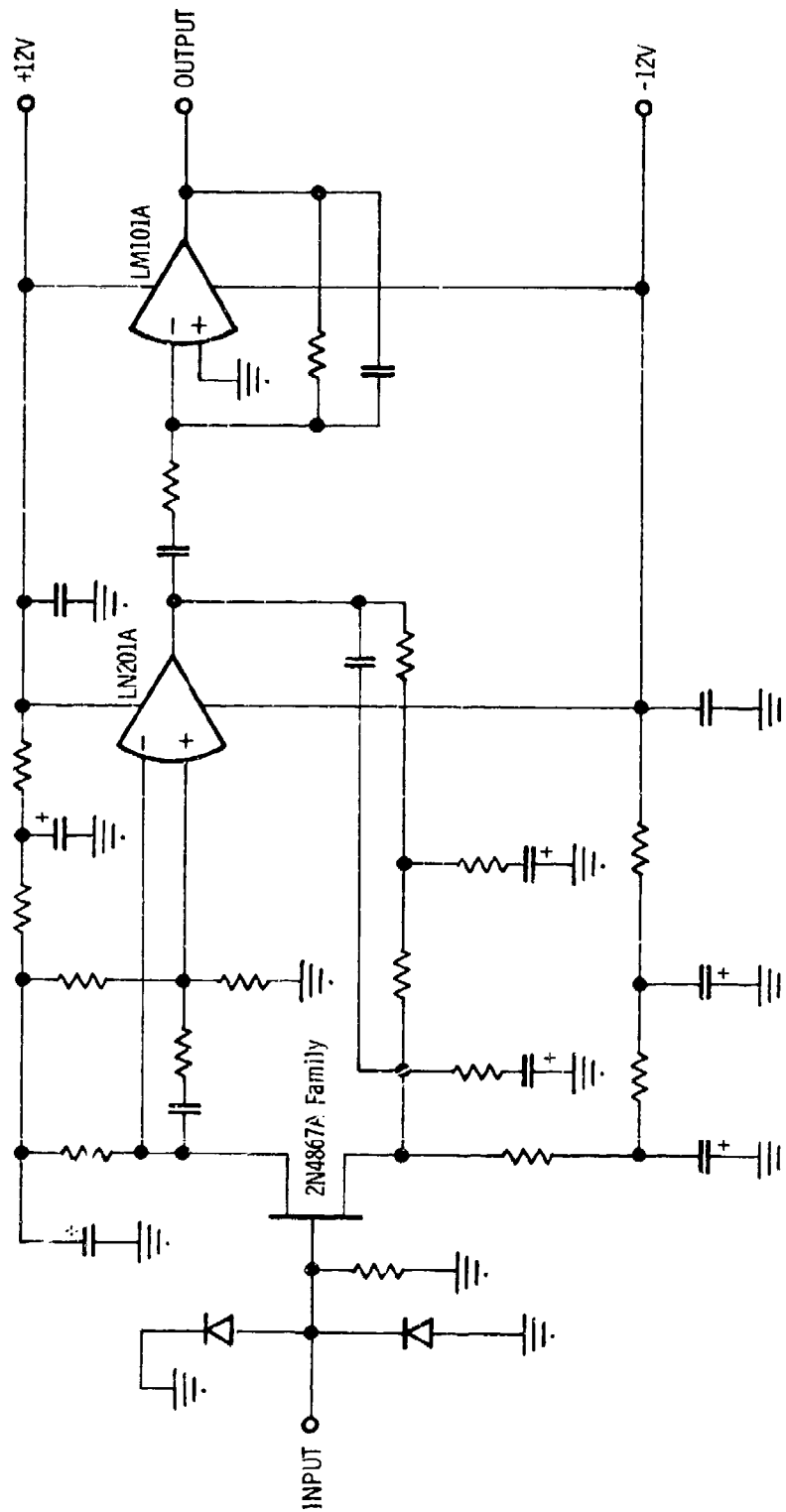


Figure 12. Preamp Topology

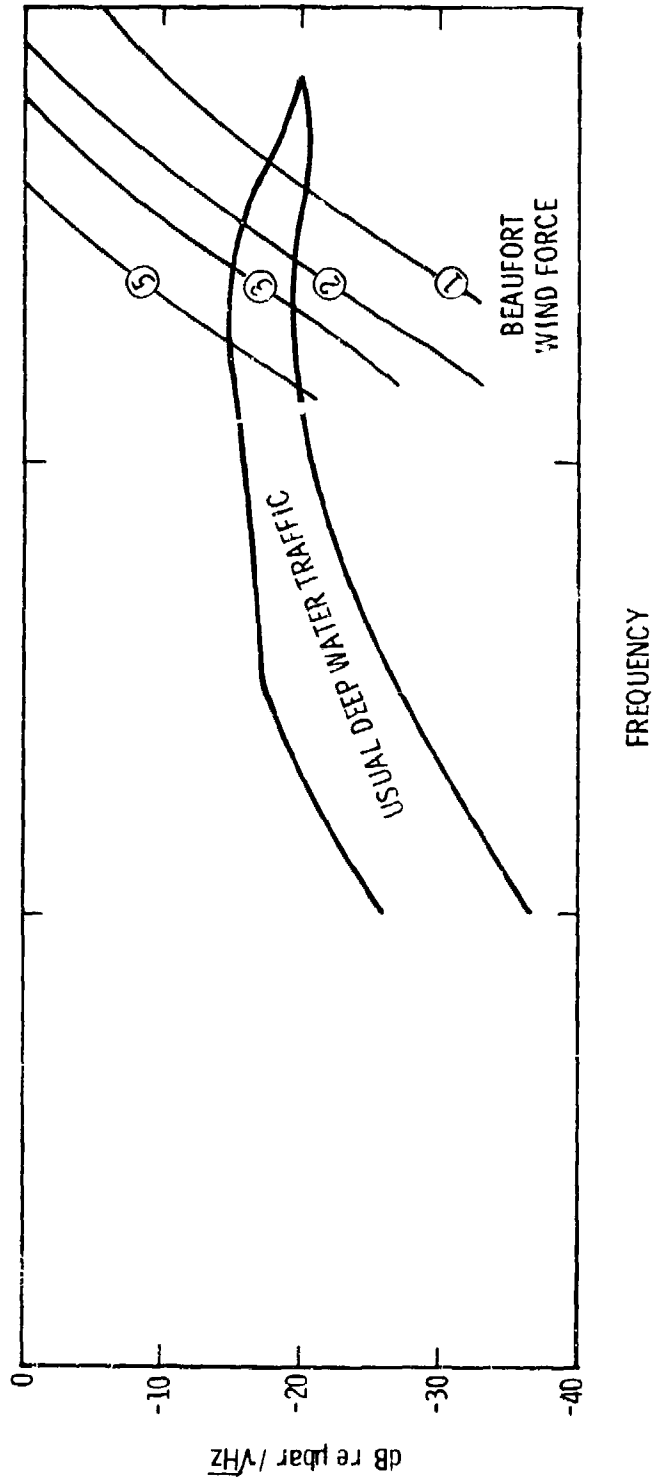


Figure 13. Noise Data Equalized by Second-Order Zero at 60 Hz

<u>Bandwidth 20 Hz To</u>	<u>Wenz's Upper Limit Integrated Noise dB re <math>\mu</math>bar</u>	<u>dB Correction</u>	<u>Wenz's Corrected Upper Limit</u>	<u>-90 dBV/<math>\mu</math>bar Hyd Total Gain Req'd for +1.5 dBV at Filter Output</u>
25	-7.289	1.390	-18.610	
30	-6.067	1.938	-17.562	
35	-4.920	2.544	-17.256	
40	-3.985	3.194	-16.906	95.5 dB
50	-2.339	4.581	-16.619	(82.25 + 13.25)
60	-1.040	6.021	-16.479	
70	-0.069	7.462	-16.238	
80	0.807	8.874	-16.126	90.7 dB
90	1.462	10.238	-15.762	
100	2.285	11.545	-15.855	(82.25 + 8.45)
110	2.828	12.792	-15.708	
120	3.306	13.979	-15.521	
130	3.771	15.109	-15.391	
140	4.182	16.184	-15.216	
150	4.586	17.207	-15.093	
160	4.984	18.182	-15.018	86.5 dB
170	5.329	19.112	-14.888	(82.25 + 4.25)
180	5.820	20.000	-15.000	
190	6.113	20.850	-14.650	
200	6.647	21.664	-14.836	
250	7.918	25.278	-14.722	
300	9.252	28.299	-15.201	82.25 dB
400	11.098	33.150	-16.350	
500	12.544	36.957	-18.043	

Table II. +40 dB/Decade Preamplifier Slope  
(Double Zero at 60 Hz)

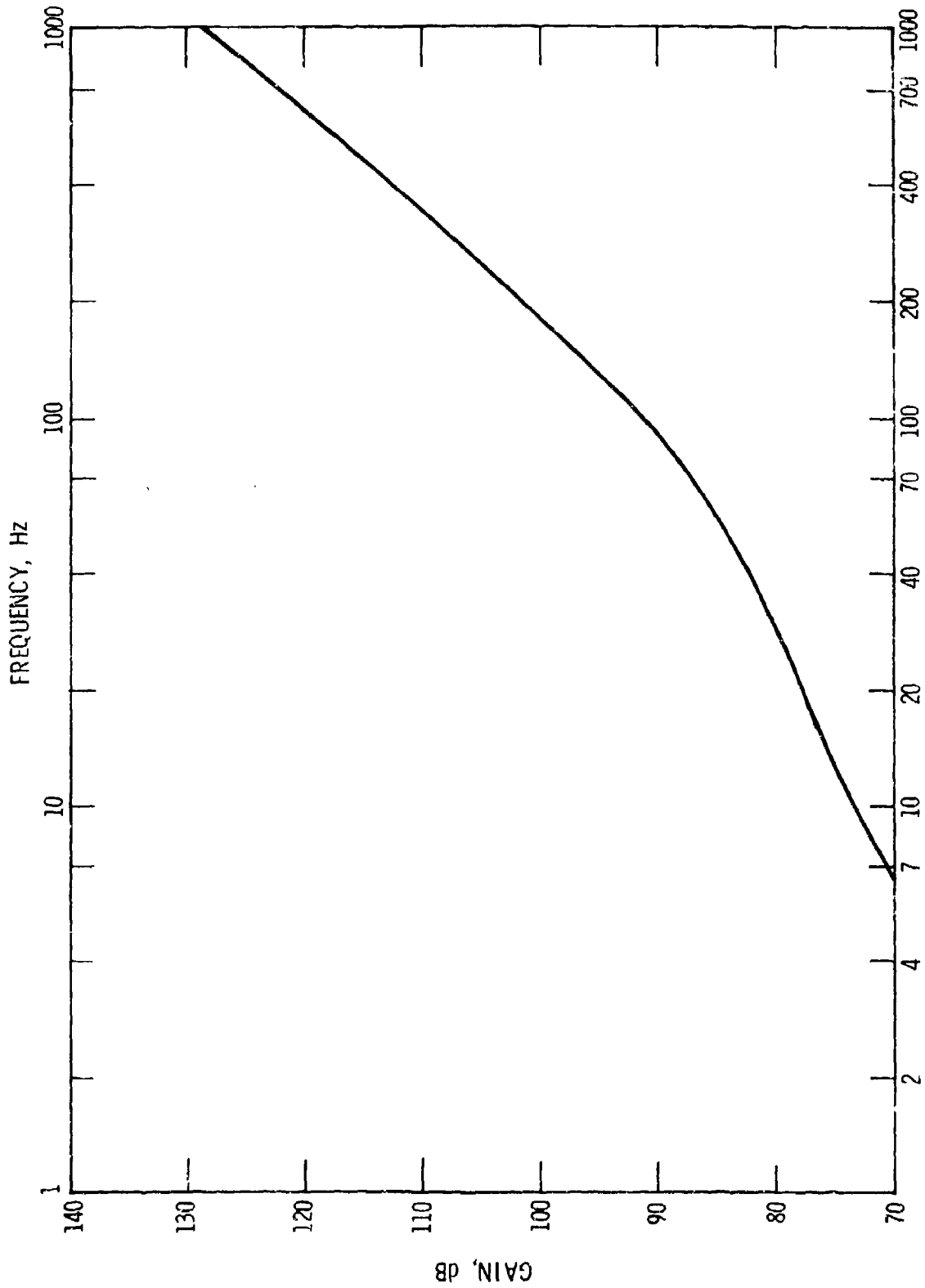


Figure 14. Pre-amplifier Gain vs Frequency

Since the system is designed to operate in one of three frequency bands, three sets of 15 filters are required. It is expected that these filters will have low-pass characteristics. The cutoff frequency (3 dB down) is determined by the highest frequency to be processed in that band. The in-band ripple is limited to  $\pm 1/2$  dB. The slope characteristics will be determined as follows: Since the sample frequency for the digital processing is exactly four times the frequency selected, the frequency at which aliasing will occur will be equal to  $3/4$  the sample frequency. The lowest frequency to be processed in the band determines where this point is. This critical frequency is equal to three times the lowest frequency in the band. Since an 8-bit (sign + 7 magnitude bits) A/D conversion takes place, the critical frequency and higher should be suppressed by greater than -42 dB. This reduces the unwanted frequency components to a level lower than the least significant bit. Since the ratio of the highest frequency to lowest frequency in each band is about 1.5, the critical frequency is about one octave away from the cutoff frequency.

The low pass filters are required to have -3 dB cutoffs of nominally 40, 80, and 160 Hz and be greater than -42 dB down at twice the cutoff frequency. A 5th order elliptic filter with 0.01 dB ripple in the pass band having ultimate attenuation reached at  $2 \times$  cutoff frequency is chosen. This design is mechanized with a two-section active filter whose topology is shown in Figure 15.

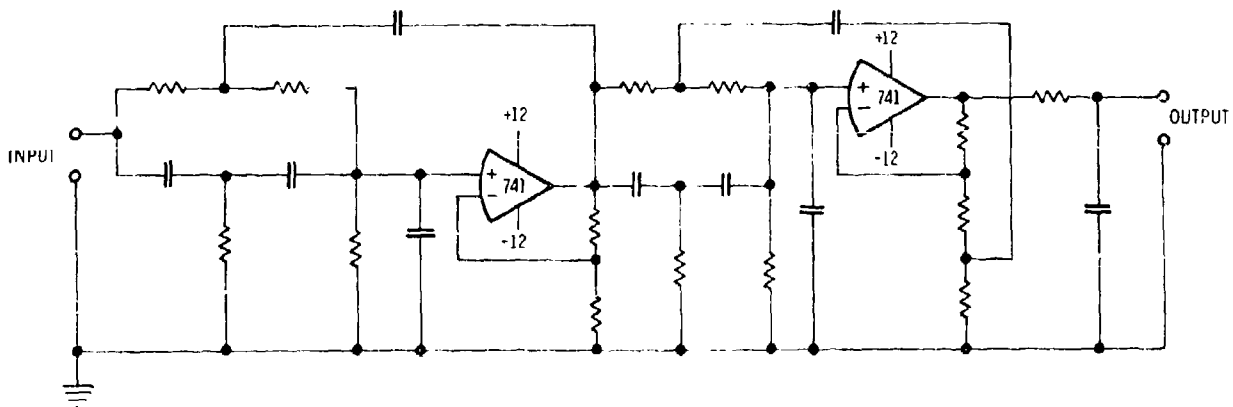


Figure 15. Filter Topology

The array selection and multiplexer portion of the BAND electronics performs the function of selecting the appropriate set of 15 filter outputs and then sampling them in sequence. The array selecting function takes place less often than eight minutes, while the multiplexing occurs at a rate of 64 times the frequency selected. Multiplexing occurs during the one minute processing period. Signal inputs and outputs are analog, while the control signals from the discrete Fourier processor are digital.

The multiplexer is implemented by using p channel FET's as shown in Figure 16. This arrangement allows for a very simple interface between the logic and the multiplexer. Extreme accuracy is not required here; hence the operational amplifier summing connection enhances the simple interface.

The requirements for the analog-to-digital converter are low power consumption and conversion rates up to 64 times the highest interrogated frequency. These characteristics are difficult to obtain in a single analog-to-digital converter. Conventional converters have high speed capabilities but their power consumption is too high. Datel Systems, Inc, model ADC-CM has low power requirements but its maximum sampling rate is low. Four of these units operating in parallel would satisfy the BAND requirements for the highest frequency.

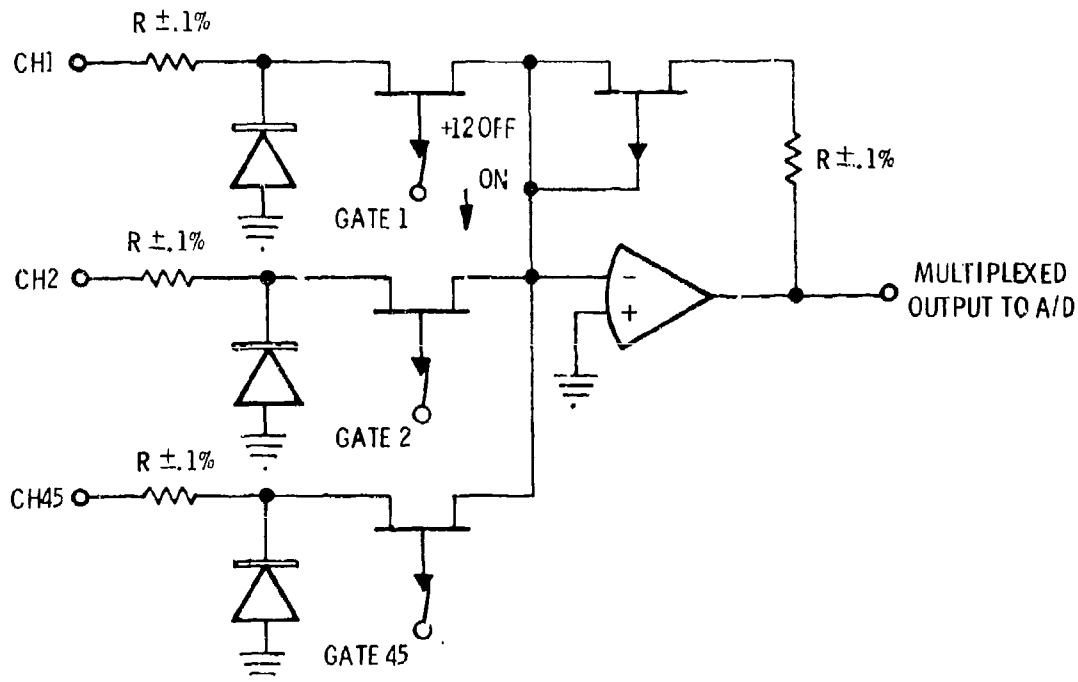


Figure 16. Multiplexer

However, the manufacturer's data do not describe the power consumption versus frequency characteristics of the device. It is recommended that additional tests be made on this unit. From these tests, the number of A/D converters can be specified with sufficient power source to drive them.

### DISCRETE FOURIER PROCESSOR

The Discrete Fourier Processor (DFP) is the heart of the BAND system. It solves the Discrete Fourier Transform (DFT), Equation 1:

$$A_k = \sum_{j=0}^{N-1} X_j e^{\frac{i2\pi jk}{N}} \quad (1)$$

where  $A_k$  is the complex Fourier coefficients for the  $k^{\text{th}}$  frequency and  $X_j$  is the  $j^{\text{th}}$  input time sample. In a conventional DFT or FFT processor,  $N$  is fixed and determined by the ratio of the sample rate and the filter bandwidth to be synthesized. In these processors, all input time samples are stored and an output is computed for every value of  $k$ . However, since the BAND processor is interested in only one frequency during any one eight-minute sampling interval, certain liberties can be taken with Equation 1. This means that  $A_{\text{out}}$  is computed for only one value of  $k$  and that there are no storage requirements for the input time samples. Further, if we choose the sample rate to be exactly four times the frequency of interest (setting  $k/N = 1/4$ ), Equation 1 reduces to:

$$A_{\text{out}} = \sum_{j=0}^{N-1} X_j e^{\frac{i\pi j}{2}}$$

This means that the real and imaginary parts of the exponential term have values of only plus one, zero, or minus one. By limiting the DFT to these conditions the processor is simplified and its operation consists of either adding or subtracting the data sample to either the real accumulator or the imaginary accumulator. For example of a single data channel for the first data sample ( $j=0$ ), the cosine term equals plus one, the sine term equals zero, the data sample is added to the cosine register and the sine register is left alone. For the second data sample ( $j=1$ ), the cosine term equals zero, the sine term equals plus one, the cosine register is left alone and the data sample is added to the sine register. Similarly for data samples 3 and 4, the data samples are subtracted from the appropriate registers.

Figure 17 shows a mechanization of the DFP. It consists of 30 registers, a parallel adder, and an exclusive OR gate. The purpose of the exclusive OR gate is to complement the data whenever a subtraction is indicated by the reference signal. The two's complement of the data is completed by adding a one to the least significant bit of the data. The 30 registers are grouped in two sets, 15 registers for the cosine accumulators and 15 registers for the sine accumulators. Data are shifted through the registers in parallel so that the input data sample from one of 15 input channels is either added or subtracted to the appropriate bin. The data input rate and the shift rate of the registers are set at 16 times the sample frequency. One clock pulse is inhibited, since there are only 15 data channels. The reset pulse occurs every 1/2 second. This sets the integration time of the accumulators and sets the filter width at 2 Hz. Before the reset pulse occurs, data are transferred to the frequency beamformer.

Figure 18 is a diagram of the DFT reference generator. Up to eight predetermined frequencies are coded in binary numbers at the input of the selector. These frequency words are sequentially selected and entered in the rate multiplier where a signal is generated whose repetition rate is exactly 16 times the sample rate. This signal is used as the clock for both the DFT and the A/D and is the input to a  $\div 16$  binary counter. The binary counter's output serves as the address for the multiplexer. The repetition rate of this signal is the sample rate. The reference signal to the DFT is 1/4 of the sample frequency and is an exact replica of the center frequency of the filter being formed.

There are 17 bits in the parallel adder and each register. This is sufficient to prevent overflow when the 8-bit input data samples are accumulated for 1/2 second at the highest sample frequency.

#### FREQUENCY BEAMFORMER

Every 1/2 second, data from the DFP are transferred into the frequency beamformer, Figure 19. Although the DFP has 17 bits, only 13 bits are passed to the beamformer. The 15 words are loaded into the recirculating registers. Data in the recirculating register are recirculated 32 times, 29 times for each of the 29 beams being formed and three times in which no beams are formed. These three times include an input channel that is passed to the output directly, two adjacent channels that are added together and passed to the output, and two terminal channels that are added together and passed to the output.

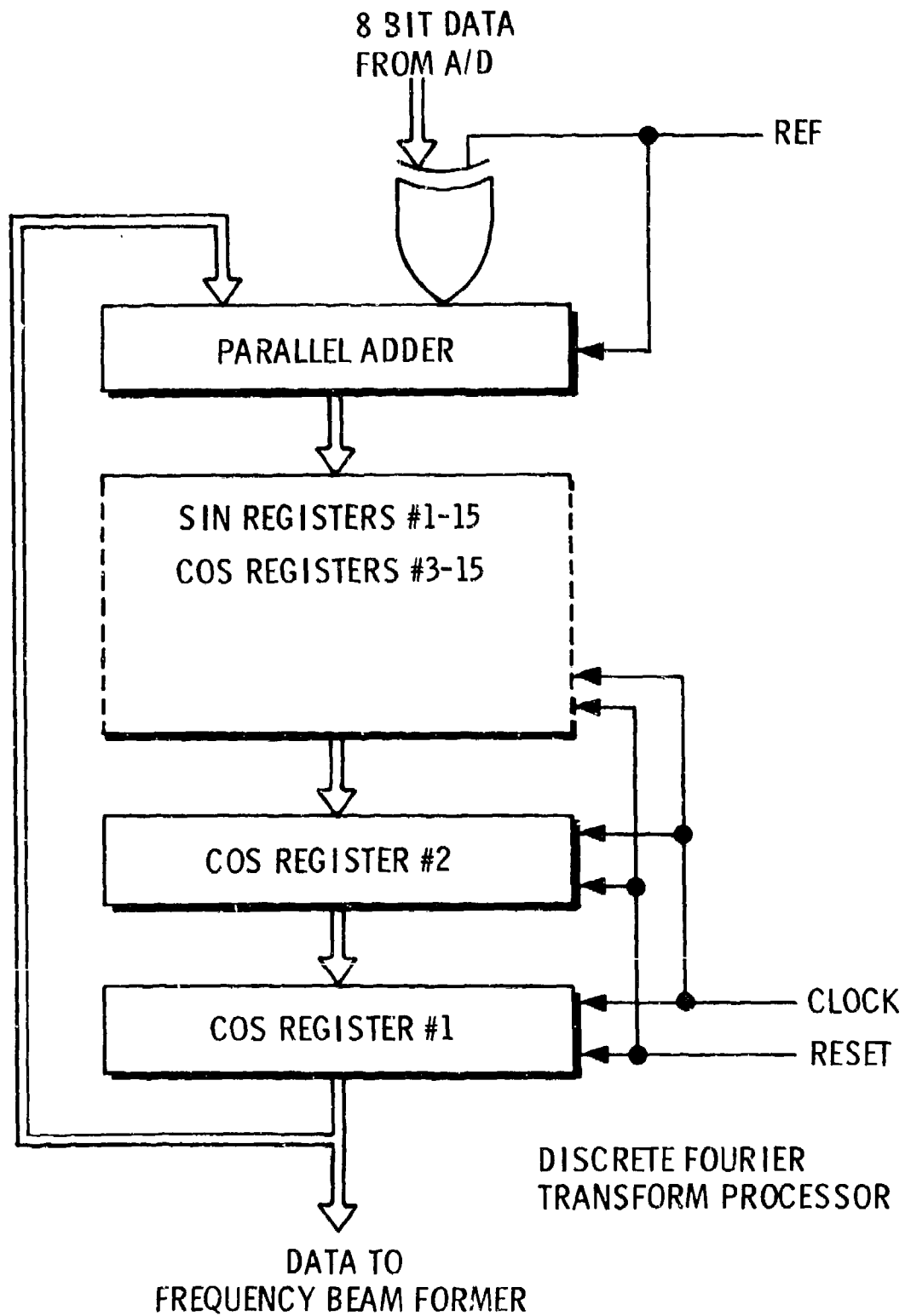


Figure 17. Discrete Fourier Transform Processor

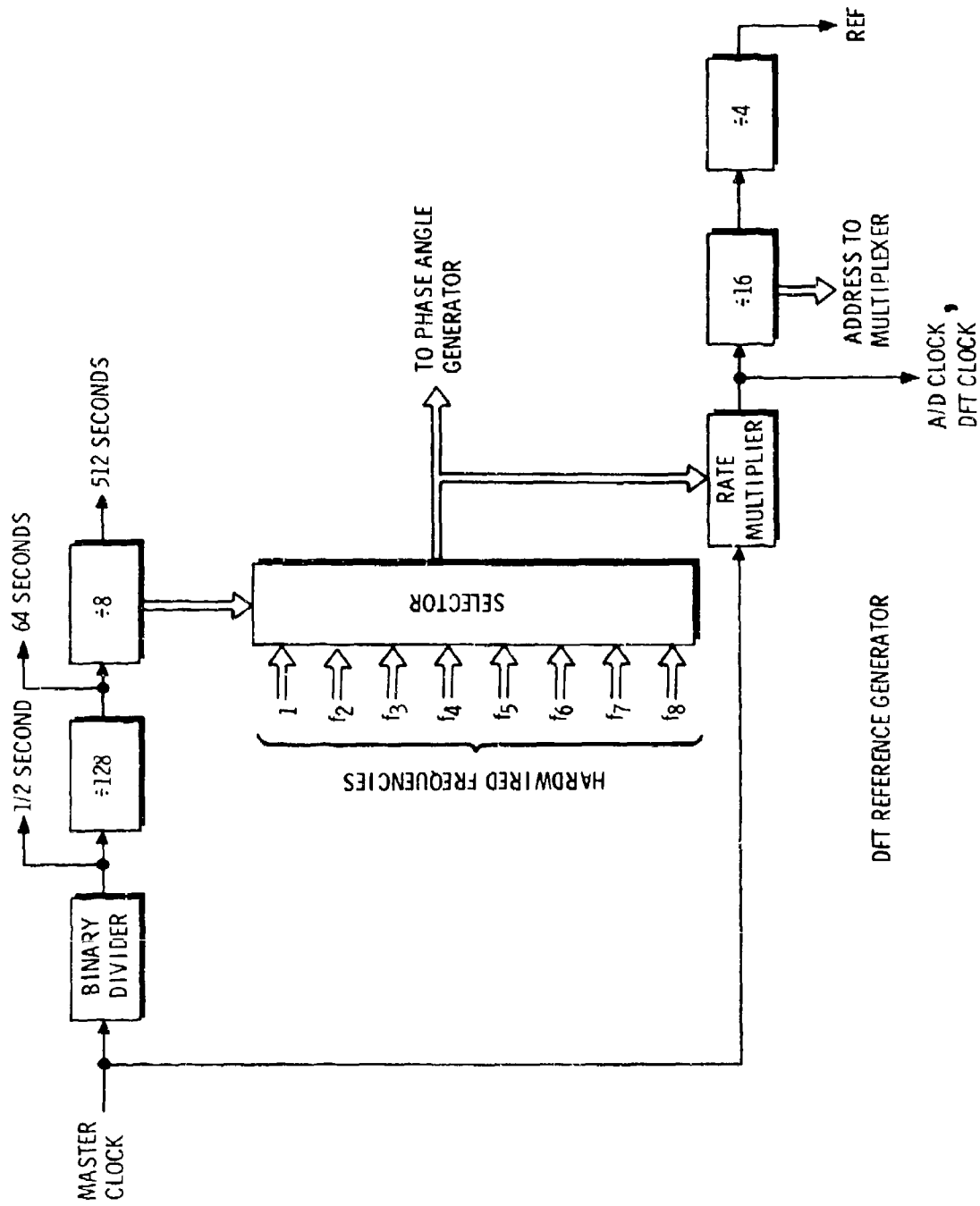


Figure 18. DFT Reference Generator

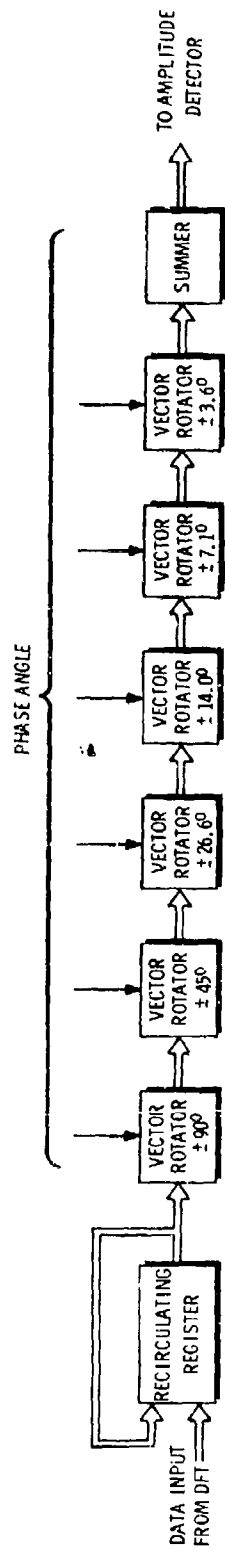


Figure 19. Frequency Beamformer

The beam displacement angles measured from broadside are proportional to the quantity  $k/16$ , where  $k$  is an integer equal to  $0, \pm 1, \pm 2 \dots \pm 14$ . Formation of these beam angles requires linear increments of delay. In addition, adjacent beams will overlap at arcsine  $(k/16 \pm 1/32)$  and beam power at overlap will be the same for all beams. The beam displacement angles are shown in Figure 20. Ambiguous beams exist at  $180^\circ - \text{arcsine } k/16$ .

In the frequency beamformer, six separate vector rotators are used to phase the incoming vectors. Operation of the vector rotators are similar except for the  $90^\circ$  rotator which interchanges the real and imaginary coefficients and complements one of these terms, depending upon the plus or minus direction dictated by the phase angle generator. Operation of the other vector rotators are based upon Equations 3 and 4:

$$A_{\text{out}} = A_{\text{in}} \pm 2^{-\ell} B_{\text{in}} \quad (3)$$

$$B_{\text{out}} = B_{\text{in}} \mp 2^{-\ell} A_{\text{in}} \quad (4)$$

where the A's and B's are the real and imaginary inputs and outputs and  $\ell$  is a fixed integer depending upon the phase shift being performed. The plus or minus operation is governed by the phase angle generator. The tangent of the phase angle is equal to  $2^{-\ell}$ . These angles are  $45^\circ, 26.6^\circ, 14^\circ, 7.1^\circ$ , and  $3.6^\circ$  for  $\ell$  equal to 0, 1, 2, 3, and 4, respectively. By using these equations all that is involved in the vector rotators is shifting and adding.

A characteristic of the vector rotator is that the magnitude of the vector is amplified at the output of each vector rotator by a factor of  $\sqrt{1+2^{-\ell}}$ . This gives a final vector amplified by about 1.64. However, since it is a fixed and known constant, it will be of no consequence.

The phase angle generator, Figure 21, accepts inputs from the DFT reference generator and computes the normalized angle through which each input vector is rotated. The normalized angle varies from  $-1/2$  to  $+1/2$ , which corresponds to actual phase displacements of  $-180^\circ$  to  $+180^\circ$ . The angle is dependent upon the product  $h \times b \times f$ , where  $h$  is the hydrophone number (0 through 14),  $b$  is the beam number (0 through 31), and  $f$  is the selected frequency. The product is formed in two parts by successive additions. The product  $b \times f$  is first formed by adding  $f$  to itself  $b$  times and then this quantity is added to itself  $h$  times to form the final product. After each addition, the phase angle generator outputs a new phase angle for the hydrophone input to the beam being formed.

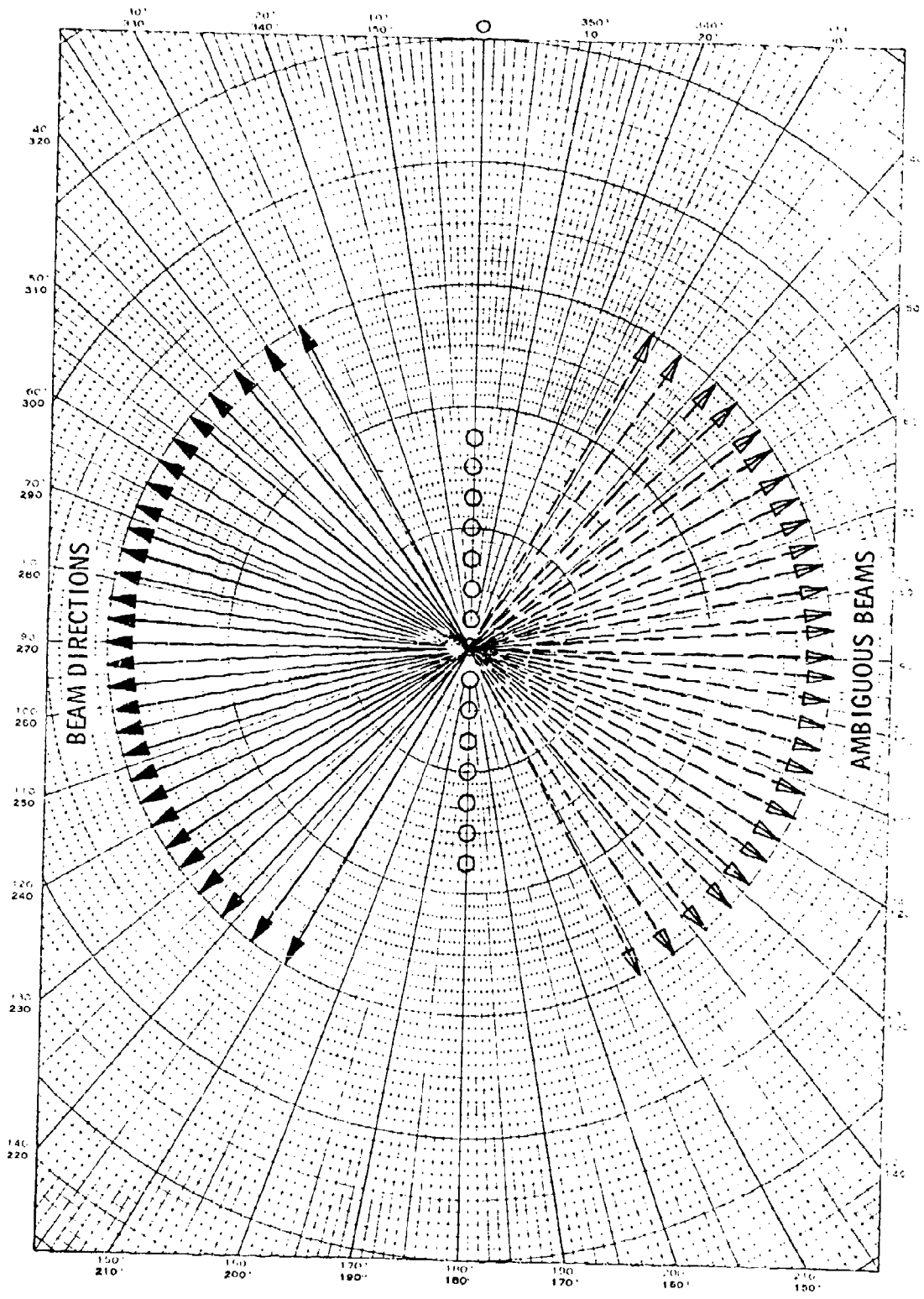


Figure 20. Beam Directions

### PHASE ANGLE GENERATOR

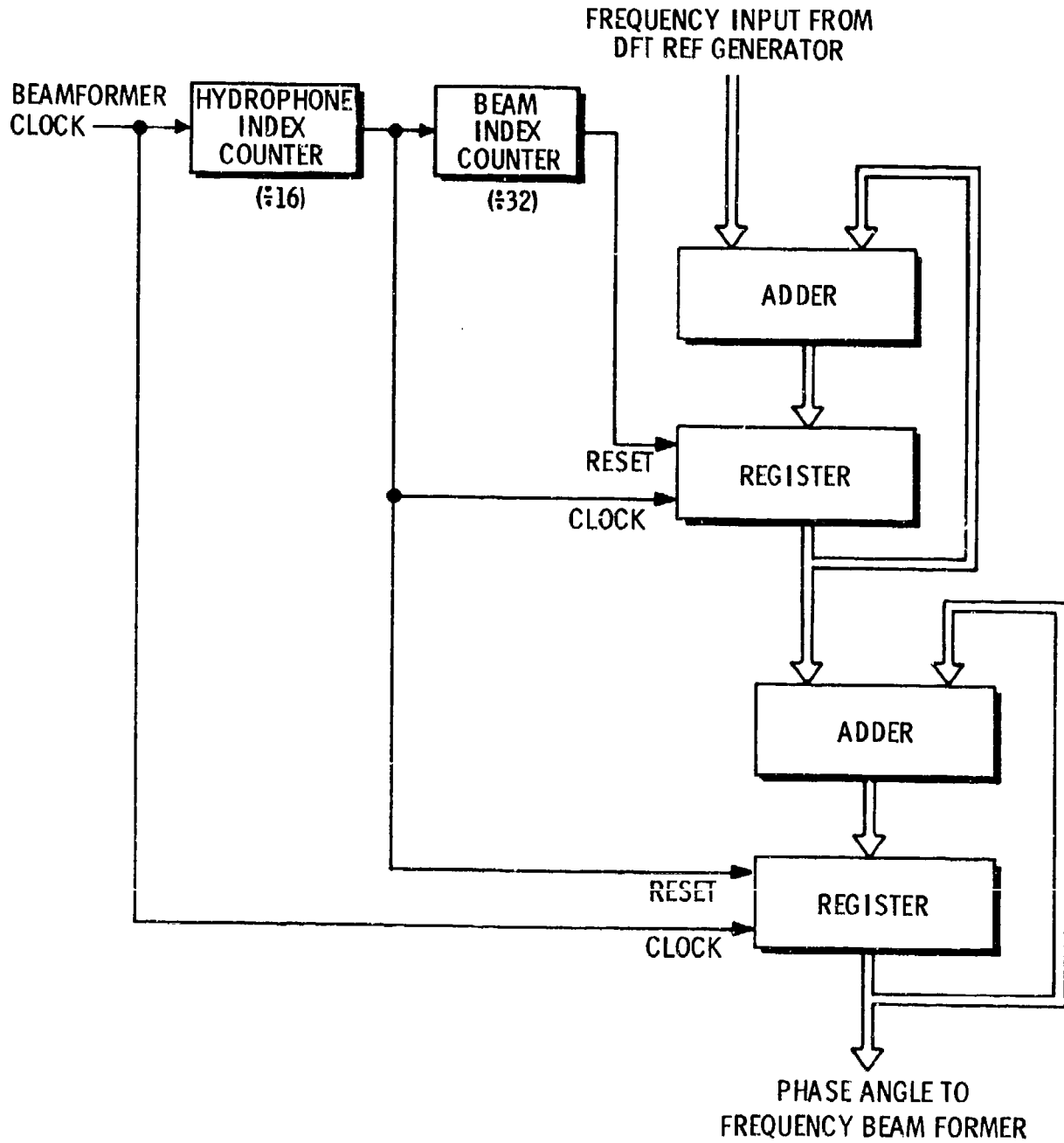


Figure 21. Phase Angle Generator

The usable output of the phase angle generator is a six-bit word whose bit weights are as follows:

- The most significant bit (MSB) indicates a phase rotation of either  $\pm 90^\circ$ .
- The next most significant bit indicates a phase rotation of  $\pm 45^\circ$ .
- The third MSB equals  $\pm 22.5^\circ$ .
- The fourth MSB equals  $\pm 11.25^\circ$ .
- The fifth MSB equals  $\pm 5.625^\circ$ .
- The least significant bit equals  $\pm 2.8125^\circ$ .

The observant reader will notice that some of these angles do not at all agree with the angles indicated in Figure 20. Table III shows a tabulation of the errors generated.

<u>Indicated Angle</u>	<u>Actual Angle</u>	<u>Error</u>
$90^\circ$	$90^\circ$	0
$45^\circ$	$45^\circ$	0
$22.5^\circ$	$26.6^\circ$	$4.1^\circ$
$11.25^\circ$	$14.0^\circ$	$2.75^\circ$
$5.625^\circ$	$7.1^\circ$	$1.48^\circ$
$2.8125^\circ$	$3.6^\circ$	$0.79^\circ$
	Maximum error	$9.12^\circ$

Table III. Phase Angle Errors

To these errors, a quantizing error of 1/2 least significant bit is added to yield a maximum error of  $10.5^\circ$  and an RMS error of  $5.4^\circ$ . Considering the lowest frequency involved and the spacing between hydrophones, the  $5.4^\circ$  phase angle will cause an error in beam centering of  $1^\circ$ . Considering the beam width at this low frequency, the  $1^\circ$  error should not be of any consequence.

The final operation in the beamformer is summing. All beams are formed in sequence with a single accumulator at the output of the device. The number of bits contained in the output register is 17; this allows for expansion of the 13-bit input words when summed over the 15 hydrophones. Of the 17, only 16 are significant and passed to the digital resolver.

## DIGITAL RESOLVER

The digital resolver, Figure 22, performs the function of a magnitude detector by generating the quantity  $\sqrt{A^2 + B^2}$ . It is based upon the same algorithm used in the vector rotators. The major difference is that, whereas the vector rotators are a group of flow-through or nonrecursive devices, the digital resolver is a recursive device. Whereas the vector rotators displace the incoming vector by a fixed angle, the digital resolver rotates the vector into the real axis. When this is done, the imaginary component is reduced to zero and the desired results lie on the real axis. Its operation is also based upon Equations 3 and 4. To form the desired quantity, the real and imaginary components are first forced into the first quadrant (both positive). Then a  $45^\circ$  rotation ( $\ell = 0$ ) takes place by a computation of Equations 3 and 4. After this is completed, the sign of the resulting imaginary component is examined to determine the direction of the next rotation ( $26.6^\circ$ ). If  $b$  is positive, a positive rotation (cw) is performed. For each computation period,  $\ell$  is incremented and a new computation is performed. Actually, about eight iteration periods are sufficient to obtain the result. Again, the final result is magnified by a factor of 1.64. Since this occurs to all beams and is known, there should be no consequences.

## POST INTEGRATOR

The post integrator, Figure 23, performs the function of temporal smoothing on all outputs of the digital resolver. The post integrator contains 32 bins (29 beam bins and three special bins). Since each 16-bit input word occurs every  $1/2$  second, each bin contains 23 bits to prevent overflow when these input words are summed over the 64 second integration period.

At the beginning of an eight minute sampling interval, the post integrator's memory is cleared of all previous results. Every  $1/2$  second, each of 32 input words are added to their respective bin. This continues for 64 seconds. At the end of this time, processing stops and the content of the post integrator memory is transferred to the incremental tape recorder.

## INCREMENTAL TAPE RECORDER

The long term storage medium selected for this application is an incremental tape recorder, Memodyne Corp. model 201. The recorder, Figure 24, is small, consumes low power and

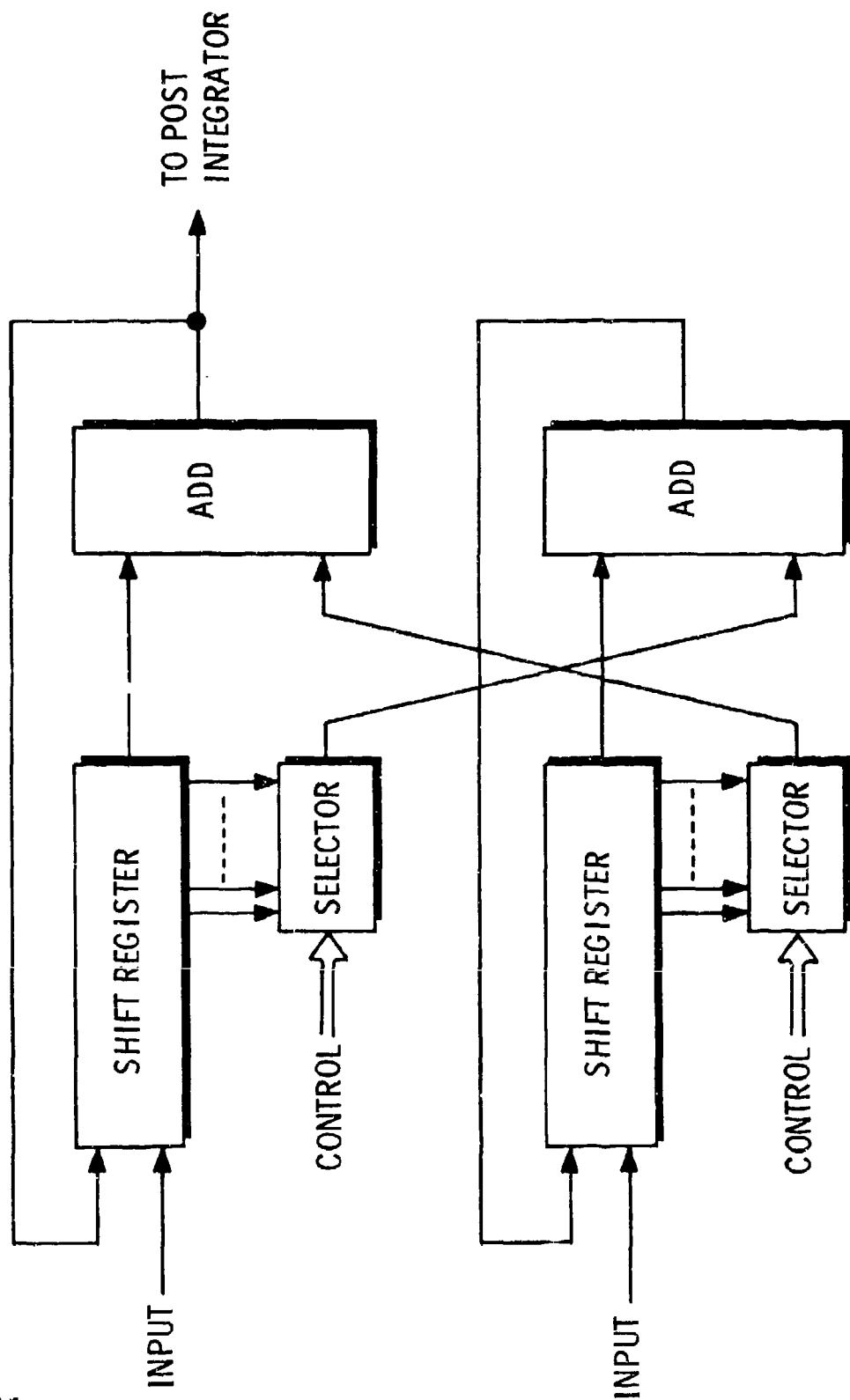


Figure 22. Digital Resolver

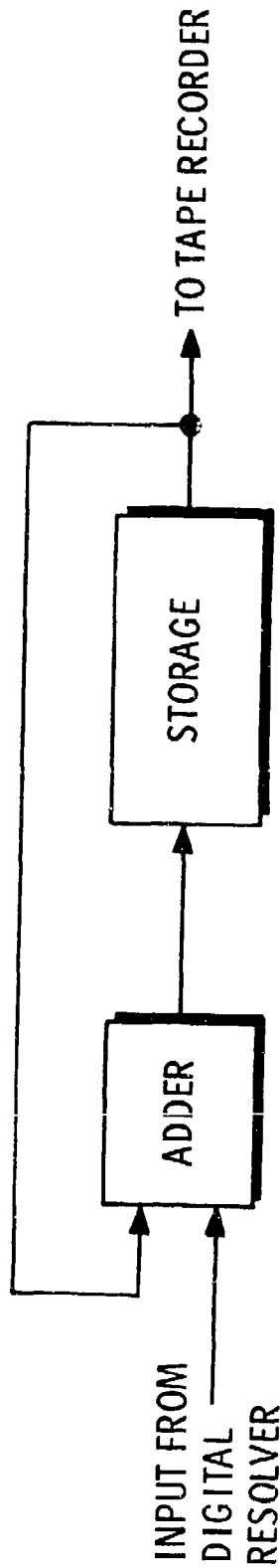


Figure 23. Post Integrator

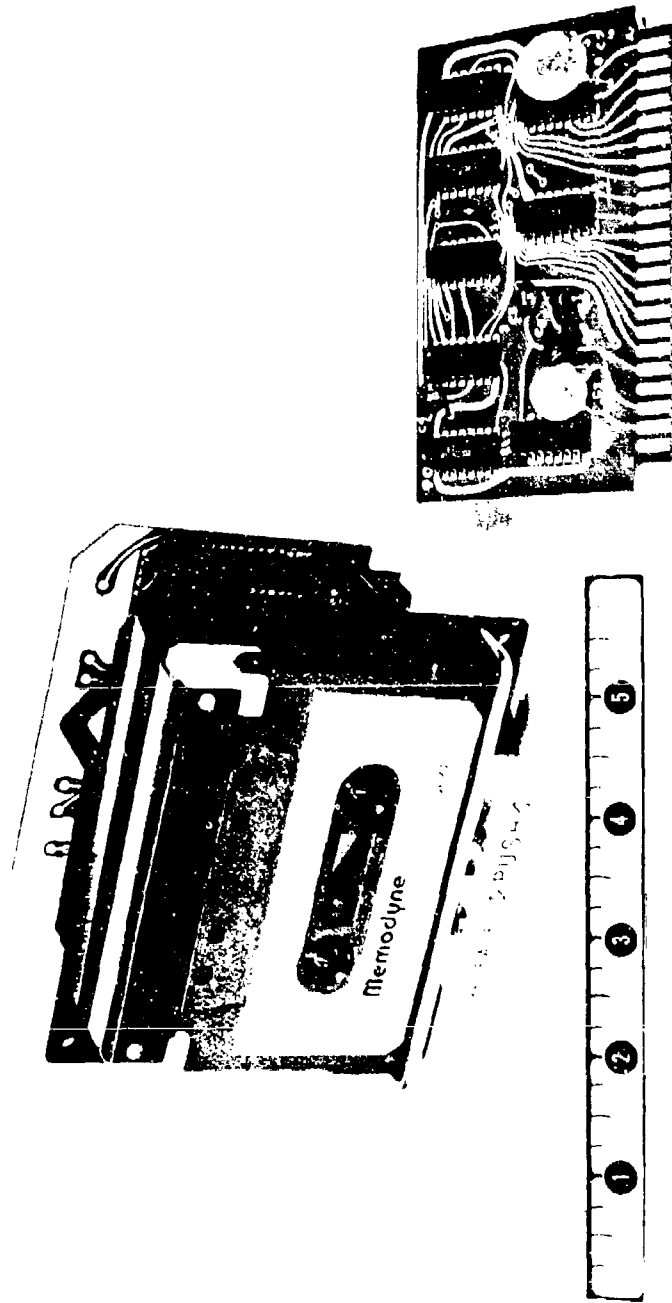


Figure 24 Recorder

has a high storage capacity. Its size is less than 64 cubic inches, permitting it to be easily contained within the BAND electronic package.

The manufacturer's specifications for maximum power consumption is 0.65 watt under continuous operation. In the interrupted mode of operation of the BAND processor, the average power for the recorder will be less than 0.01 watt. Based upon a 20-day operating period, the total power consumed will be less than 4.8 watt hours.

The tape recorder uses a 300-foot tape cassette. With a recording density of 615 bits per inch, a total storage capacity of 2.2 million bits will be obtained. Using an 18-bit word length (16 bits data and a two bit gap), a total of 120,000 words can be recorded. Thirty-three words will compose a file, 32 data words and one end-of-file word. This permits 3600 files to be recorded. A file is recorded every eight minutes. This gives a total recording time of 20 days.

#### INPUT SIMULATOR

To facilitate in-plant tests, an input simulator would be built. The device, Figure 25, will simulate signal direction and frequency. It consists of two external tunable oscillators. The first of these simulates signal frequency and is used as the data input to a 15-stage shift register. The second oscillator controls the shift rate of the register and in this manner delays the signal to each of the 15 output taps. In this manner, signal bearing is simulated. A pseudorandom noise generator with delayed output taps is used to add uncorrelated noise to each of the 15 signals. The delay between taps from the noise source is greater than the maximum propagation delay between hydrophones; hence these noise sources will be uncorrelated. After the noise is added, the resultant signals are converted to an analog signal and entered into the processor.

The device will be fabricated with commercial grade TTL integrated circuits. Since this device is only used on the shore end, no special packaging requirements are necessary.

#### READOUT SYSTEM

To facilitate in-plant tests and to scan the data after retrieval, a readout system, Figure 26, will be used. It will be capable of viewing on a laboratory oscilloscope, one complete file at a time. One file contains the data from one eight-minute sample interval. It consists

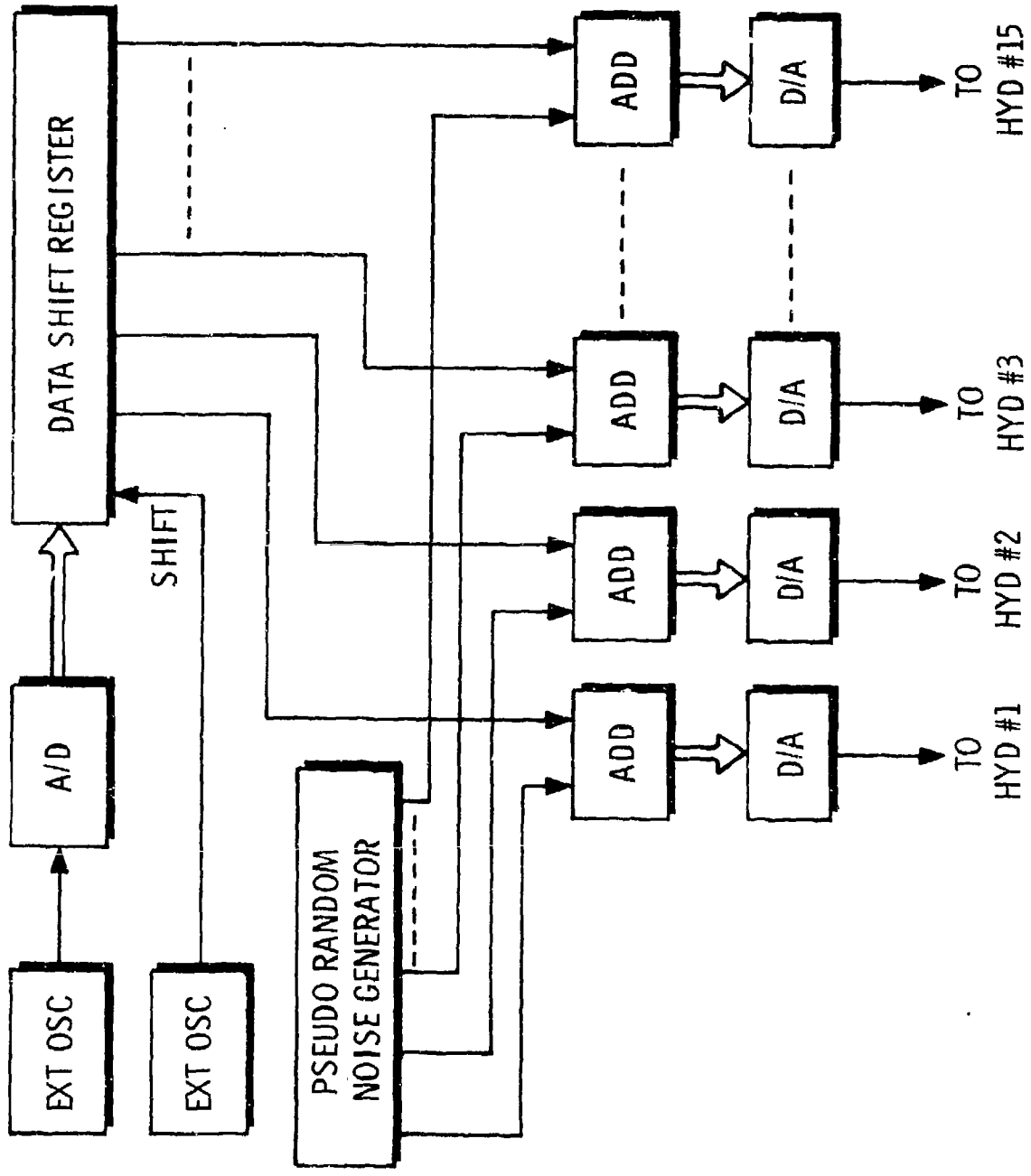


Figure 25. Simulator

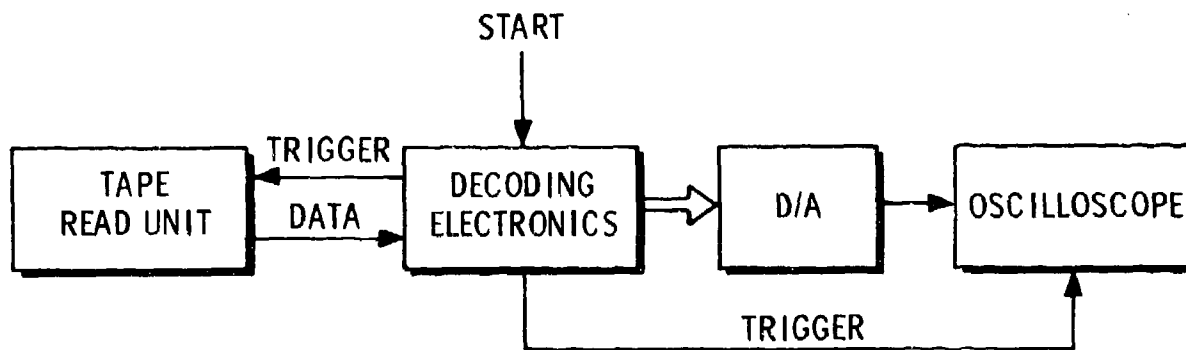


Figure 26. Readout System

of a tape readout (Memodyne Corp. model 122 read-only system, Figure 27), decode electronics, a digital-to-analog converter and an ordinary laboratory type oscilloscope. Upon initiation of the start command, the read tape transport is started and the 32 data samples are displayed as amplitude vs bearing on the oscilloscope. The start command may be initiated manually or continuously through the use of an external oscillator.

As in the case of simulation, commercial grade TTL integrated circuits will be used. No special packaging requirements are necessary.

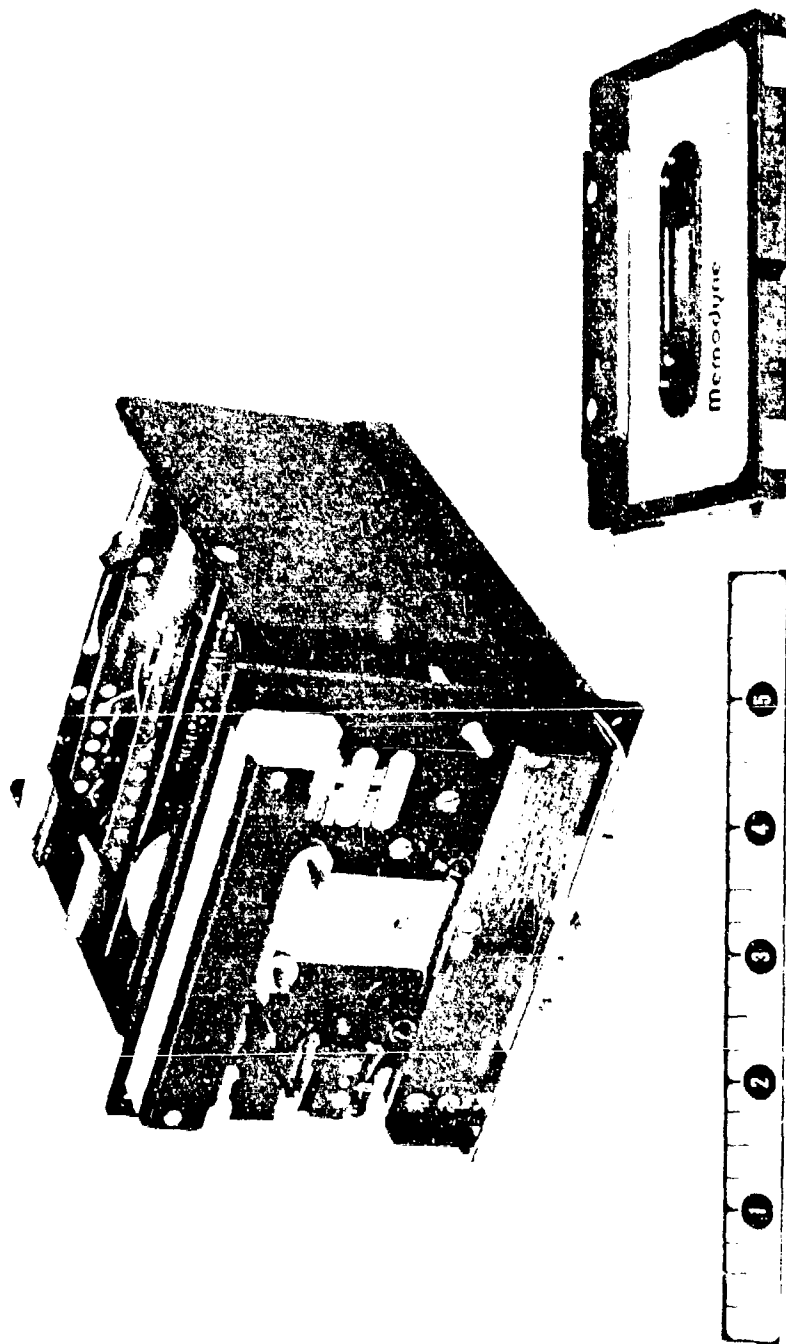


Figure 27 Tape Readout

SECTION IV  
MAJOR STRUCTURAL COMPONENTS OF THE SYSTEM

The in-water system consists of three basic assemblies:

- (1) the anchor/buoy
- (2) the electronics, processor/recorder
- (3) the acoustic array.

THE ANCHOR/BUOY ASSEMBLY (Ref. Figure 28)

The basic components of this assembly are virtually off-the-shelf, well-proven units.

The anchor is a standard cylindrical clump of cast iron connected to the buoy assembly by an oil-filled, jacketed, mechanical cable.

The buoy is structured around an acoustic release and consists of a sandwich of hollow glass spheres surrounding a central well which houses the release. The sandwich is of modular concept and can be inserted, removed, expanded, or reduced as individual layers. The spheres have been used on many programs and have a good history of reliability; they are capable of withstanding loads greater than experienced at 20,000 foot ocean depths.

In the sketch shown, two sandwich layers consisting of five and four glass spheres are concentrically sandwiched between PVC plates. During installation, the four spheres are uppermost. A stand-off ring on the base provides both a support base and a protective cage for the navigation light and the radio beacon, secured to the base plate. (NOTE: On release, the buoy inverts; hence the light and radio beacon are above the water line when the buoy surfaces.)

The acoustic release is locked to the upper and lower plates of the assembly, with the transponder extending from the top plate. The anchor cable is attached to the release clevis at the base of the acoustic release, while a limited-arc swivel connects the electronic pressure-vessel to the fixed clevis on the upper portion of the release. (A limited arc swivel is used to prevent the electronic vessel striking the transponder assembly.)

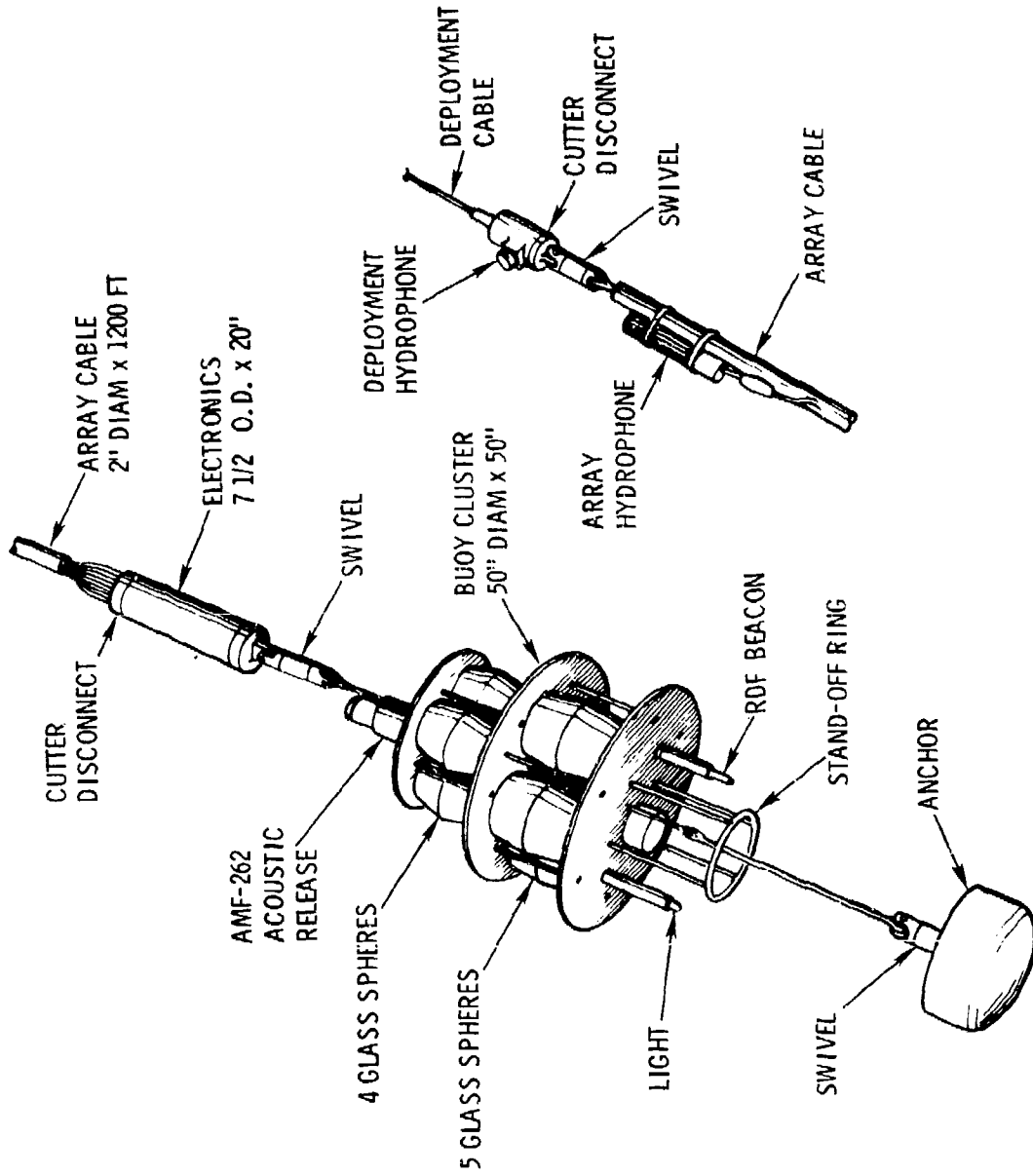


Figure 28. Anchor/Buoy Assembly

## ELECTRONIC PRESSURE VESSEL

This is a simple, cylindrical, end-capped pressure vessel. The lower end cap forms a clevis to which the buoy swivel is attached. The upper end cap is a terminator for the mechanical cable portion of the acoustic array and also a feedthrough for the electrical coaxial cables from the 29 hydrophones.

Details of these end caps are shown by Figure 29.

The design is based on redundant seals and employs oil-filled cable terminations with a pressure balancer. Glass-to-metal seals are used across the pressure bulkhead.

The cable end cap is actually a double cap wherein the outer cap is held captive to the inner cap by a ring of explosive bolts. When activated, these bolts explode and the outer end cap with the attached acoustic array is free to fall away from the inner cap.

A stand-off strain relief collar prevents the acoustic array cable from excessive bend stresses and from pull loads on the cable terminators.

The steel cable is terminated in a tapered collar and locked secure by an epoxy matrix.

The electronic assemblies and recorders are mounted on stud guides attached to the cable end cap. These components are all modular and can be easily inserted, removed, and checked. The power source is a series of 'D' cells wired and potted into cylindrical tubes which fill the interstices between the electronic blocks and the inside surface of the pressure vessel.

The BAND electronics will be housed in a tube 8" OD x 36" long. The outline is shown in Figure 30. The analog signal conditioning electronics will be mounted on printed circuit cards spaced on 0.6" centers. These preamp circuits will be housed on one card. A total of ten cards will be required. Three filter circuits will also be mounted on one card. Fifteen cards will be required. A total length of 15 inches is allocated for the analog circuits.

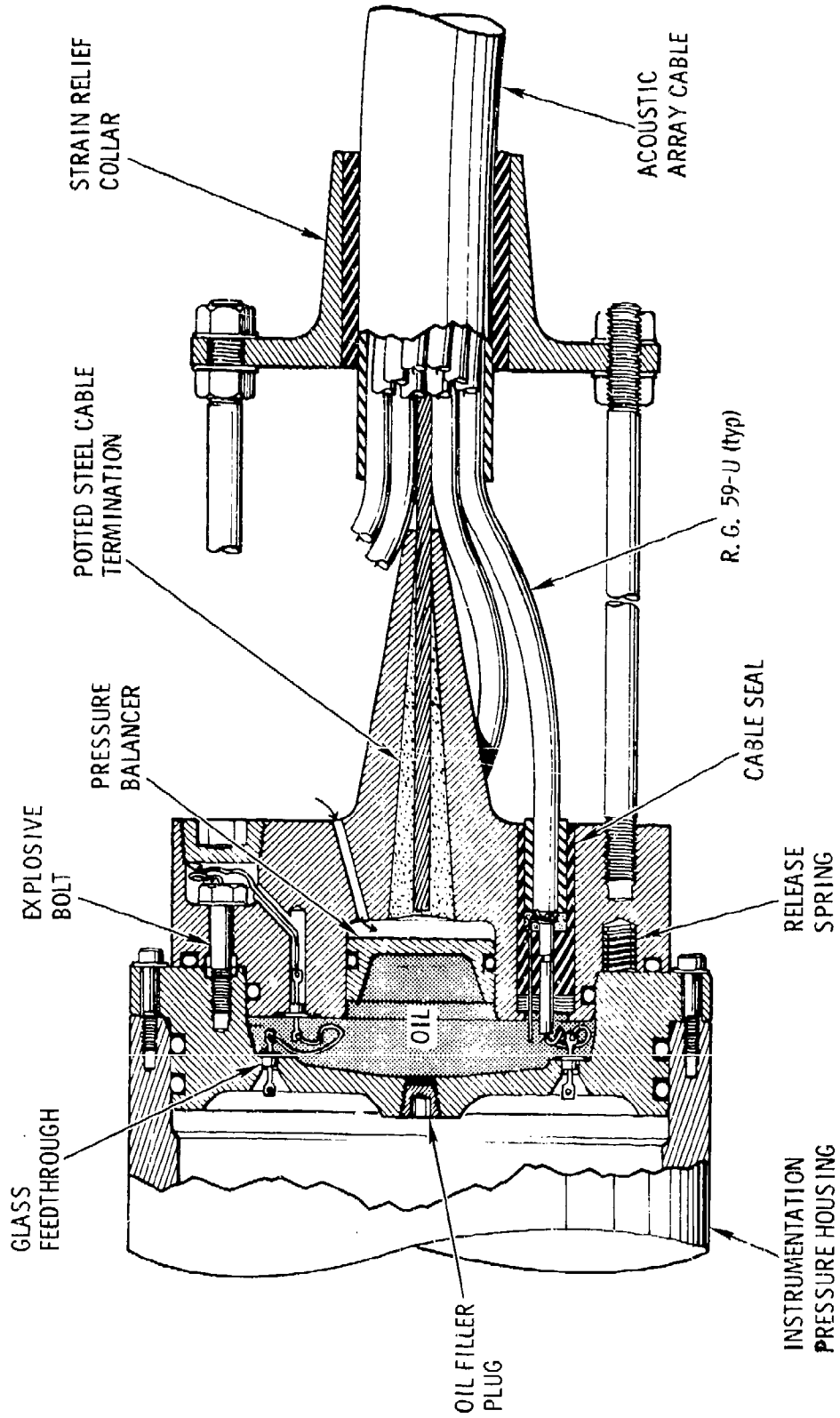


Figure 29. Pressure Vessel

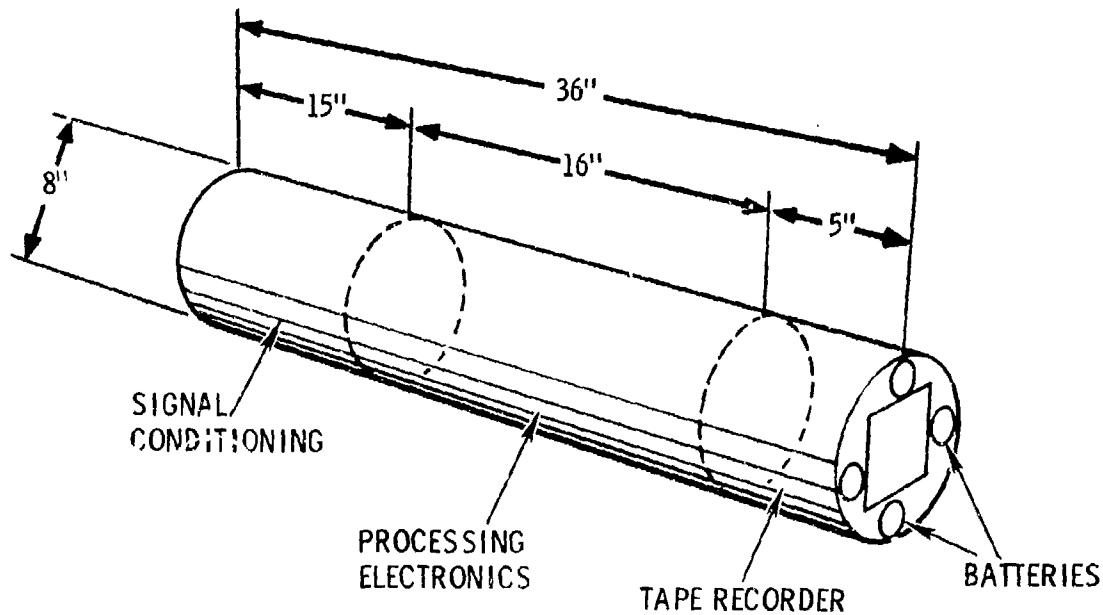


Figure 30. Electronics Package

The digital circuits will be mounted in four dual-in-time (DIP) socket carriers, Figure 31. Up to 90 circuits may be mounted in each carrier. Sixteen inches of length are allocated for the DIP socket carriers. Interconnections for the DIP sockets will be by wire wrap terminations.

The tape recorder will be mounted in the remaining five inches of length.

The "D" cell batteries will be mounted in four tubes nestled along the inside wall as shown in Figure 30.

Low power COS/MOS integrated circuit chips will be used throughout. Power consumption for these devices is proportional to the frequency of their use. Therefore, the estimate of the total power may be difficult to determine until the actual center frequencies are specified. However, a one-to-two watt power consumption estimate seems reasonable enough.

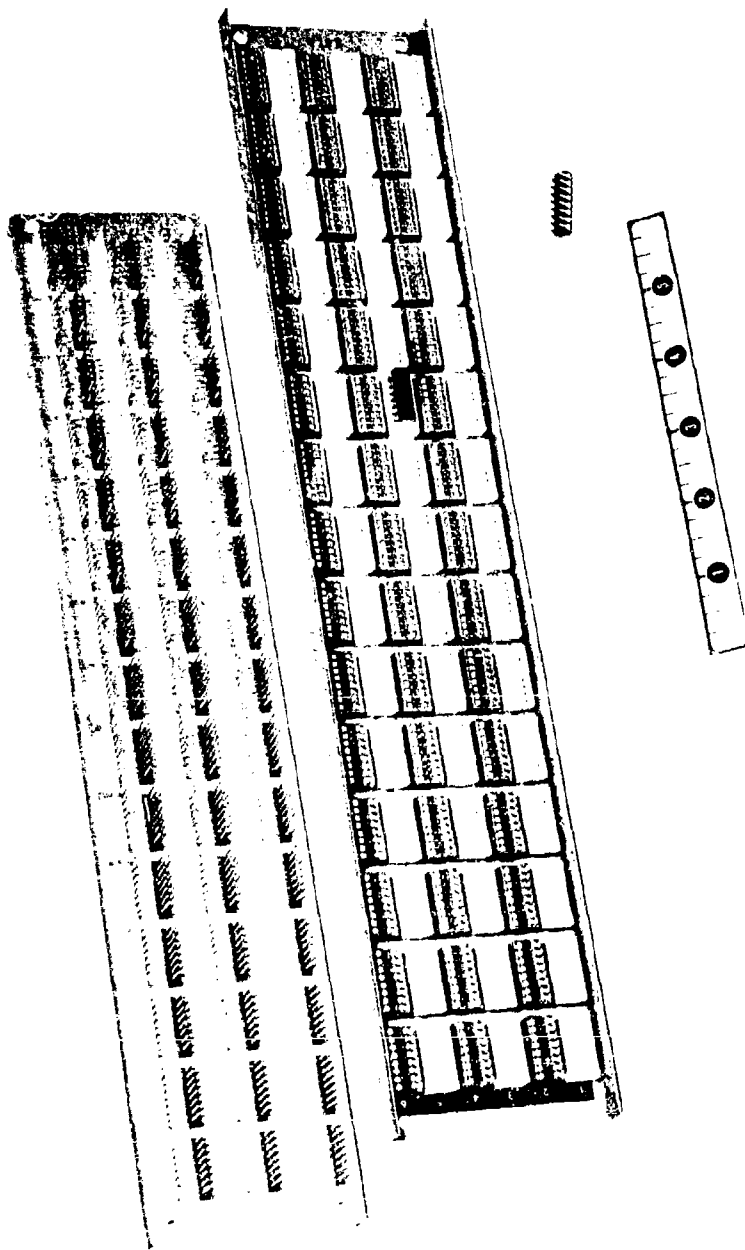


Figure 31 Digital Electronics

### THE ACOUSTIC ARRAY

The array is a 29-element string which forms, by electronic selection, three 15-element arrays. Figure 32 shows the configuration of the cable. The array is constructed around concentric layers of RG-59-U coaxial conductors. Each layer is individually jacketed with high density polyethylene. As shown, there is a total of 35 conductors which includes six spares.

The array cable, then, is a continuous length with two diameters. The outer diameter (approximately two inches) contains 18 breakouts and forms all of the connections to the elements of array No. 1 and part of array No. 2. The inner diameter (approximately 1.5 inch) contains eleven breakouts and forms the connections to the remainder of the elements of array No. 2 plus all of array No. 3.

The breakouts are made by cutting through the jacket to the requisite conductor; cutting that conductor and peeling it back about 12 inches; and placing a dummy replacement of 12 inches back into the gap created by peeling back the conductor. This portion is re-molded to provide a continuous shape and a strengthening of the breakout. A typical section is shown by Figure 32.

The hydrophone is a modular design consisting of four cylindrical elements mounted in parallel stacked between rubber end caps. A rubber boot encloses the ceramics and is filled with castor oil. Connections are made through glass-to-metal seals in the end cap. This assembly is supported on three struts suspended between two cable clamp-ons. A second boot is clamped between the cable clampons and its cavity is also filled with castor oil. The coaxial breakout from the array cable is connected to the glass-to-metal seals through a Morrison seal in the clamp-on. The assembly is illustrated by Figure 33 (Ref. Dwg. R00219).

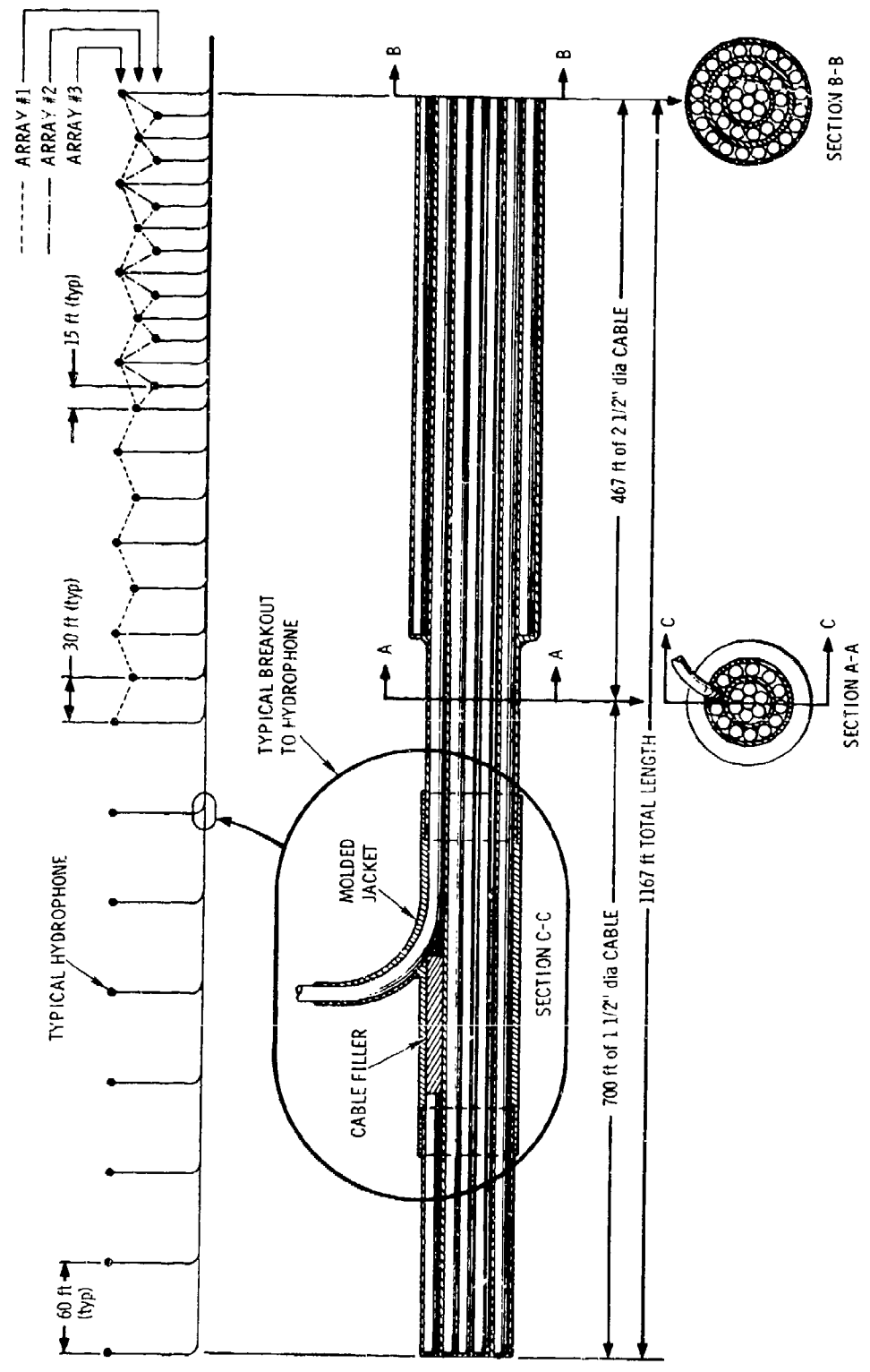


Figure 32. Cable Configuration

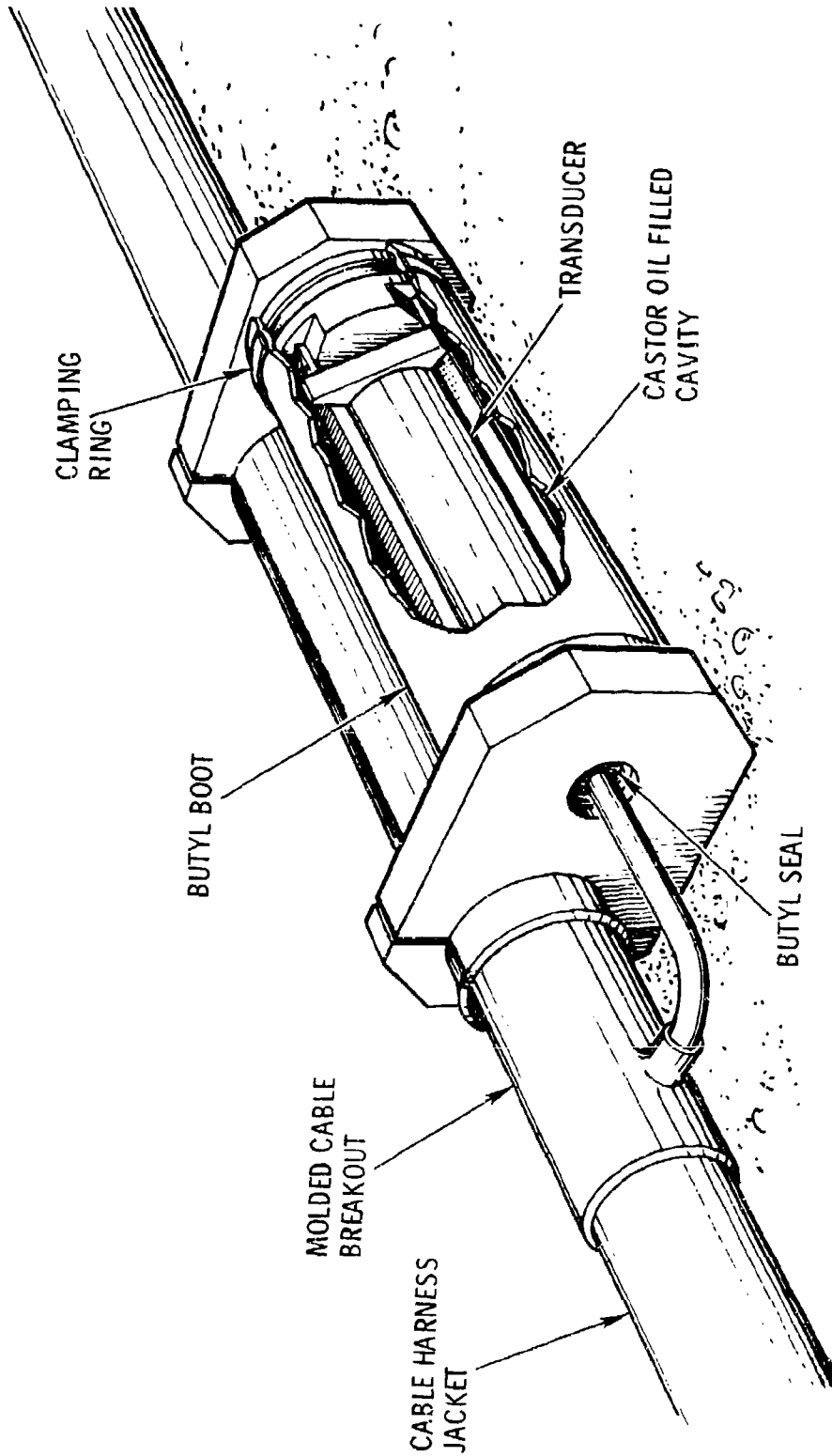


Figure 33. Clamp-on Assembly

## SECTION V TESTS

Tests were conducted to check the feasibility of the deployment systems. These tests were followed by explosive disconnect simulations for the array. Tests were also conducted on some of the major electronic components and subassemblies.

### DEPLOYMENT SYSTEMS

Two systems of deployment were analyzed and designed (with interchangeable components), Figures 34 and 35. These systems were built and assembled. In both cases, pingers were designed to be attached to each end of the simulated array to assist in tracking the system during deployment in the SCARF tracking range. These pingers were successfully pressure-tested, while operating, at the equivalent depth of 4300 ft for 72 hours before use.

The deployment systems were checked in the SCARF range at a depth of 4000 ft over a two-day period. Both systems showed that the concepts are feasible. Some components of the design had to be further investigated to improve performance (e. g., in the swing-away system the paravane/buoy needed redesigning to slow its descent compared to the main anchor). With the vertical implantment, a further test, using the free-fall bale concept, was scheduled.

The first attempt at the swing-away system showed a bottom separation of the array as 640 ft and a direction error of  $21^{\circ}$ . The impact point was 330 yd from the designed designated coordinates.

In the first attempt at the vertical implantment, bottom separation was 720 ft (after straightening out the array from a free implant of 420 ft) and the direction error  $27^{\circ}$ . The impact point was 56 yd from the designated coordinates. (Note: The directional error was approximately the same in each case and was probably due to an excessively high current, 0.4 knots, running at the time of deployment.)

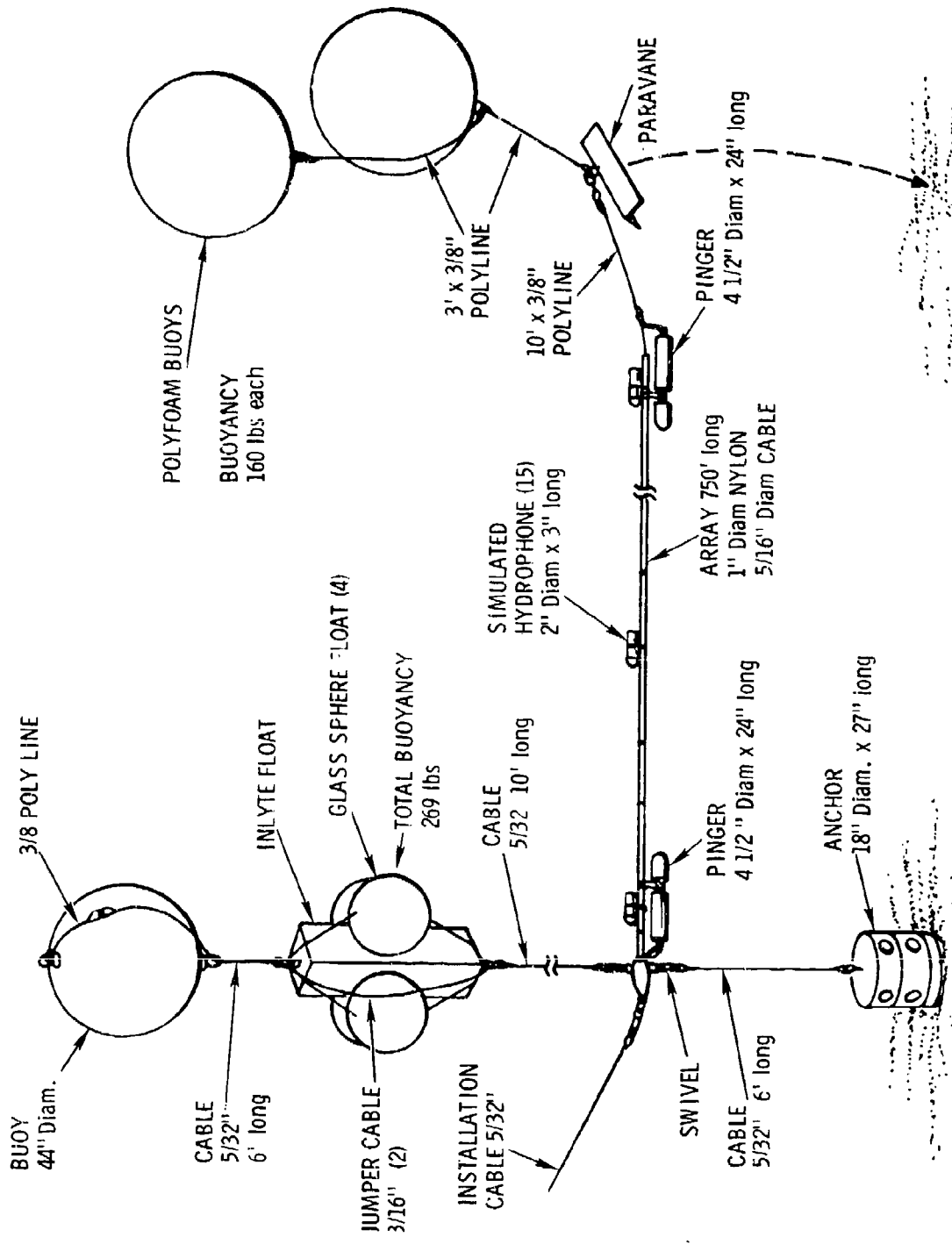


Figure 34. BAND Swing-In System

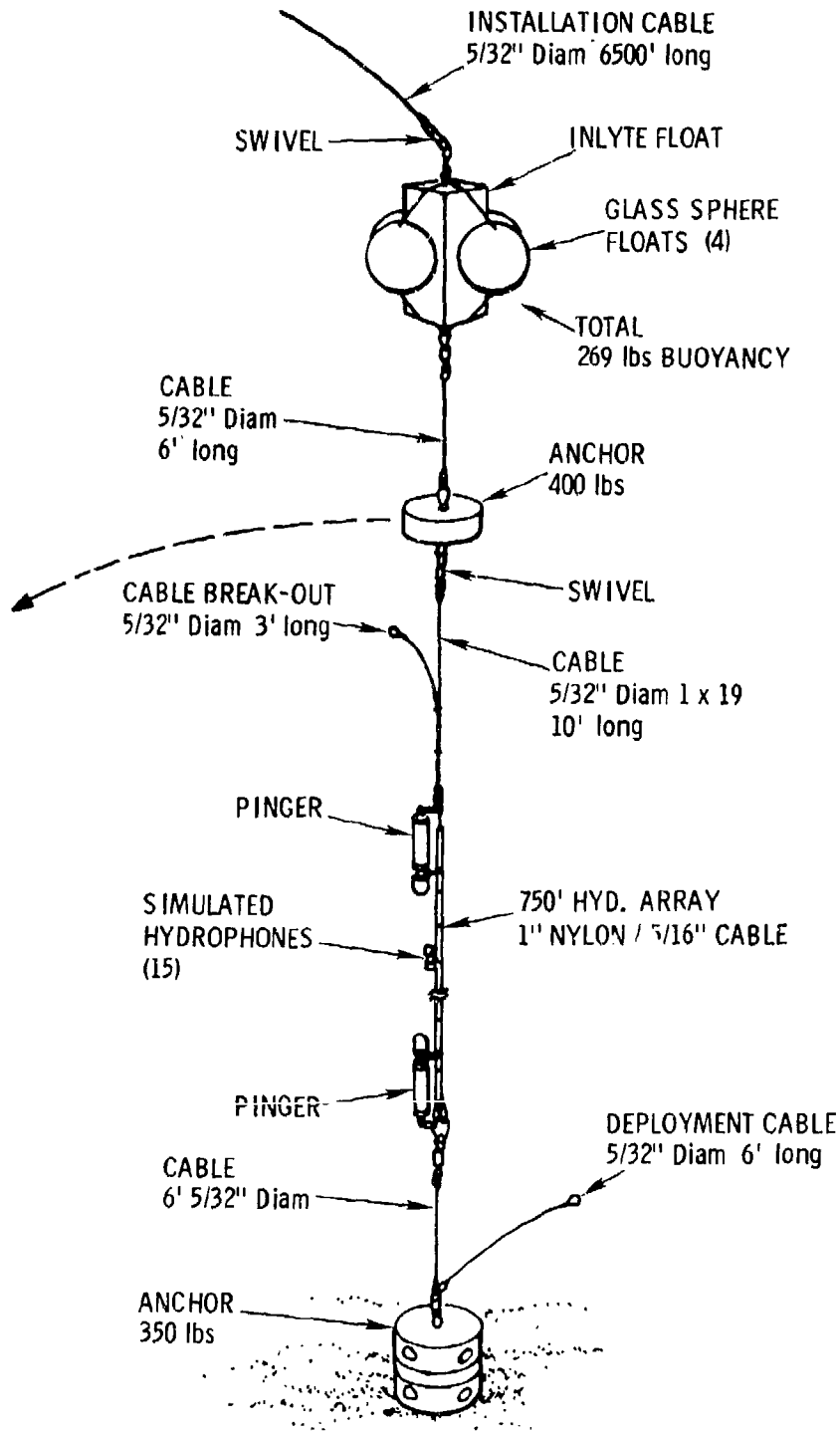


Figure 35. BAND Vertical Implantation

A second test of the deployment systems was conducted at SCARF. In the first test of the swing-away system, it was concluded that the rear hydrophone struck an escarpment before the forward hydrophone struck the sea bed. In the second test, the deployment run was reversed (i. e., going from deep water into shallow water) such that the hydrophone could not hit any projections. To prevent the rear hydrophone accelerating past the forward hydrophone, the collapsable polyform buoys were replaced with a rigid syntactic foam float. This test resulted in the array finally stretched out the full 720 ft with a bearing error of only  $4^{\circ}$ . The impact point, however, was 1200 ft from its designated coordinates.

The second test of the "lay-in" system was similar to the first test. The deployment cable, however, was too light to form the catenaries quickly enough to fully stretch out the array after the leading pinger struck sea bed. In this case, the array separation was 600 ft and the bearing error  $9^{\circ}$ . The impact point was 250 ft from the target. By relifting the forward pinger, the bearing error was reduced to  $1/2^{\circ}$ ; however, time prevented further maneuvering to fully stretch out the array.

Figures 36 and 37 show the xy plots of the pingers and the SWAN during the deployment.

In summary, feasibility of the deployment system has been shown; however, it must be remembered that ideal conditions existed in deployment tests (i. e., flat seas, little wind forces, and the use of an acoustic tracking range to direct ship movement during implantment). None of these conditions is liable to exist in deep ocean. With the "swing-in" system, at deeper depths, a long quantity of cable must be stretched out and buoyed along the sea surface before it is deployed. Even in moderate seas, the chances of maintaining a straight line are slim. Also the drop must be activated from the ship and with distributed buoys this would require multiple releases.

The lay-in system is the preferred technique, particularly employing a heavier deployment cable and a "catenary-former" anchor. The system is applicable to a "free-fall" system, wherein the cable container now becomes the "catenary anchor" after the cable is deployed. By using the installation method described elsewhere, the array should be readily stretched to its full potential and in close proximity to the desired bearing.

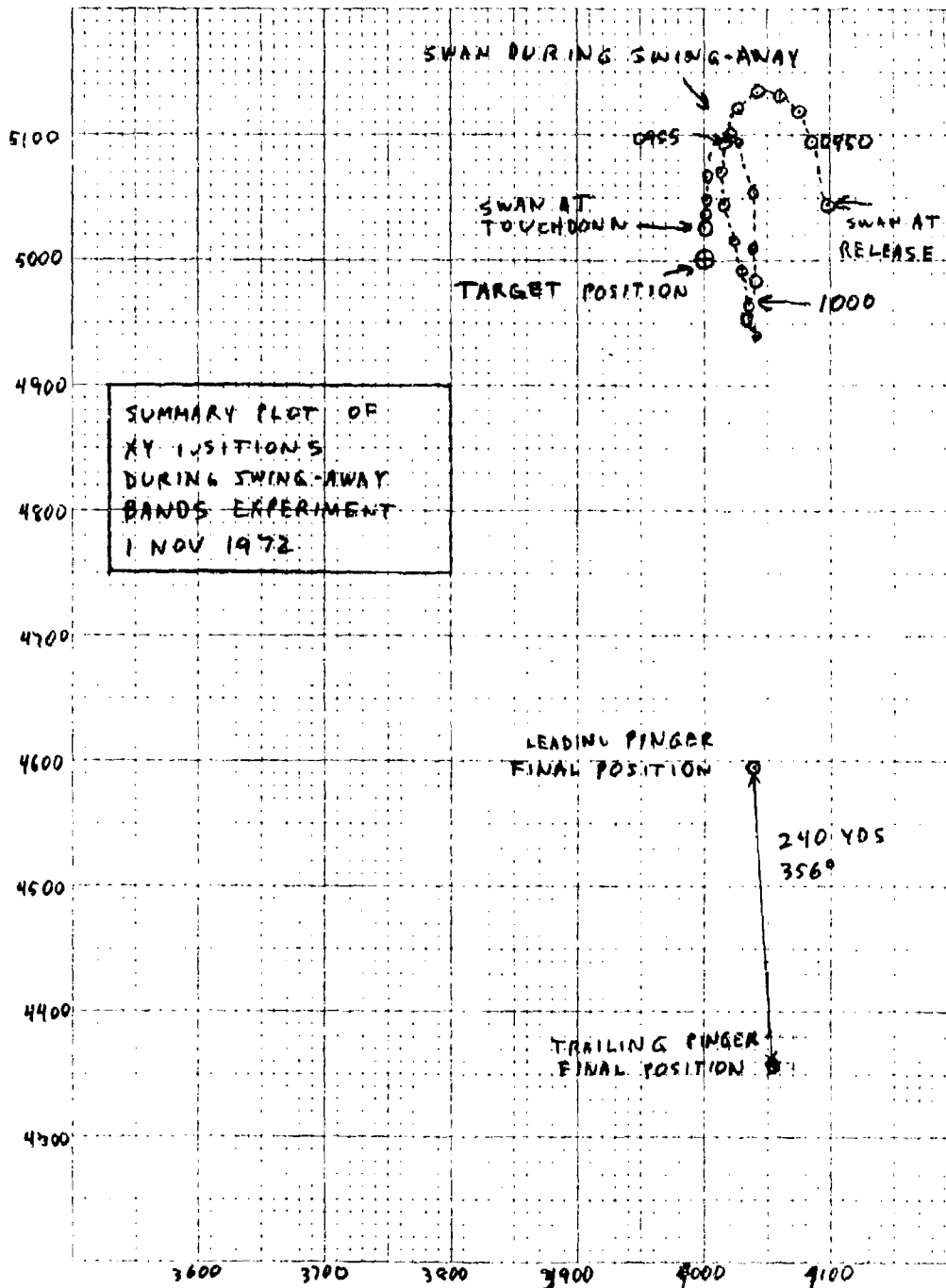


Figure 36. Summary Plot of XY Position During Swing-Away BAND Experiment, 1 Nov. 1972

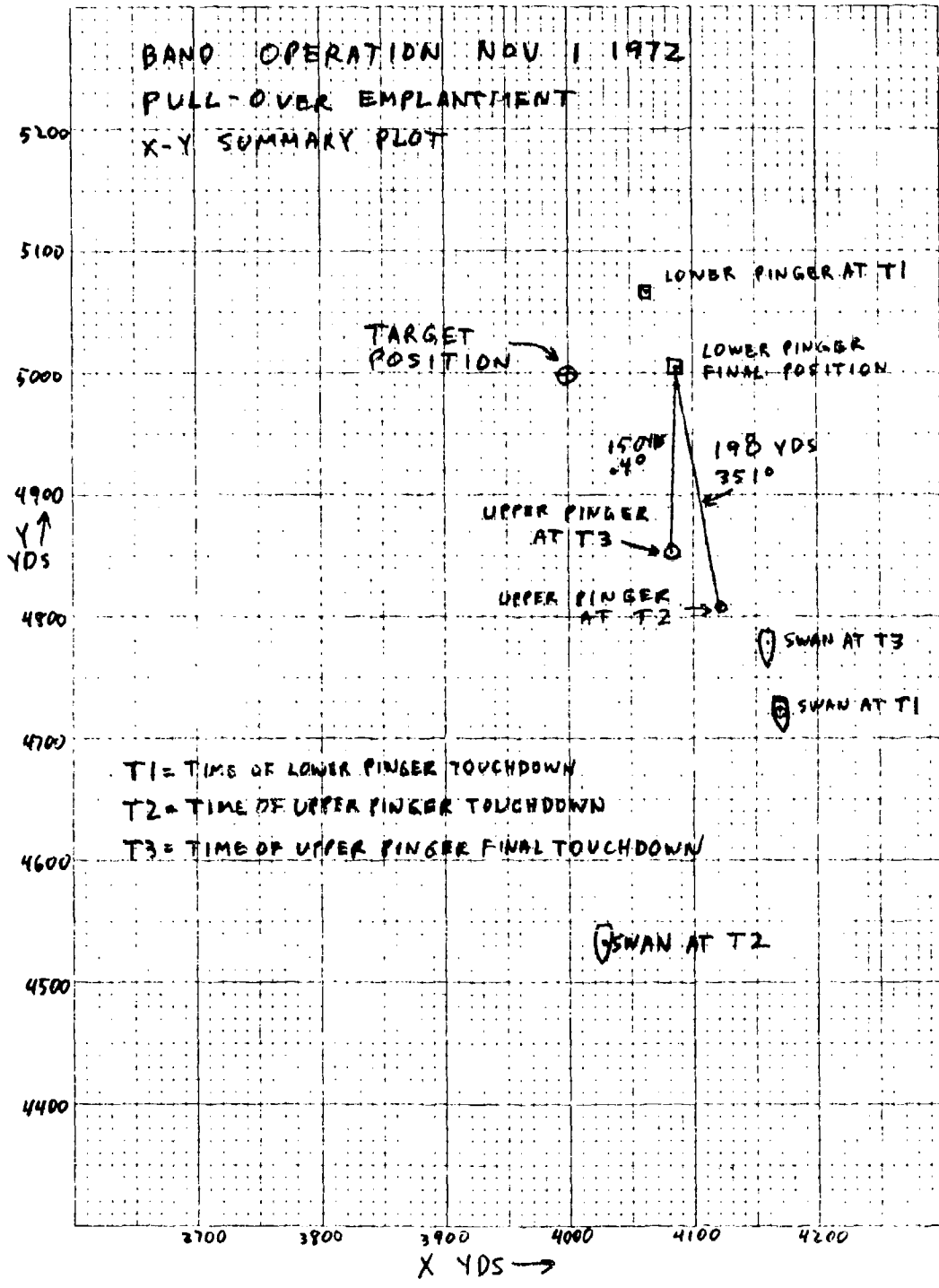


Figure 37. X-Y Summary Plot of Pull-Over BAND Emplantment, Nov 1, 1972

#### CABLE ARRAY DISCONNECT TESTS

The purpose of these tests was to prove that, in case of emergency (such as cable snagging), the total acoustic array can be jettisoned from the electronic pressure vessel. A fixture was made (see Figures 38 and 39) to test the structural strength of the electrical feed-throughs and the effect of the bolt explosions.

The structures were subjected to a static pressure of 8000 psi. The bolts were activated while the system was at 8000 psi. The structural integrity of the sealing system and the electrical feed-throughs was sound. The explosive bolts activated as expected and separation of the simulated array system was accomplished. The tests showed, however (Figure 39), that the "O" ring locating glands had been made too close to the bolts. This is not detrimental to its operation but means that for re-use, the glands would have to be re-machined. The final design allows a greater amount of metal between the glands and the bolts.

#### RECORDER TESTS

The recorder has been successfully tested at Delco at a temperature of 0°C over a 5-day continuous operating period. No defects were noted under these test conditions. Manufacturer's specifications for maximum power consumption under continuous operation is 0.65 watts. Measured value in laboratory tests was less than 0.5 watt.

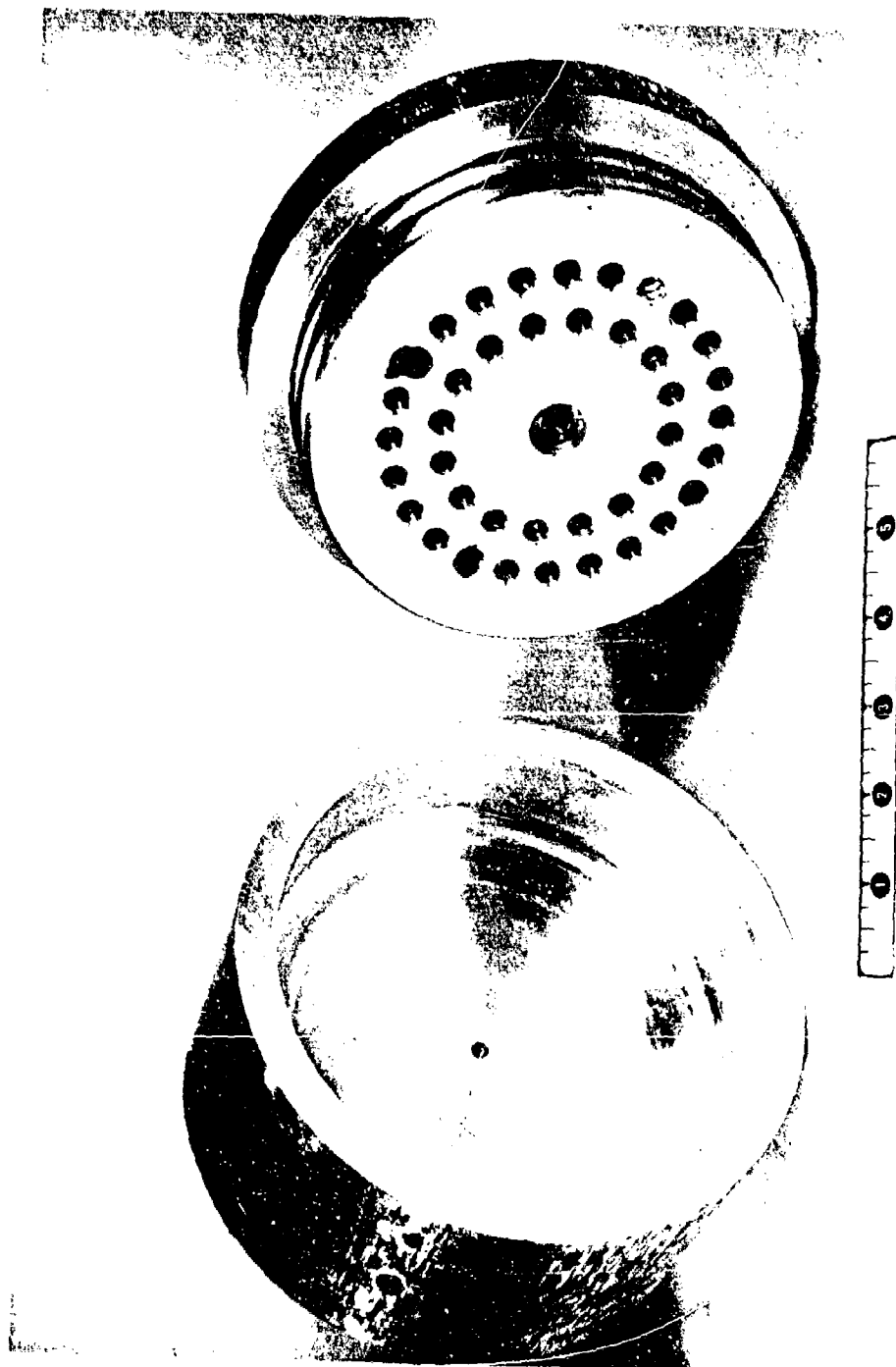


Figure 38 Test Fixture

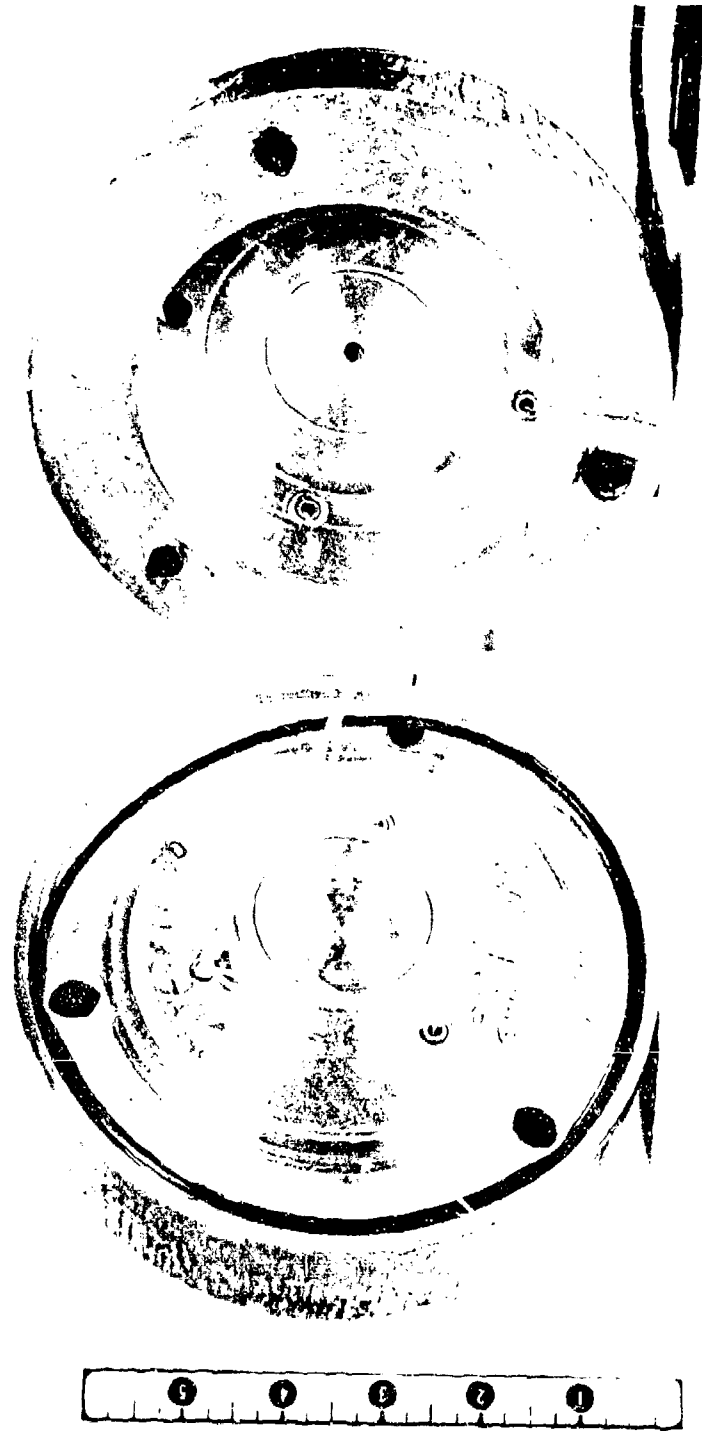


Figure 39 Test Fixture

## SECTION VI IMPLANTMENT AND RECOVERY

### THE IMPLANTMENT SYSTEM

A major factor in the array implantment is to determine the true length of the extended array. Without this knowledge, serious deviations in the final analyses can be expected. A system has been devised, utilizing components already in use in the system, to give an accurate measurement of the array length. This measurement can be made before the installation cable is disconnected.

Since the array already uses an acoustic release to separate the recovery buoy from the anchor, this unit is employed as part of the array length measurement system. Referring to Figures 40 and 41, a deployment hydrophone, electrically connected through the deployment cable to the ship, is located on the deployment cable-cutter disconnect. The AMF acoustic release is cocooned in the center of the recovery buoy cluster. The acoustic array lies between the buoy and the deployment cable cutter disconnect; this distance is accurately measured and is a short extrapolation of the actual acoustic array length.

In deployment, then, the anchor and the recovery buoy are lowered to the sea bed via the array cable and deployment cable. Bottom contact is measured by load-cell monitor. The deployment ship moves to new coordinates, reflecting the direction in which the array is to lie and the displacement needed to form an installation catenary. A secondary "catenary" anchor is strategically located on the deployment cable to provide the tangential lay of the acoustic array. Sufficient deployment cable has been paid-out during the ship transition to form the correct catenary profile. (NOTE: the recovery buoy is used as part of the array tensioning system to maintain a straight array.)

Measurement of the length of the stretched array is now made:

- 1) On board ship, the AMF transponder sends a signal to the pinger on the acoustic release; this is mark  $T_0$ .
- 2) The installation hydrophone is the first to receive this signal and it is recorded as  $T_1$ .
- 3) The acoustic release hydrophone receives the signal; this is designated  $T_2$ .

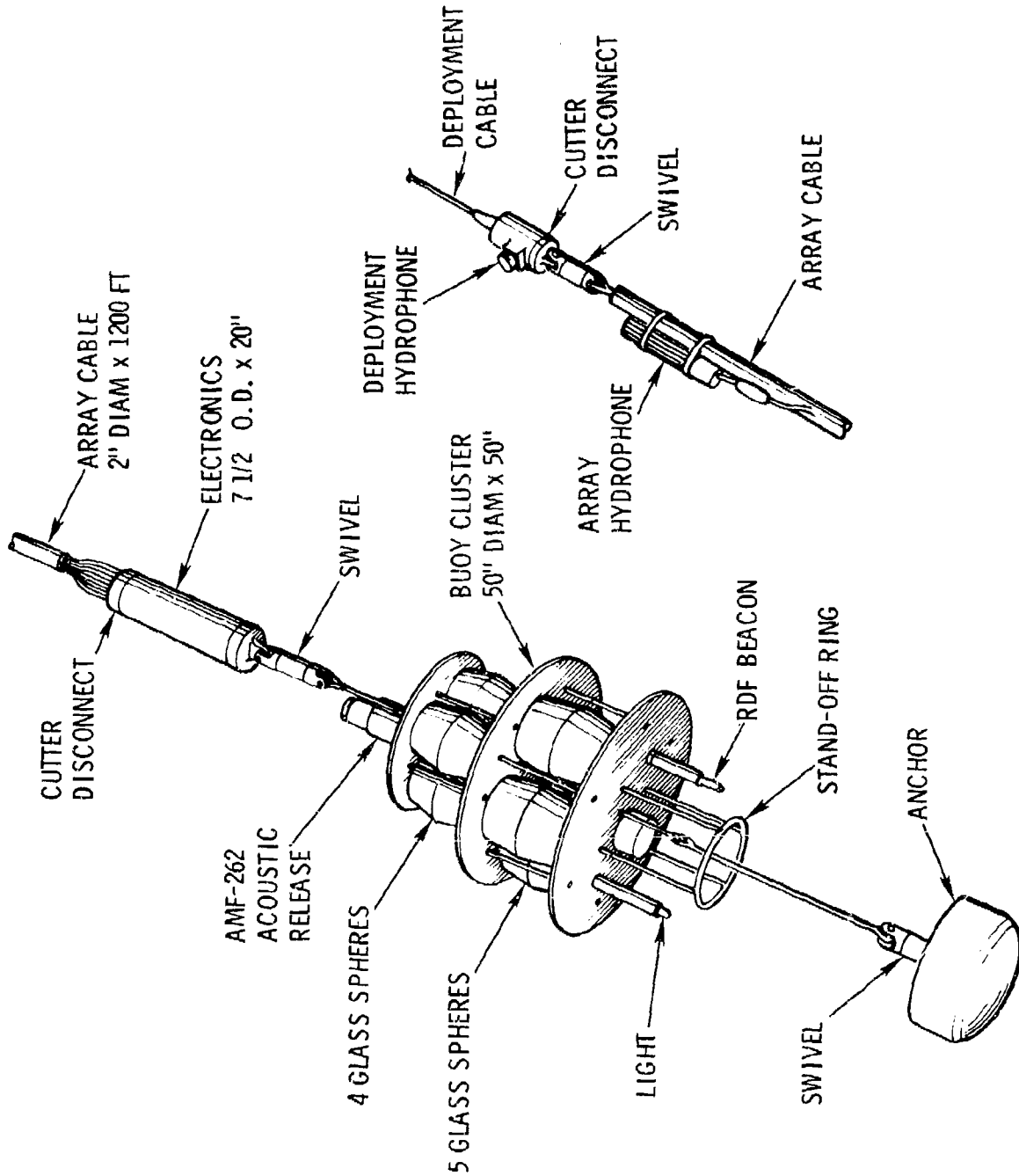


Figure 40. Anchor/Buoy Assembly

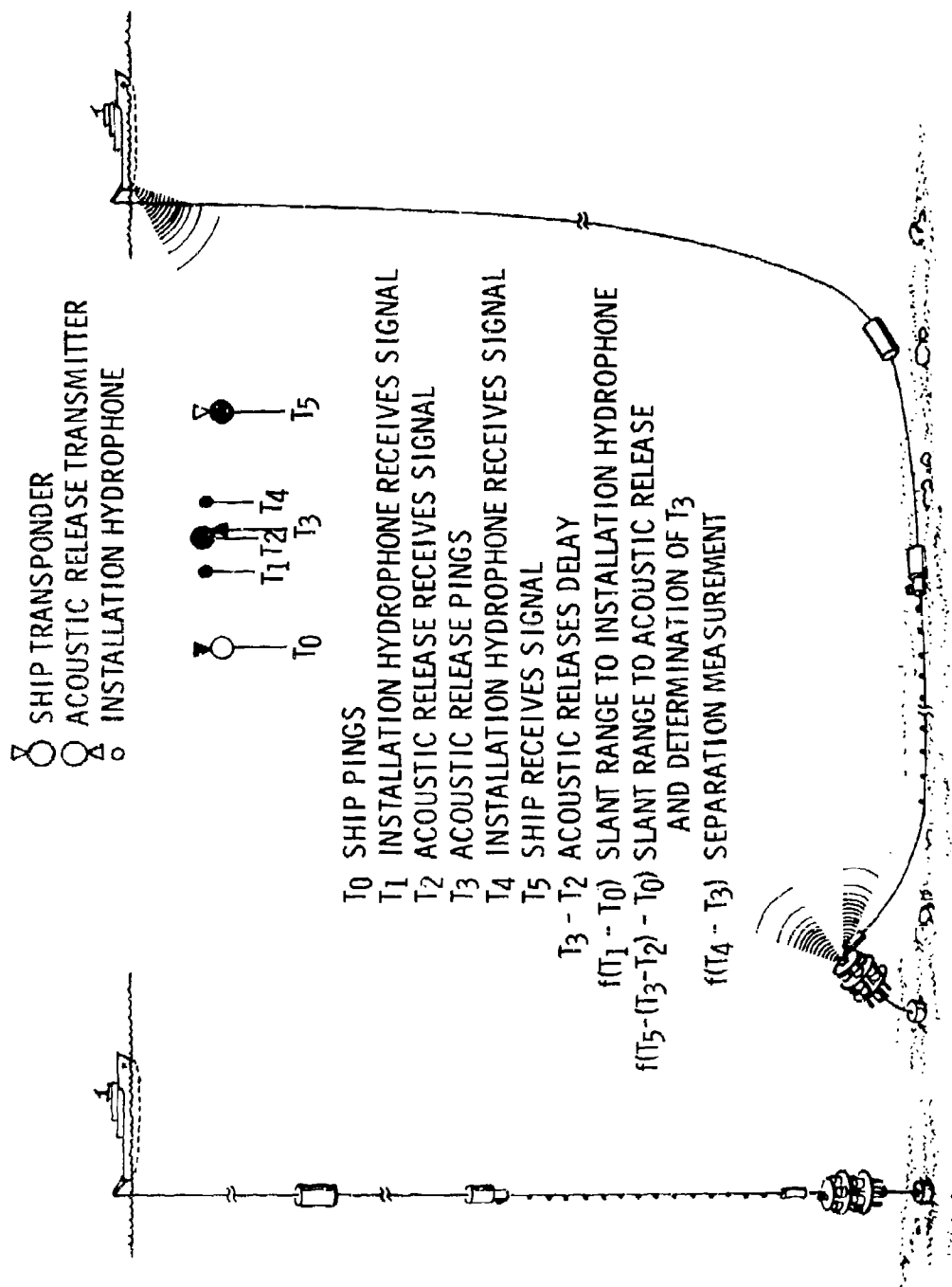


Figure 41. Implantment and Recovery System

- 4) The acoustic release pinger sends a signal activated from the incoming command; this is designated  $T_3$ .  
(Note that  $(T_3 - T_2)$  is the inherent delay in acoustic release and is already established.)
- 5) The installation hydrophone now receives the signal emitted from the acoustic release; this is recorded as  $T_4$ .
- 6) The transponder on the ship now receives the signal emitted from the acoustic release; this is recorded as  $T_5$ .

From these conditions, it is easy to calculate the time of pinger signal emission from the AMF acoustic release and the time of arrival at the deployment hydrophone.

Knowing or deducing the velocity of sound at that location and depth, a simple calculation gives the distance of separation.

At a depth of 12,000 ft the total elapsed time of the total emitted and received signals is less than 10 seconds; hence errors due to ship drift etc., are minimal (e.g., a ship drifting at 2 kts would be displaced about 30 ft; at a slant range of 15,000 ft, this is negligible).

To reposition or extend the array, the "catenary" anchor is lifted and repositioned until the desired conditions are met. The deployment cable is then disconnected from the array by firing the cutter disconnect.

#### RECOVERY SYSTEM

To recover the system, the ship uses its satellite navigation to reestablish its coordinates. From this position, the AMF transponder communicates with the acoustic release and the position of the array is established. The transponder now transmits a coded signal to activate the release. Activation of the release separates the recovery buoy from the anchor mass.

The buoy begins to rise and inverts itself into the recovery mode (see Figure 42) dragging the array behind it. At buoy inversion, a timer switch is activated (Figure 43) (note that it cannot activate until a near vertical attitude is attained) that controls the power supply to the explosive bolts securing the acoustic array to the buoy system. Should the buoy

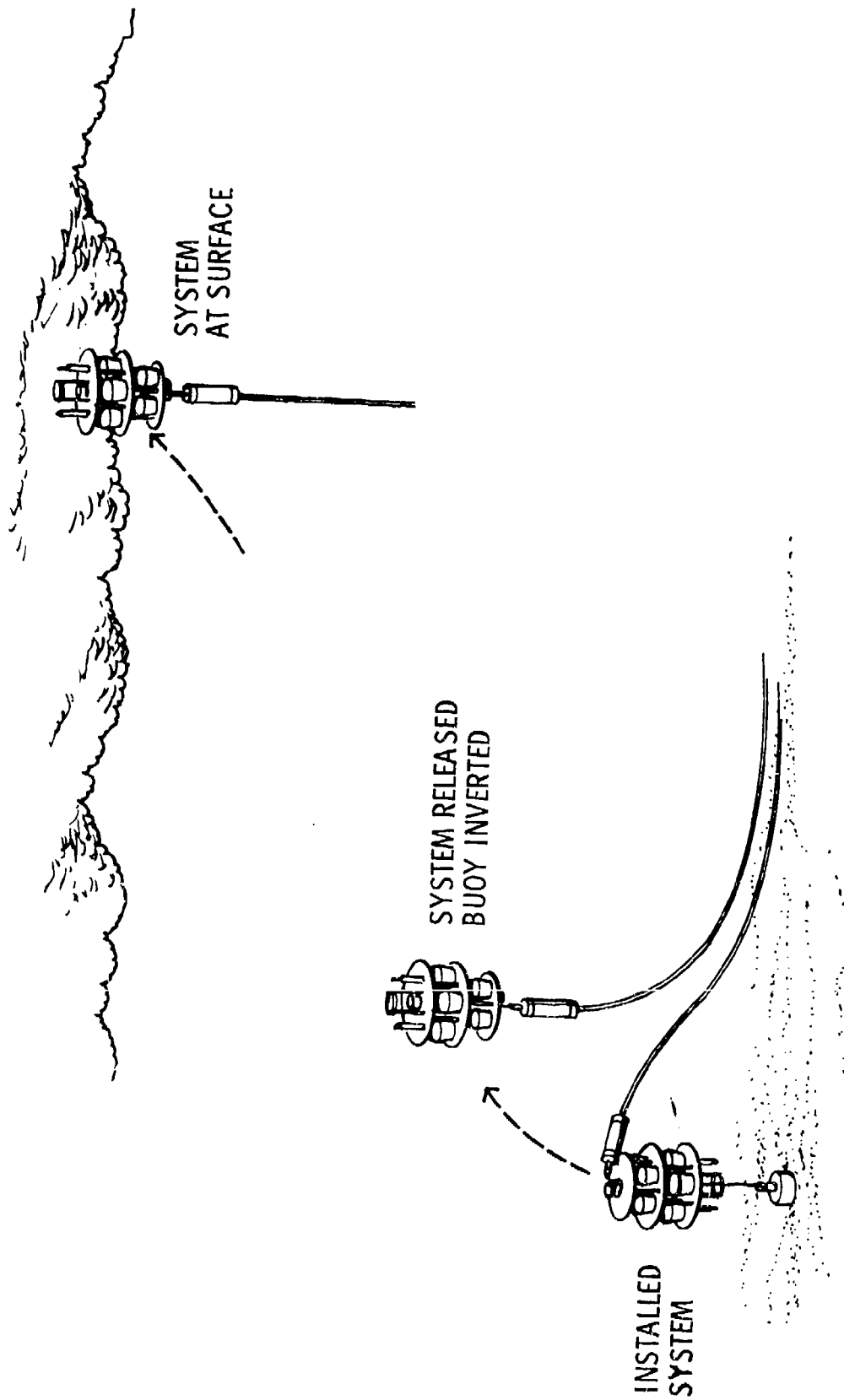


Figure 42. Recovery Sequence

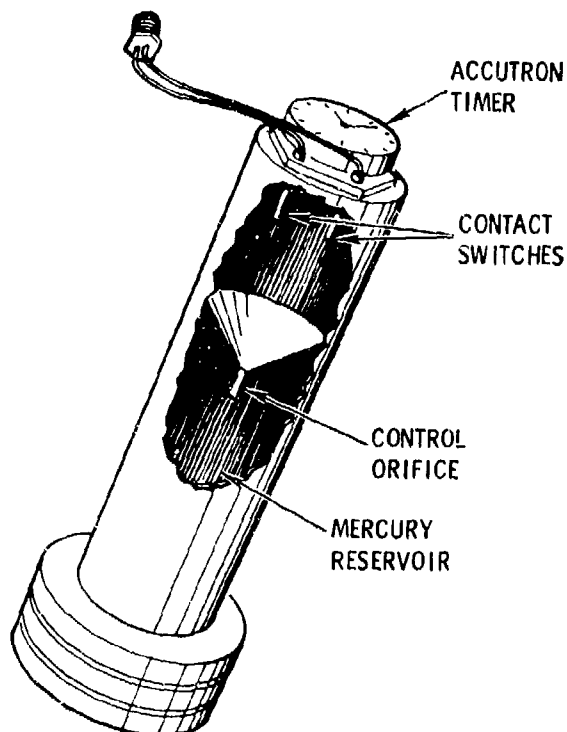


Figure 43. Timer

not be recovered in a set interval (say 4 hours), the bolts explode and the buoy with the electronics is released from the array.

This protective mode is primarily to guard against the array being snagged, hence preventing the buoy from reaching the surface.

When the buoy is recovered, it is re-inverted, thus disconnecting the timer; or the timer can be manually deactivated. The array is disconnected from the buoy system and wound onto its storage reel.

All that is required for re-use is:

- (a) replacement of the battery power supply
- (b) installation of a new cassette into the recorder
- (c) addition of a simple anchor clump.

SECTION VII  
PHASE II REQUIREMENTS AND SCHEDULES

Phase I was a design and feasibility study. Some hardware was purchased and test assemblies manufactured to check out problem areas of the design concept.

Phase II will consist of the completion of the design, fabrication, test, and assembly of the prototype unit; assistance in the sea operations; analyses of the recorded data; and publication of a final report.

Some components in the electronic package have been bought and will be applied to the prototype unit. The major purchasing still left includes the cable for the array, the hydrophones, and minor electronic components. Long lead items now remaining are the hydrophones and the array cable.

The system design has been virtually established and most assembly drawings are complete. Detail drawings for manufacture need to be made.

The major tests of components have been completed, although the system simulator must be detailed and built. Electronic bench tests and a mechanical pressure test still must be accomplished.

Schedules for Phase II are shown by Figure 44.

The sequence would be:

- (a) Ordering long-lead items
- (b) Completing details of manufacturing drawings (in conjunction with (a) )
- (c) Making and assembling the components
- (d) Bench testing and simulating test the system
- (e) Operationally testing the system in the SCARF
- (f) Refurbishment of equipment
- (g) Operationally testing the system in the deep ocean
- (h) Publishing a report on the total project.

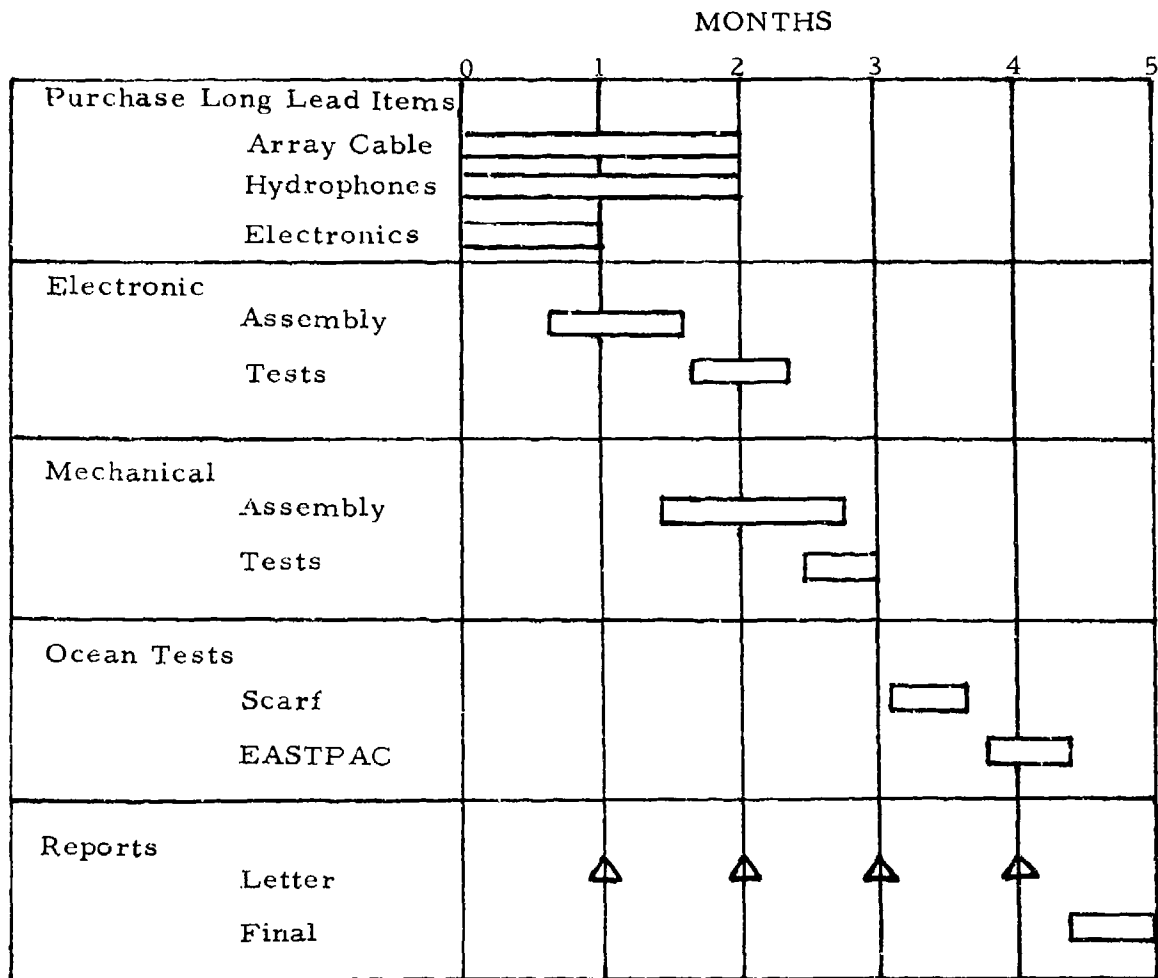


Figure 44. Phase II Schedules

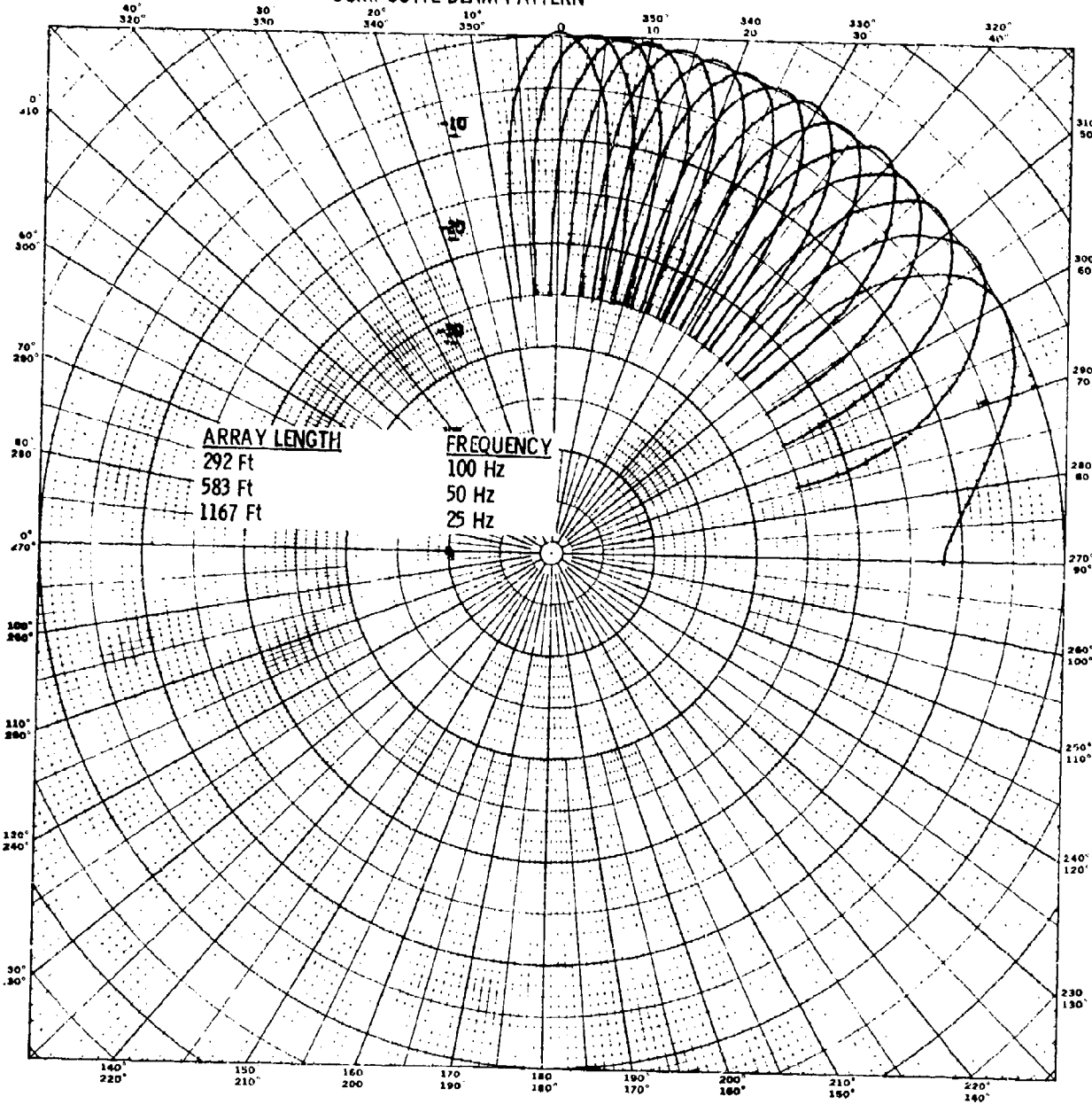
APPENDIX  
POWER BEAM PATTERNS

The appendix contains overlap plots of the main beams for various steering directions. Additionally the power beam pattern for each steering direction is plotted as a function of azimuth referenced to the array normal. For frequencies of 100, 50, and 25 Hz, see pages A-1 through A-16; for frequencies of 86.4, 43.2, and 21.6 Hz, see pages A-17 through A-32; and for frequencies of 150, 75, and 37.5 Hz, see pages A-33 through A-48.

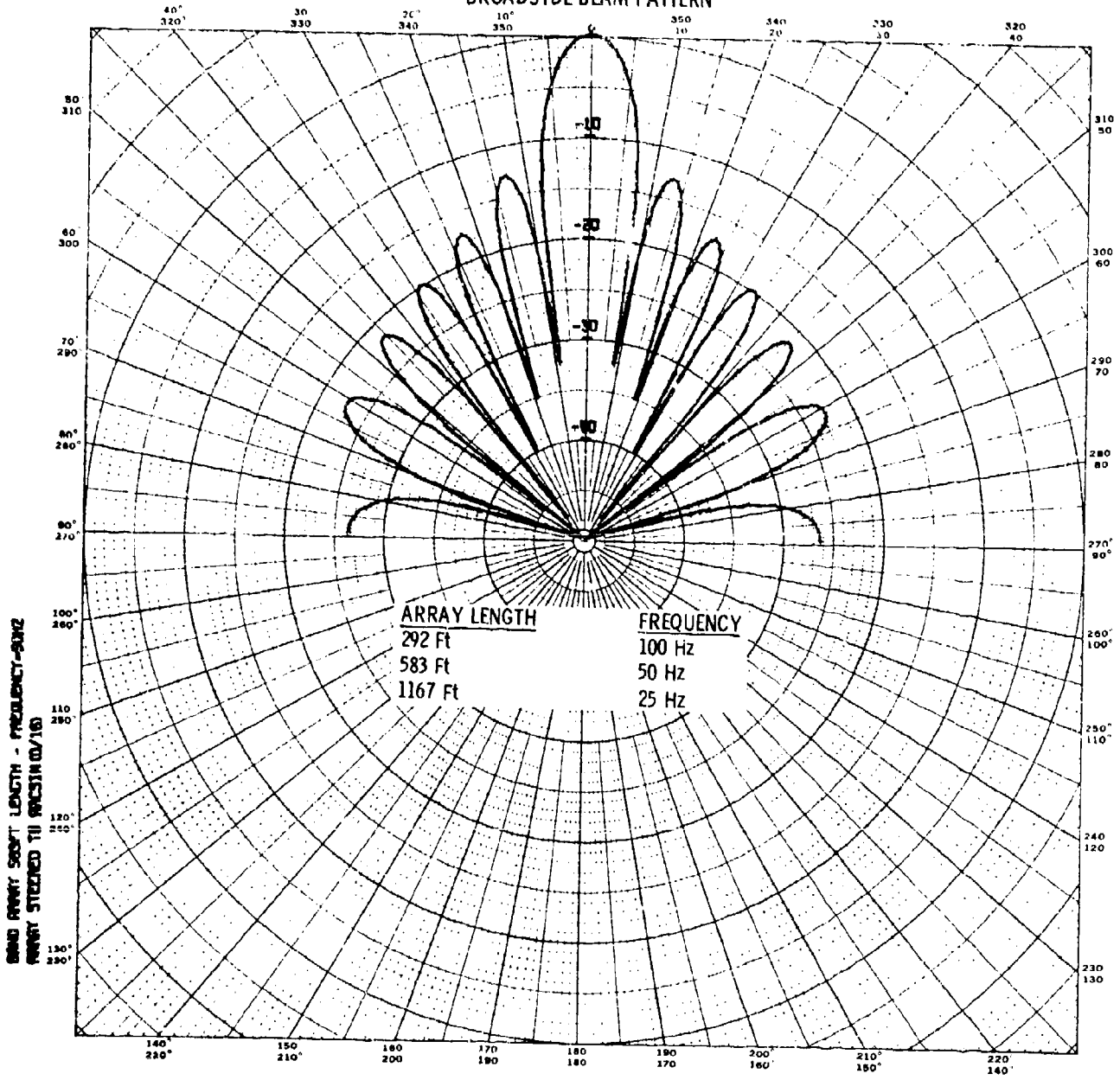
APPENDIX

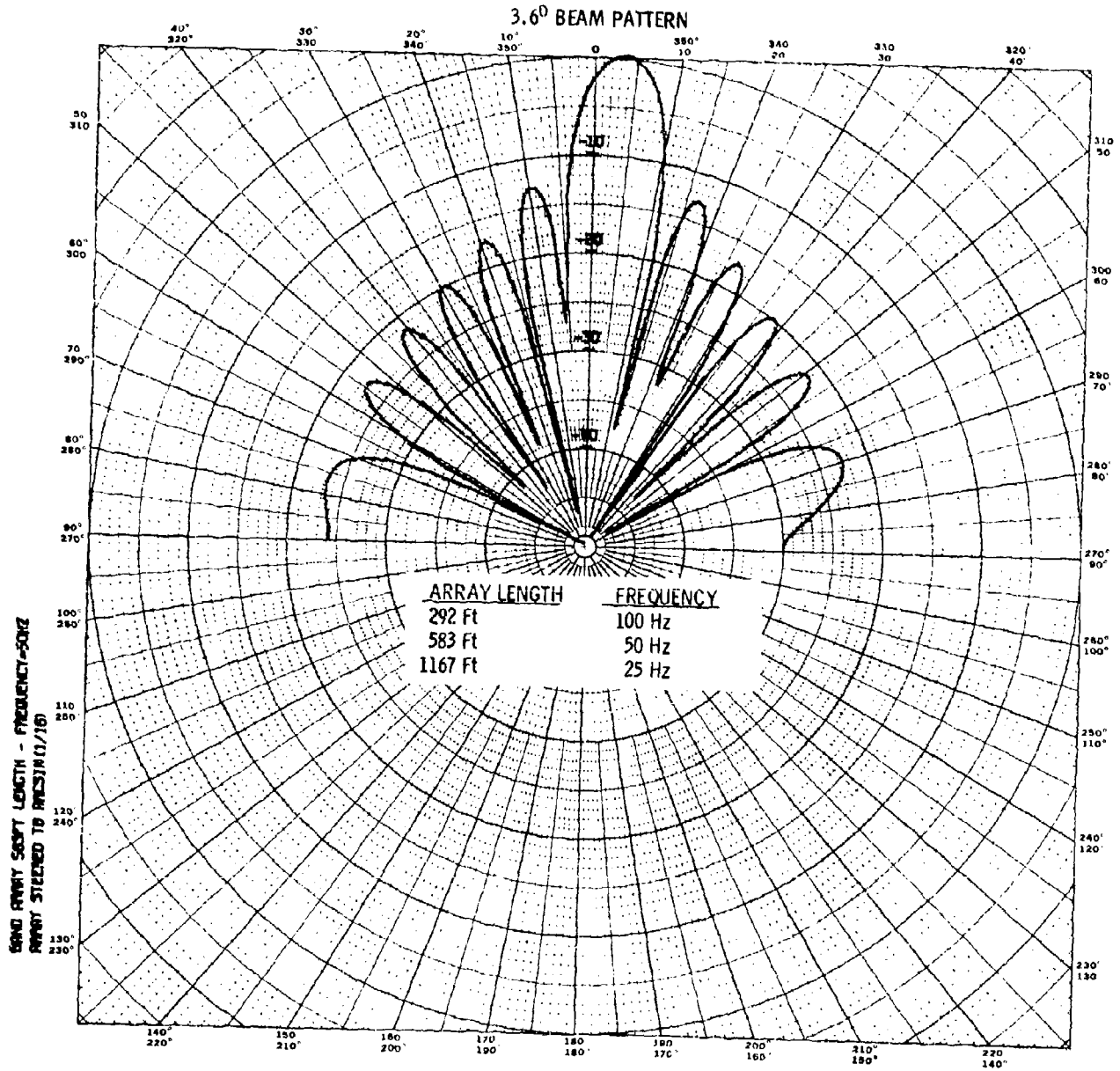
A-1

COMPOSITE BEAM PATTERN

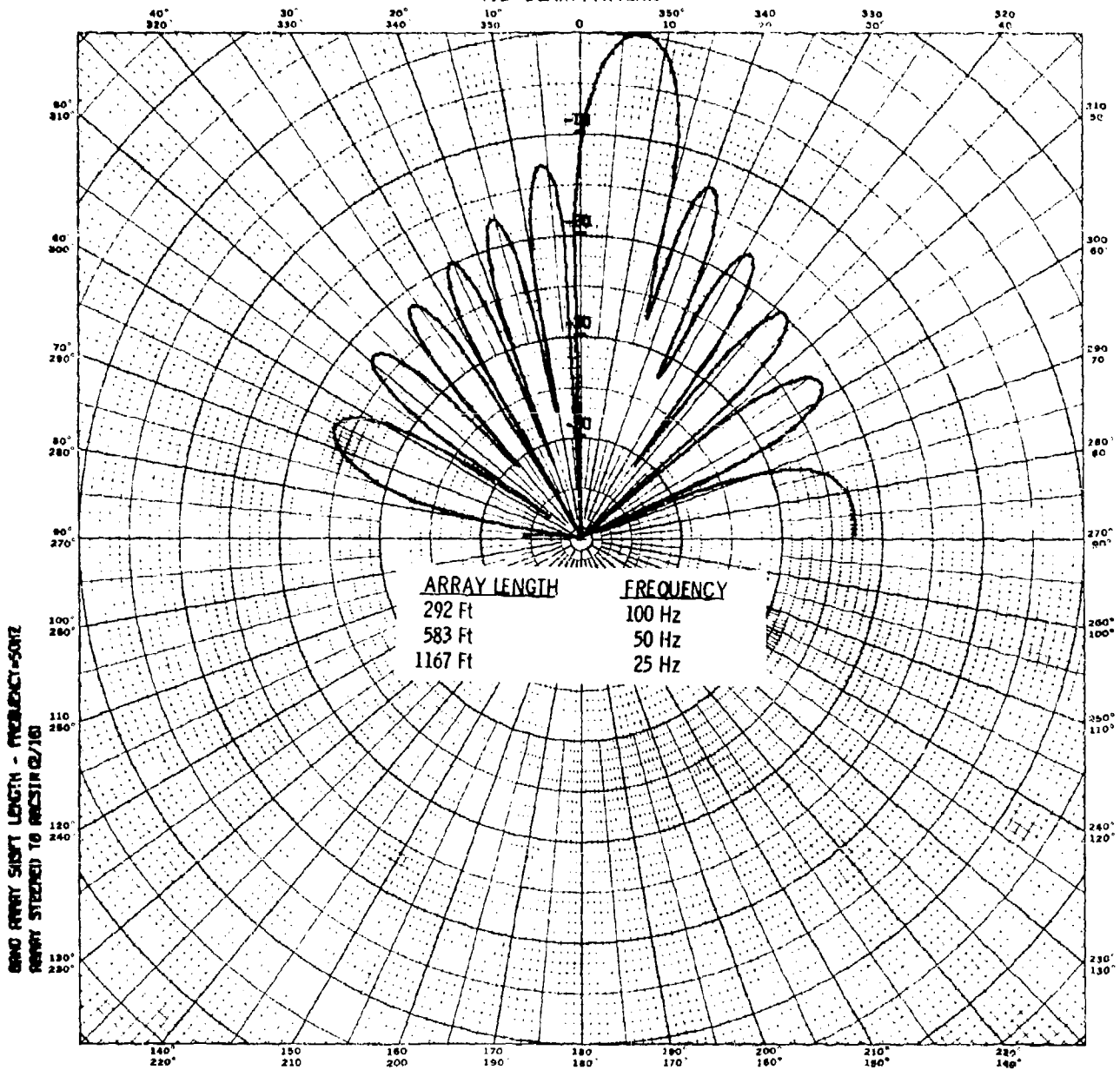


BROADSIDE BEAM PATTERN

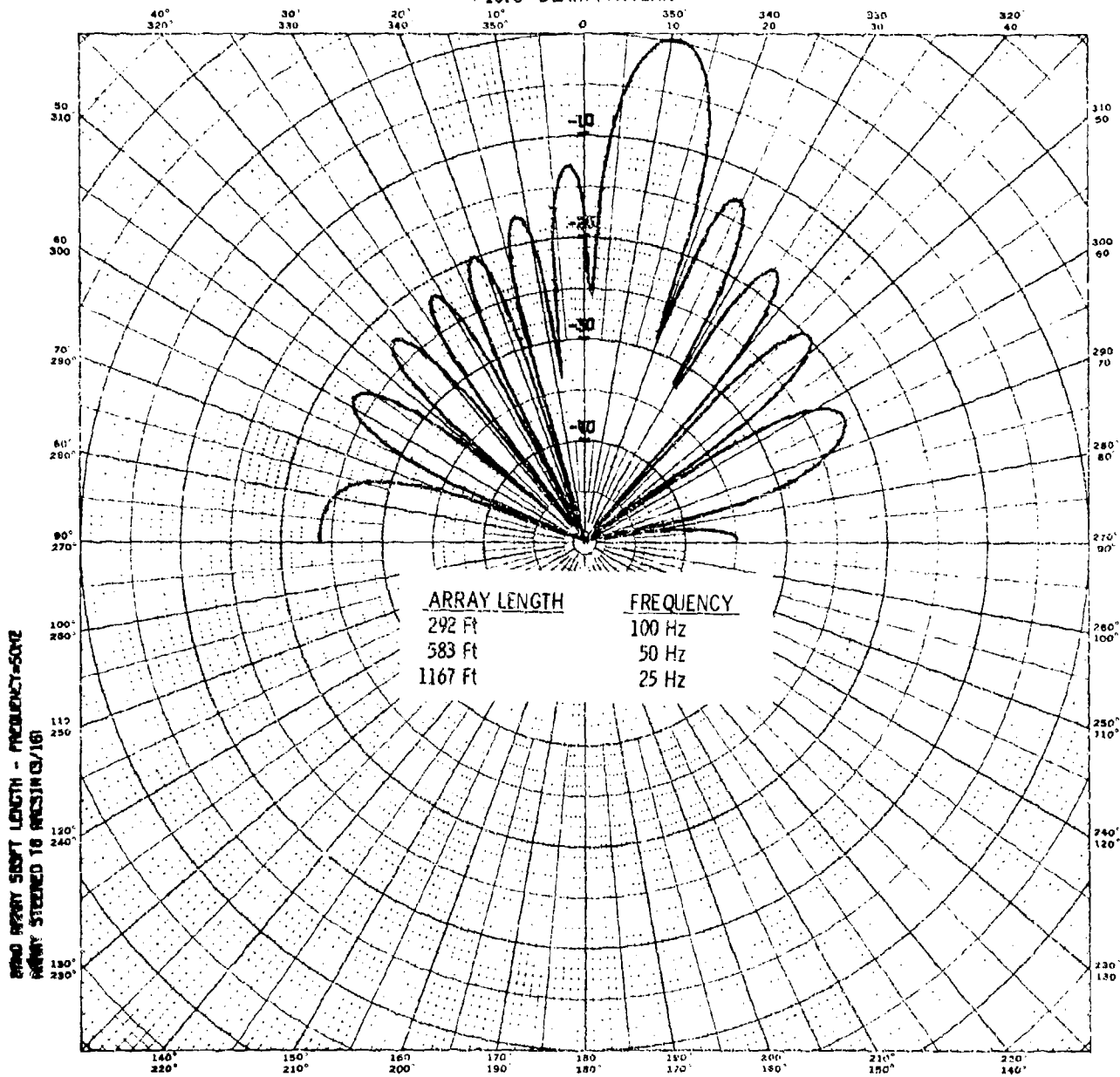




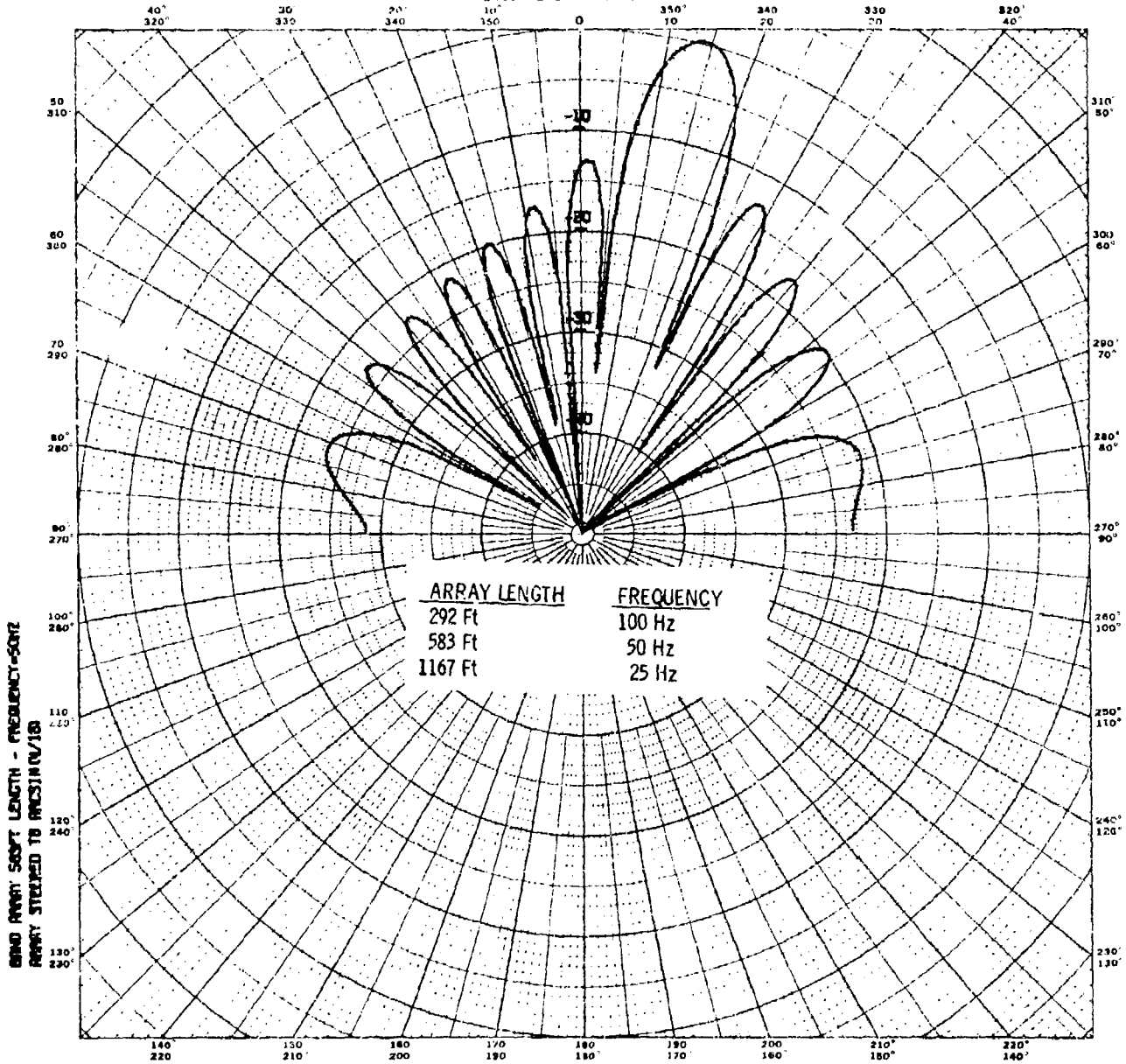
7.2° BEAM PATTERN



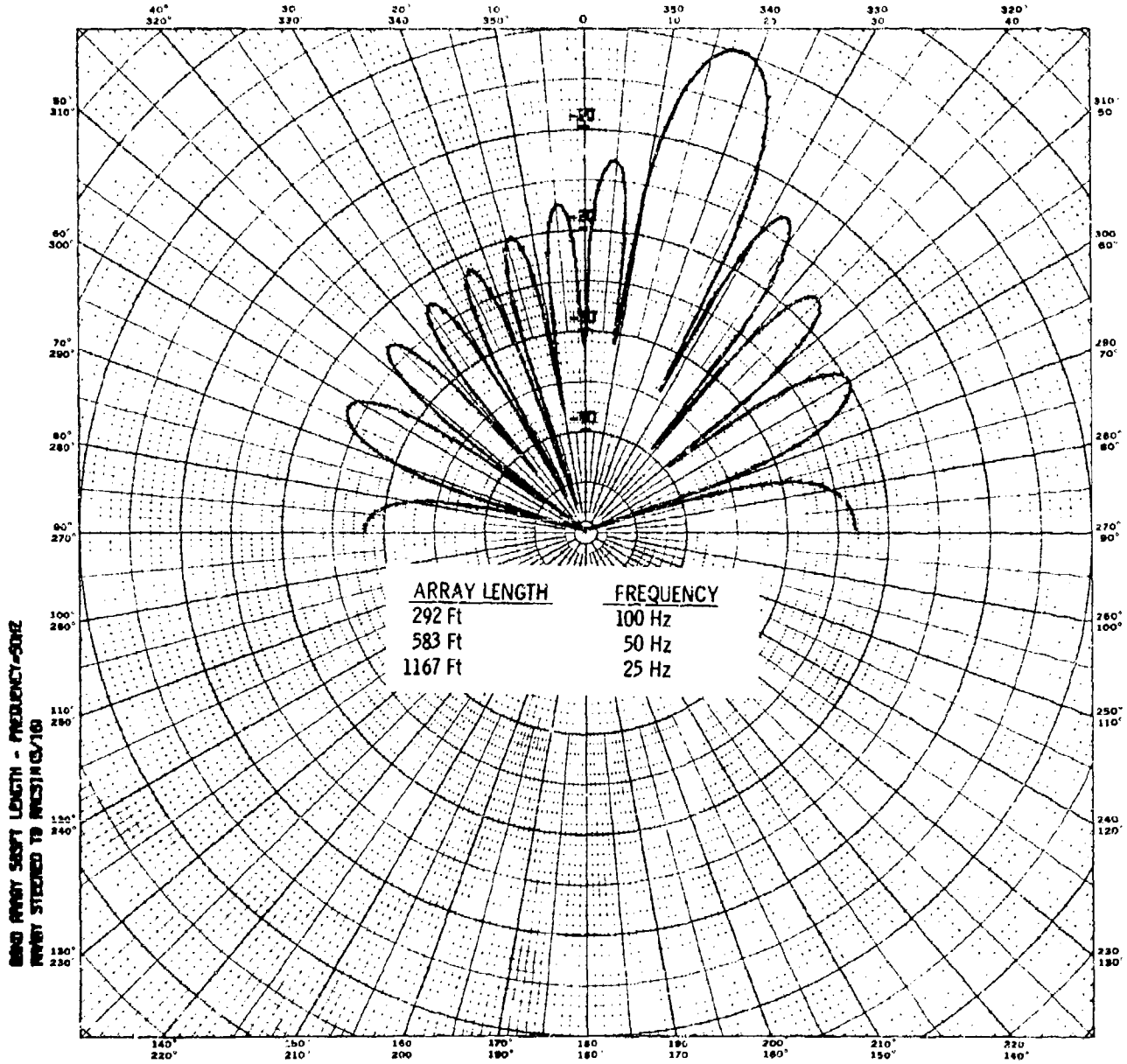
10.8° BEAM PATTERN

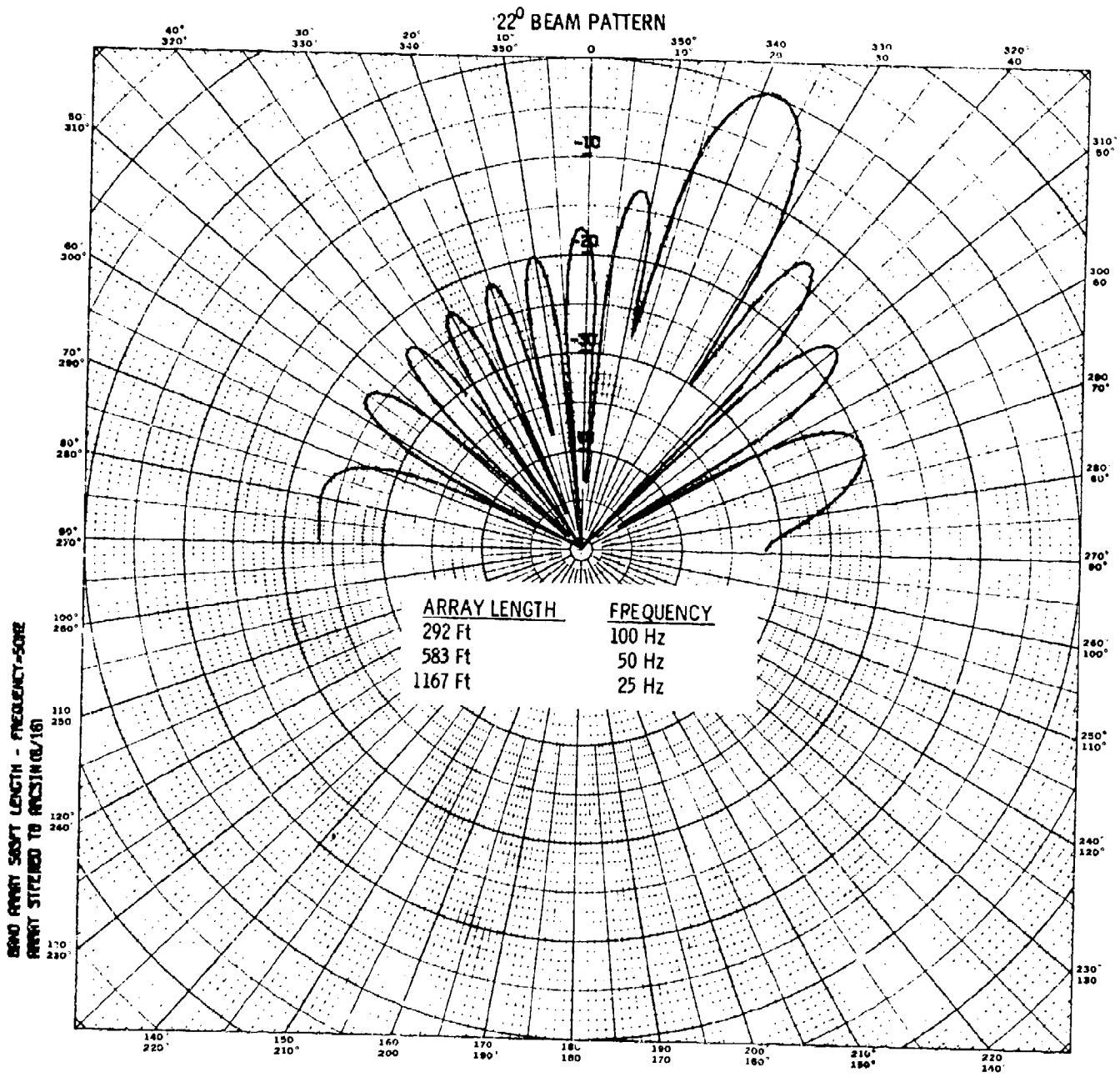


14.5° BEAM PATTERN

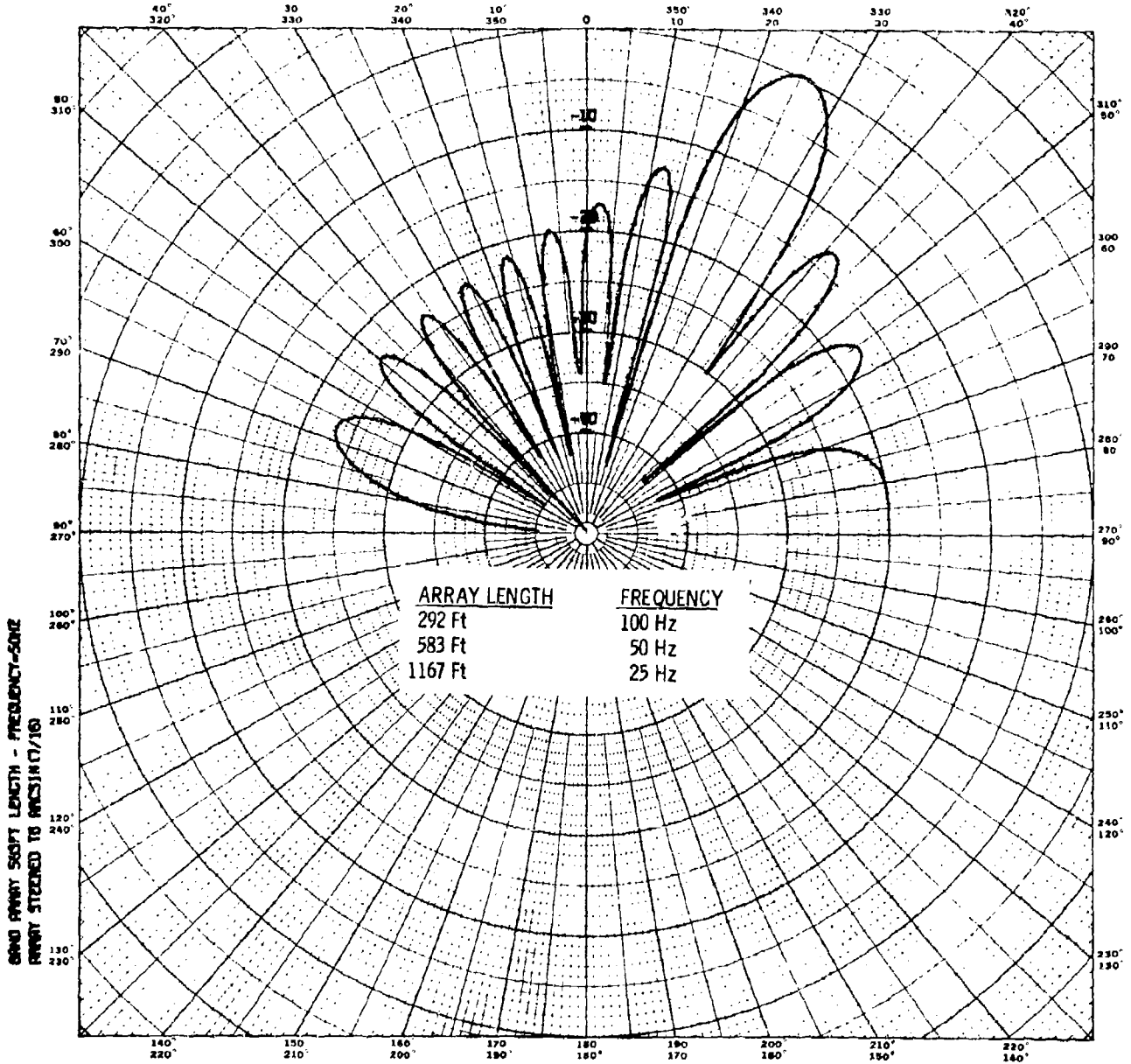


18.2° BEAM PATTERN

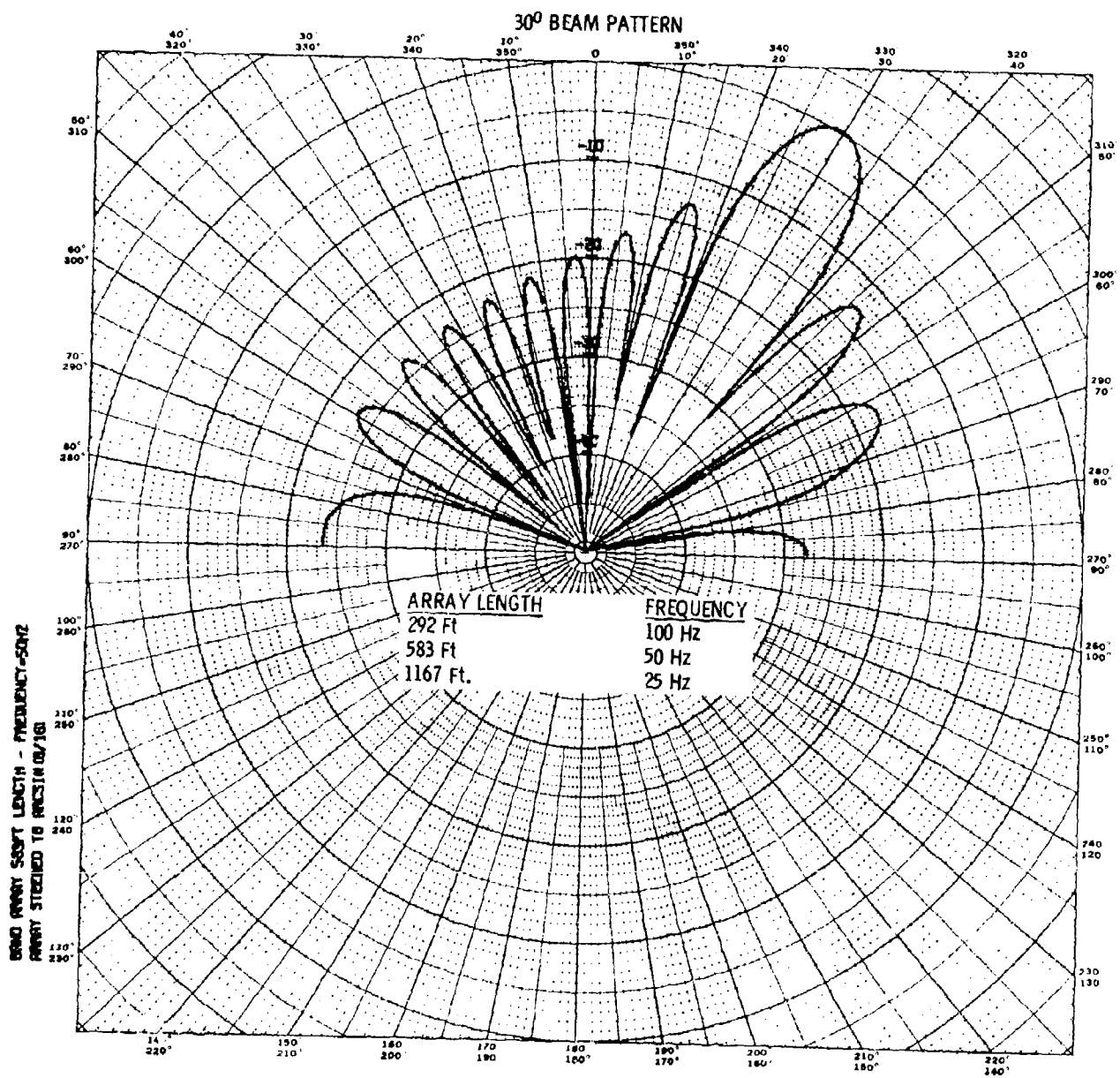


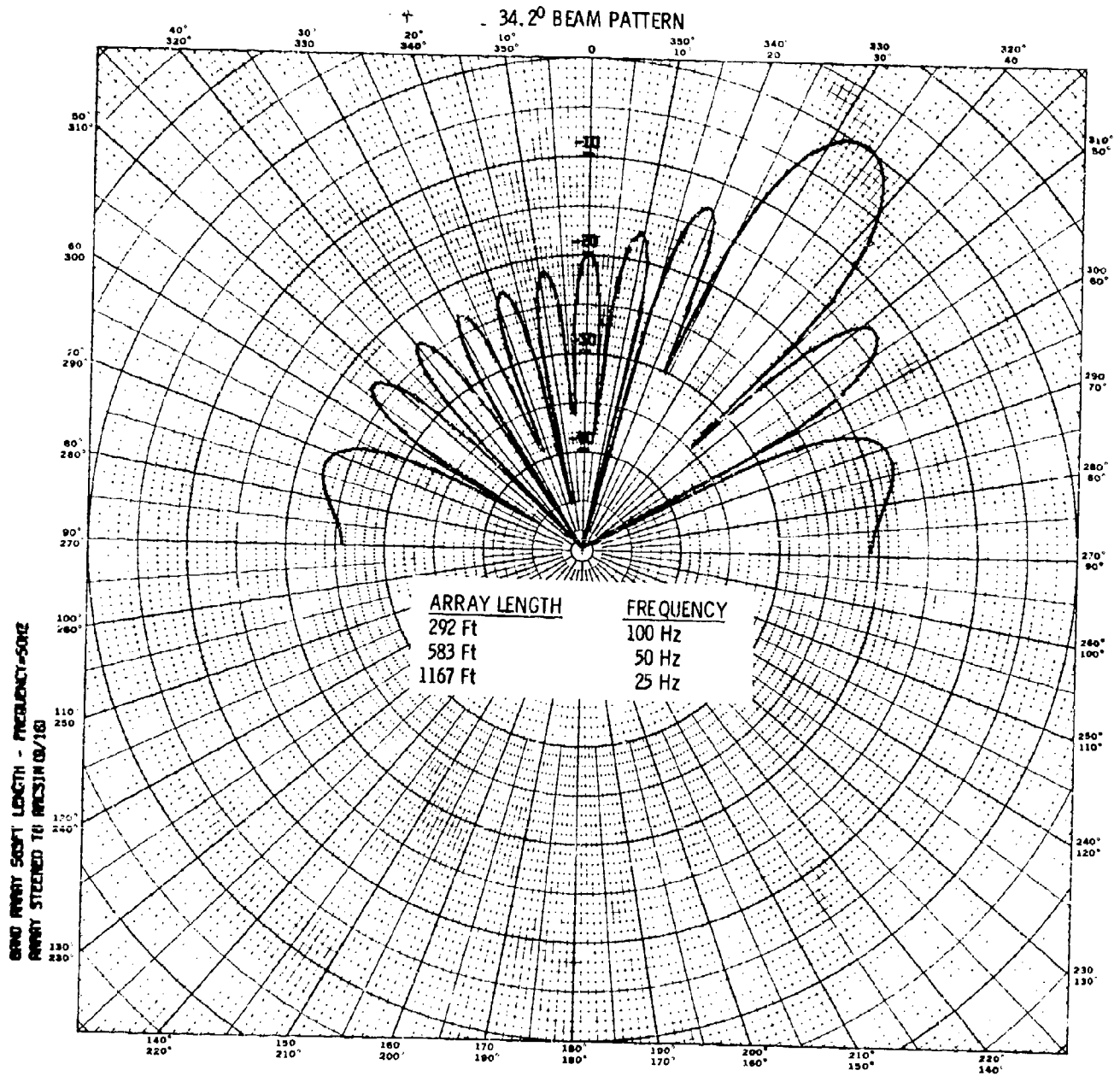


26° BEAM PATTERN

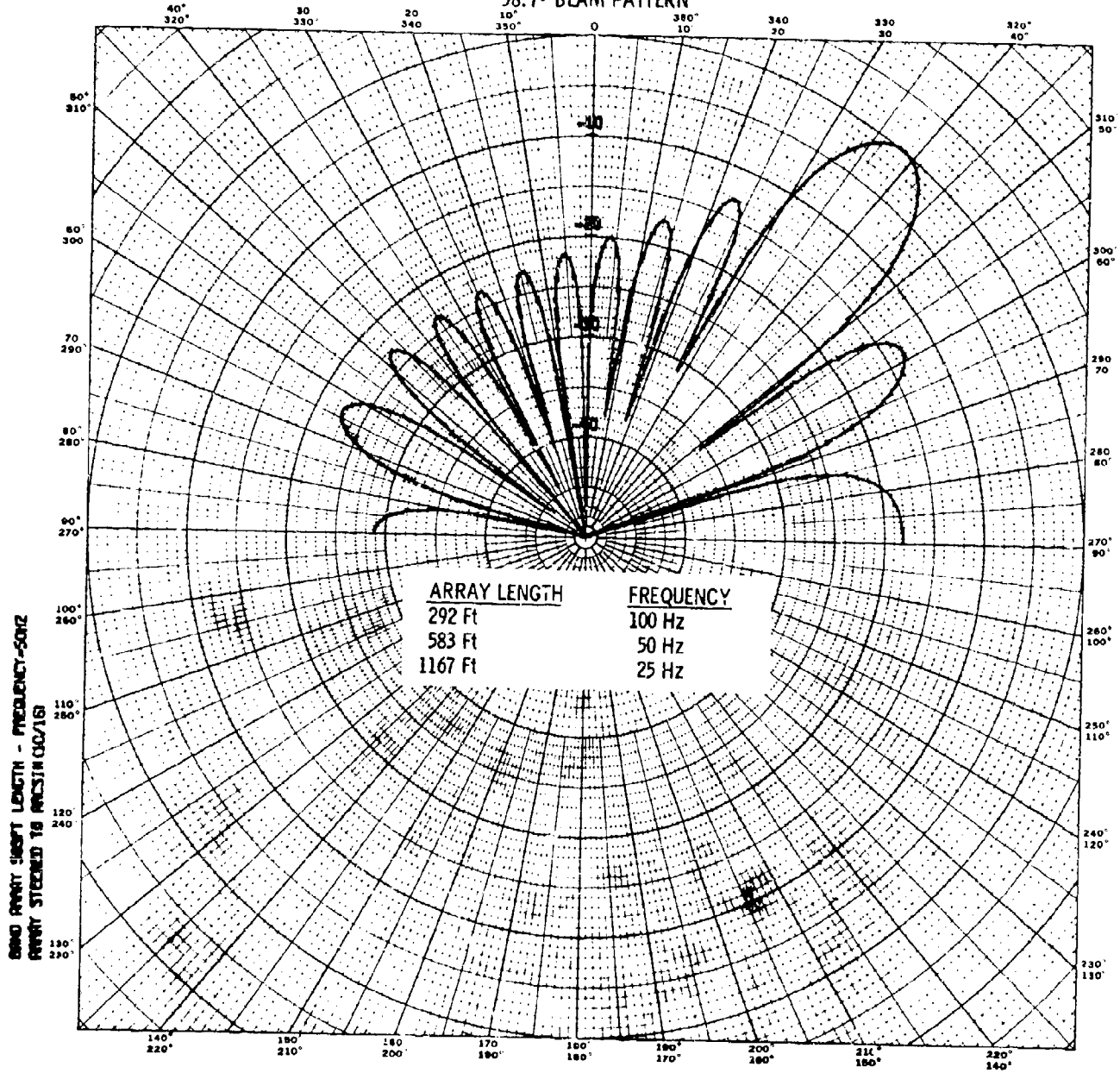


6000 ARRAY 560FT LENGTH - FREQUENCY-SOME  
 ARRAY STEREO TO INCSJIN (7/16)



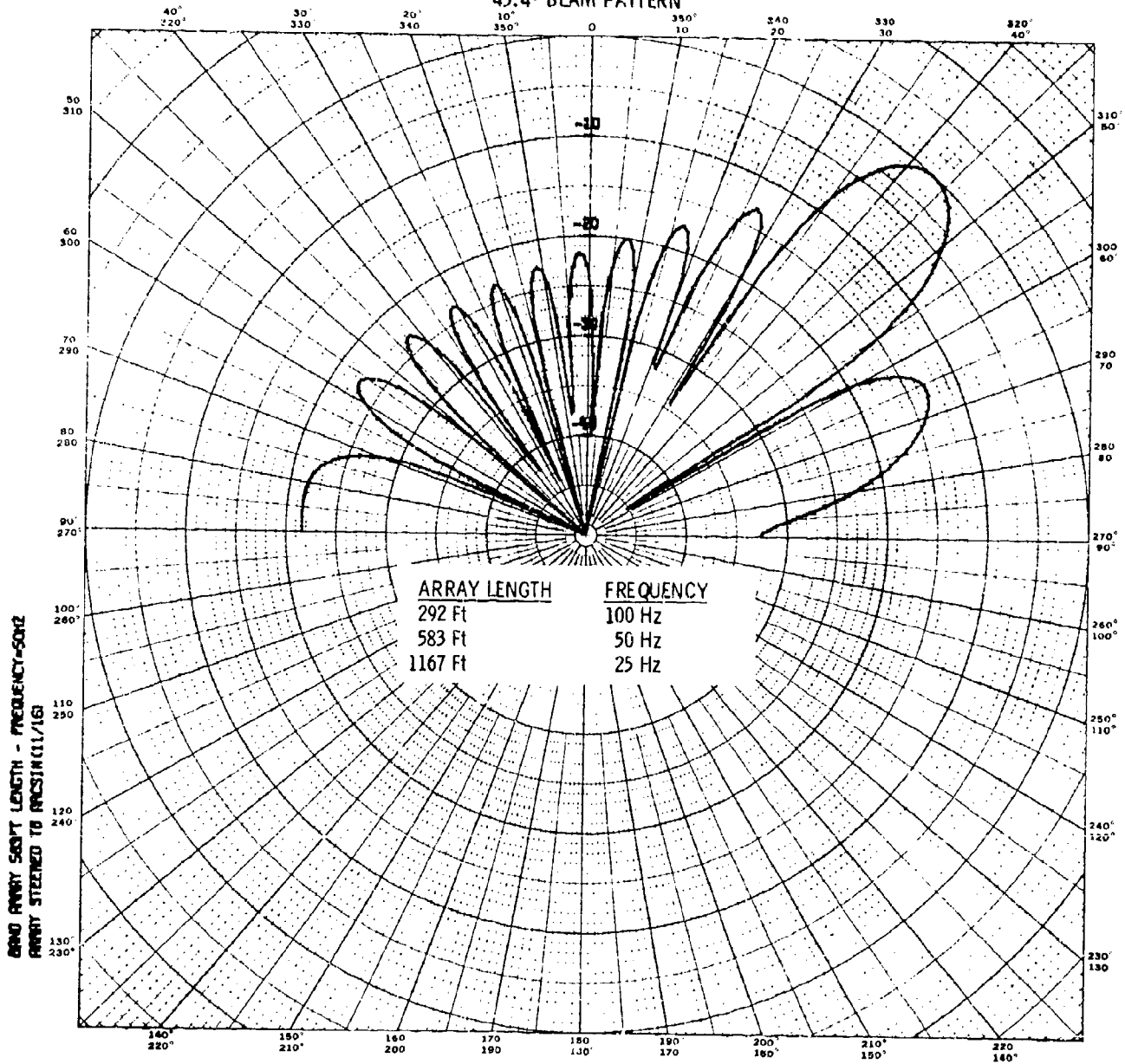


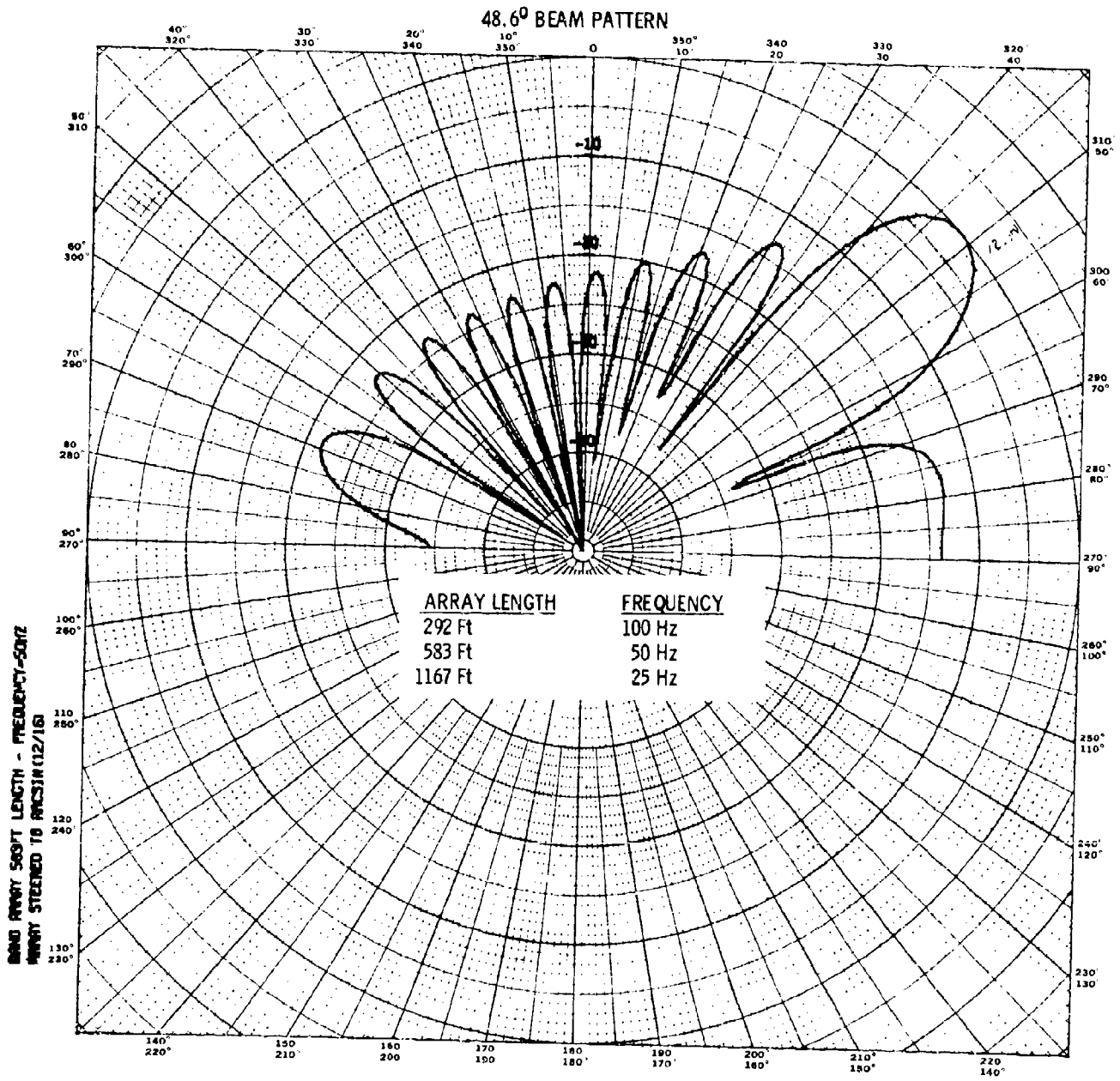
38.7° BEAM PATTERN



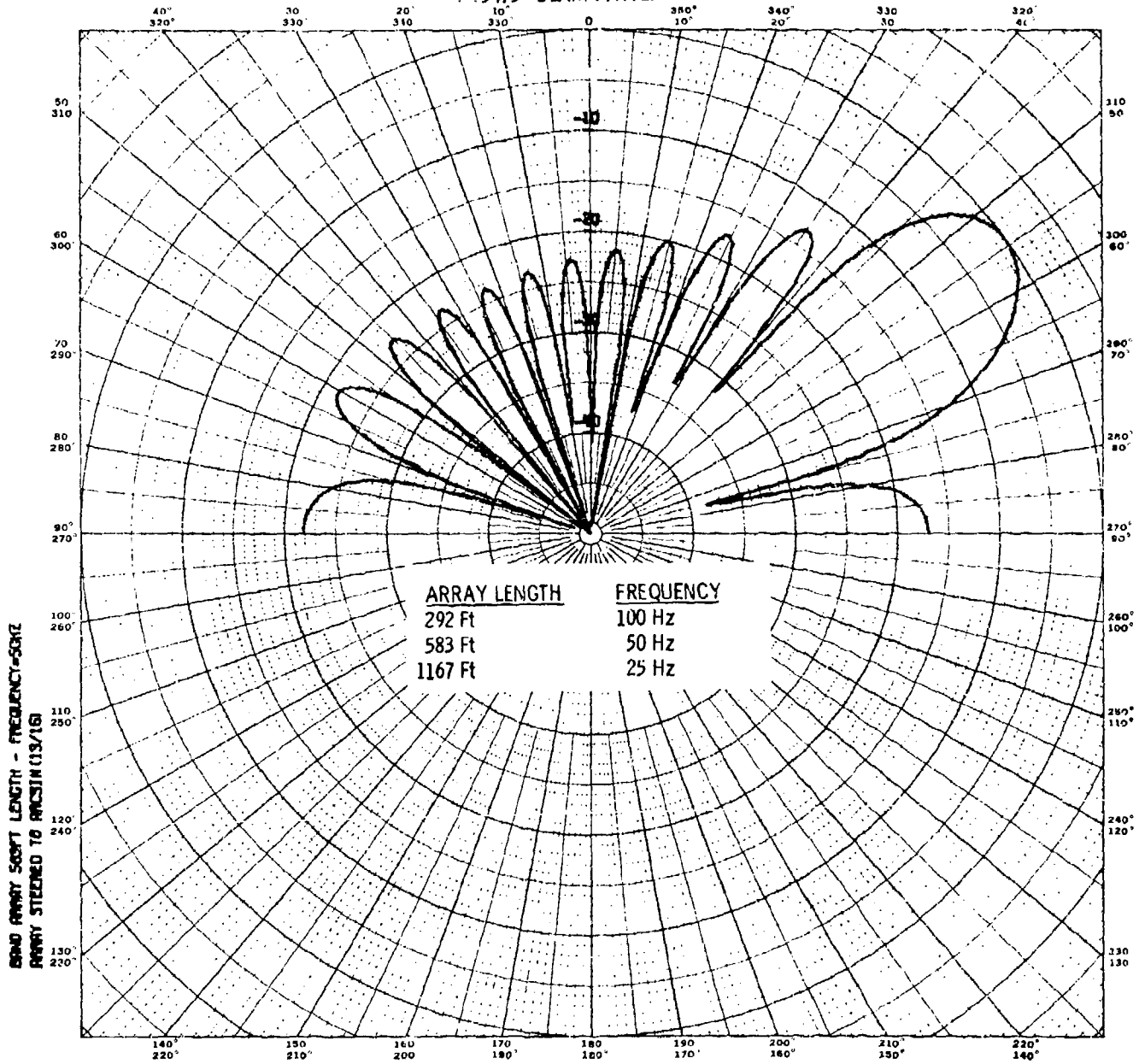
GAIN ARRAY LENGTH - FREQUENCY-SONZ  
 ARRAY STEERED TO MAXIMUM GAIN

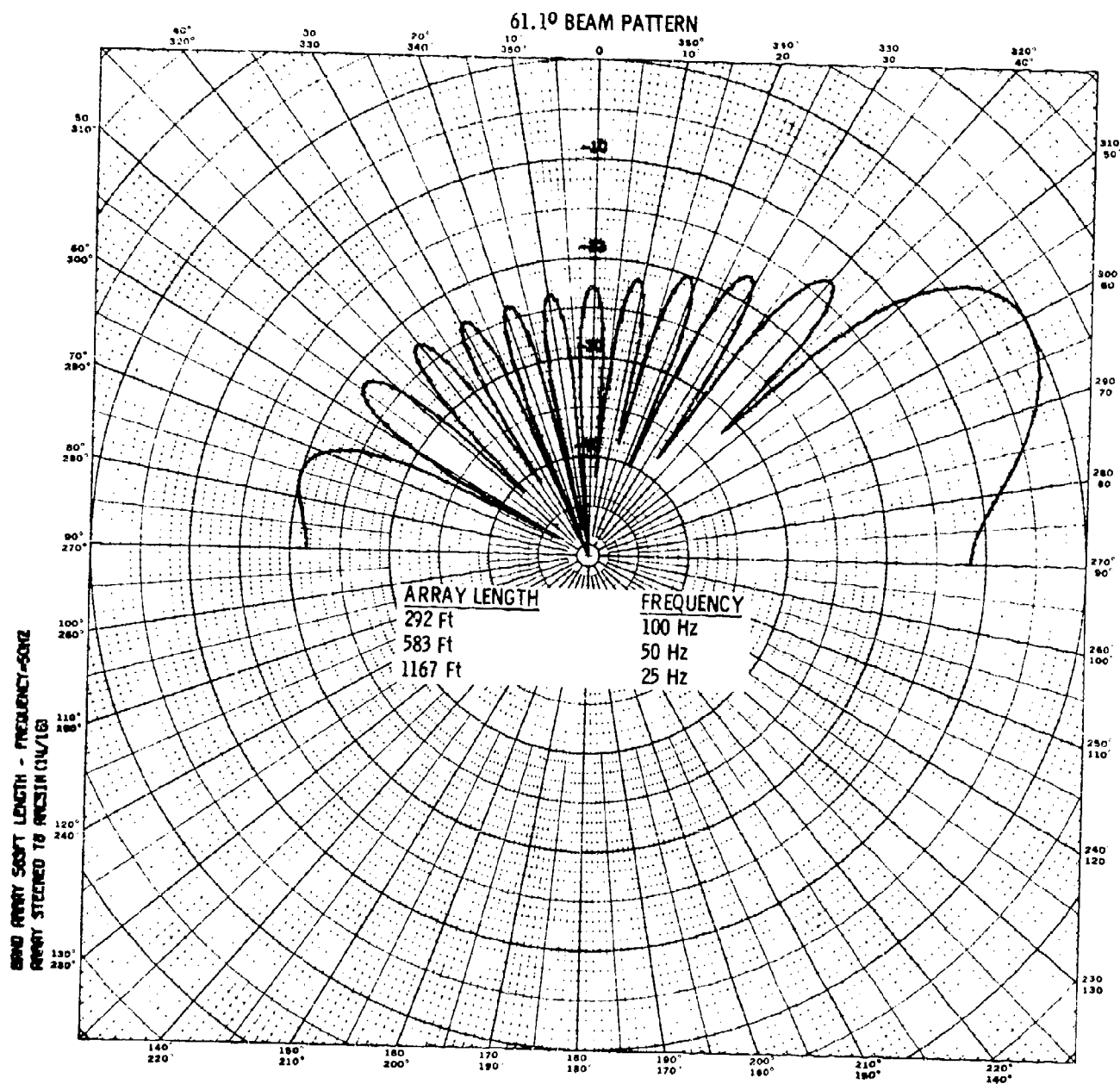
43.4° BEAM PATTERN



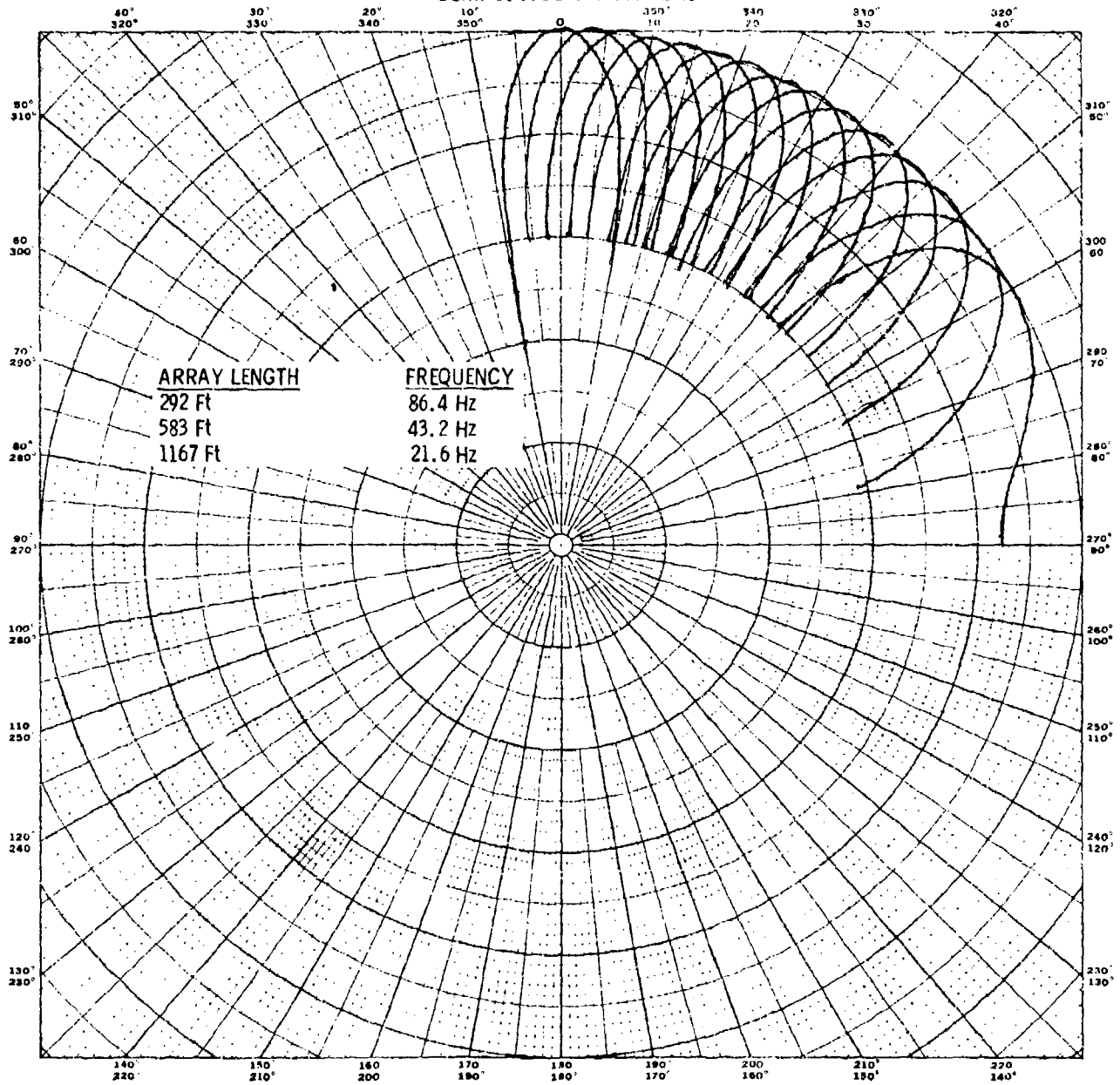


54.3° BEAM PATTERN

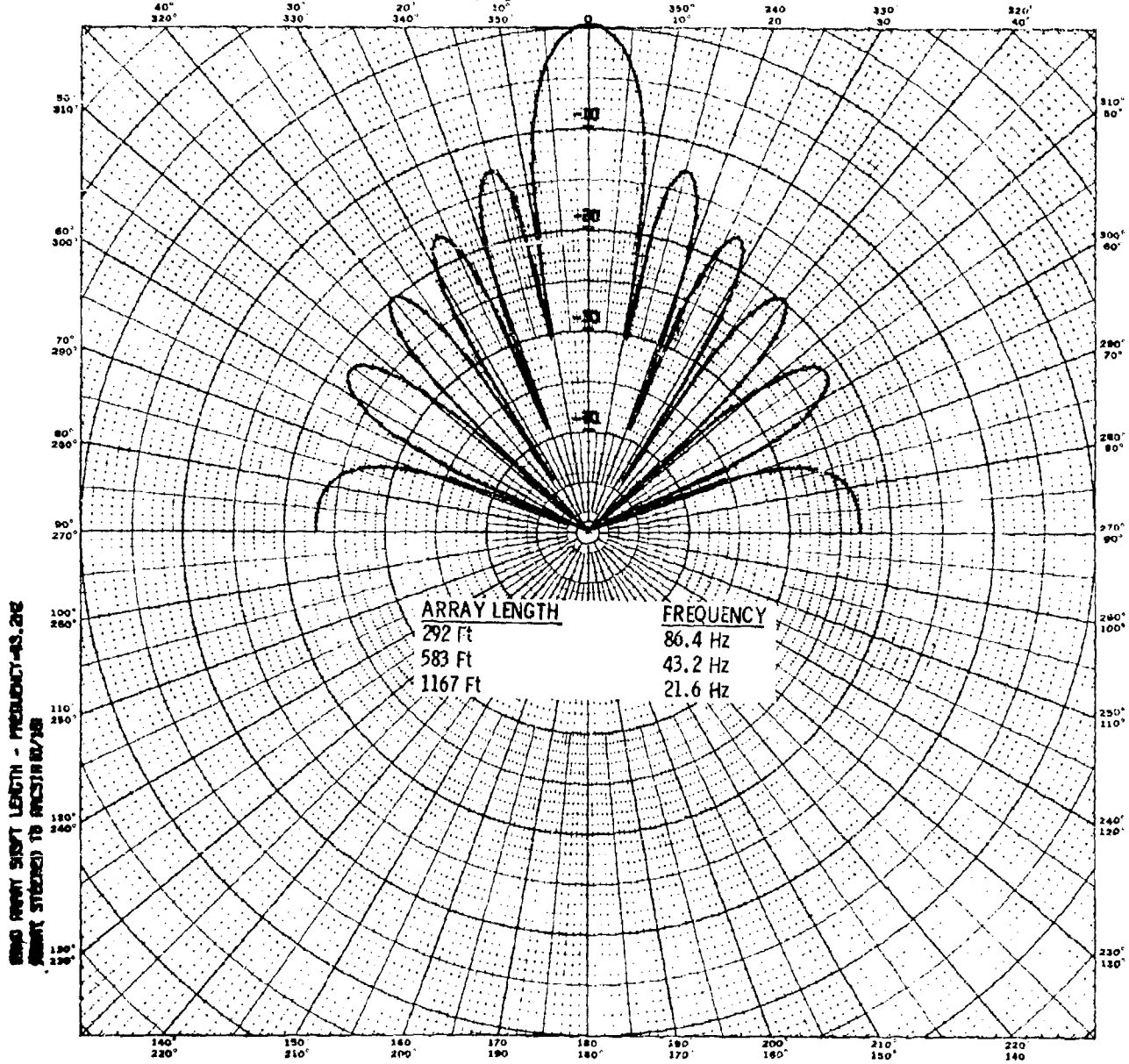


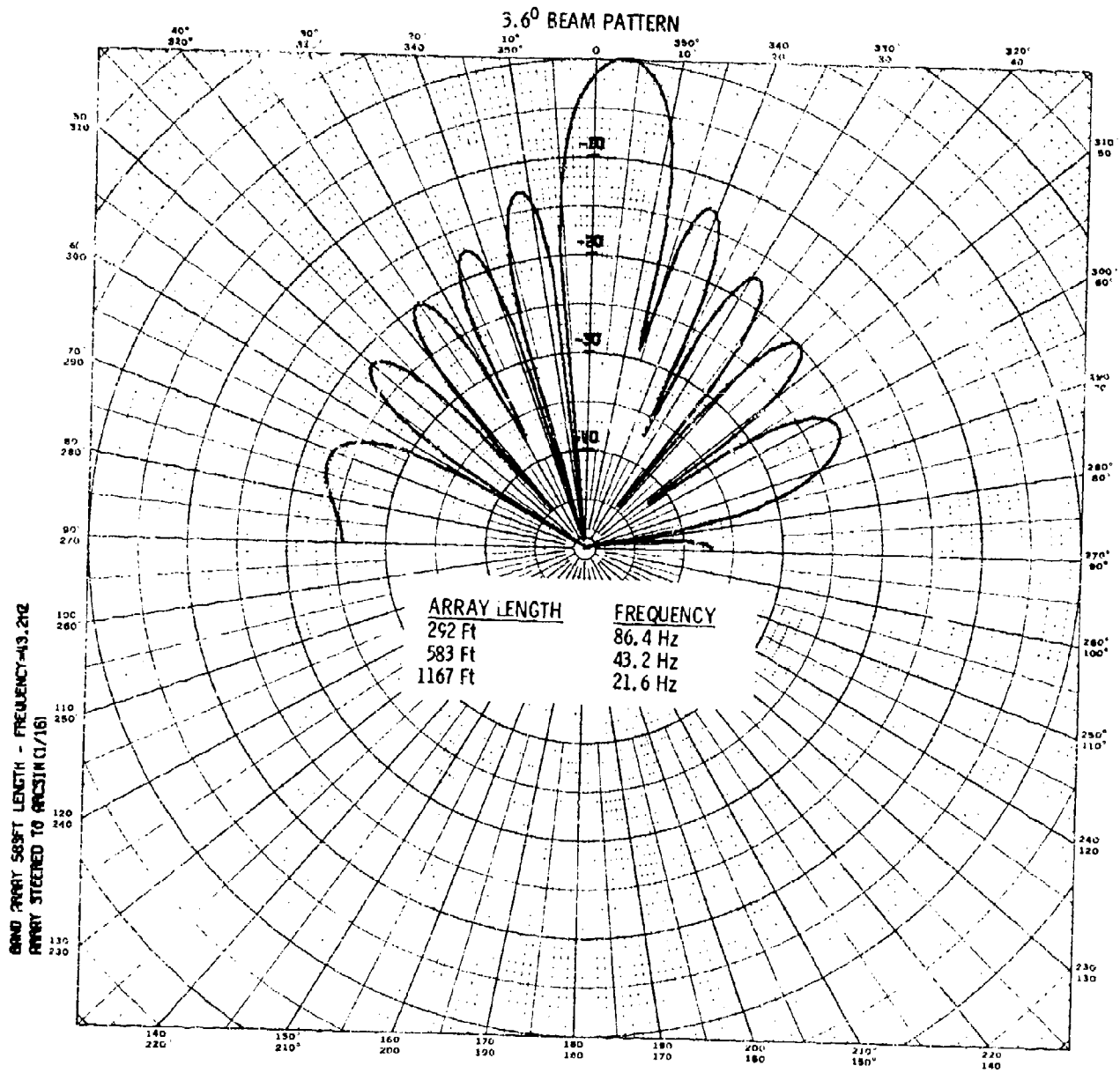


COMPOSITE BEAM PATTERN

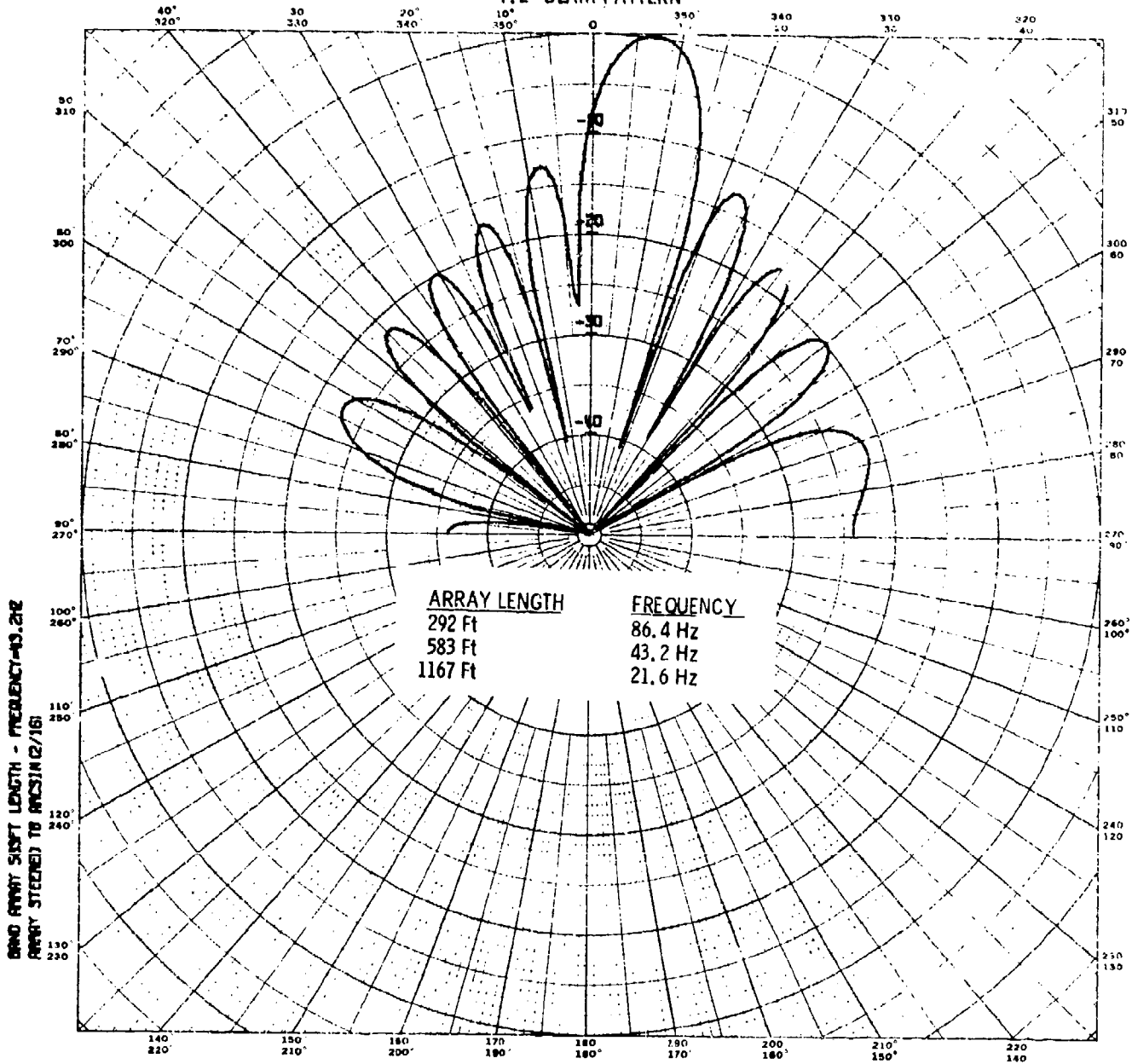


BROADSIDE BEAM PATTERN



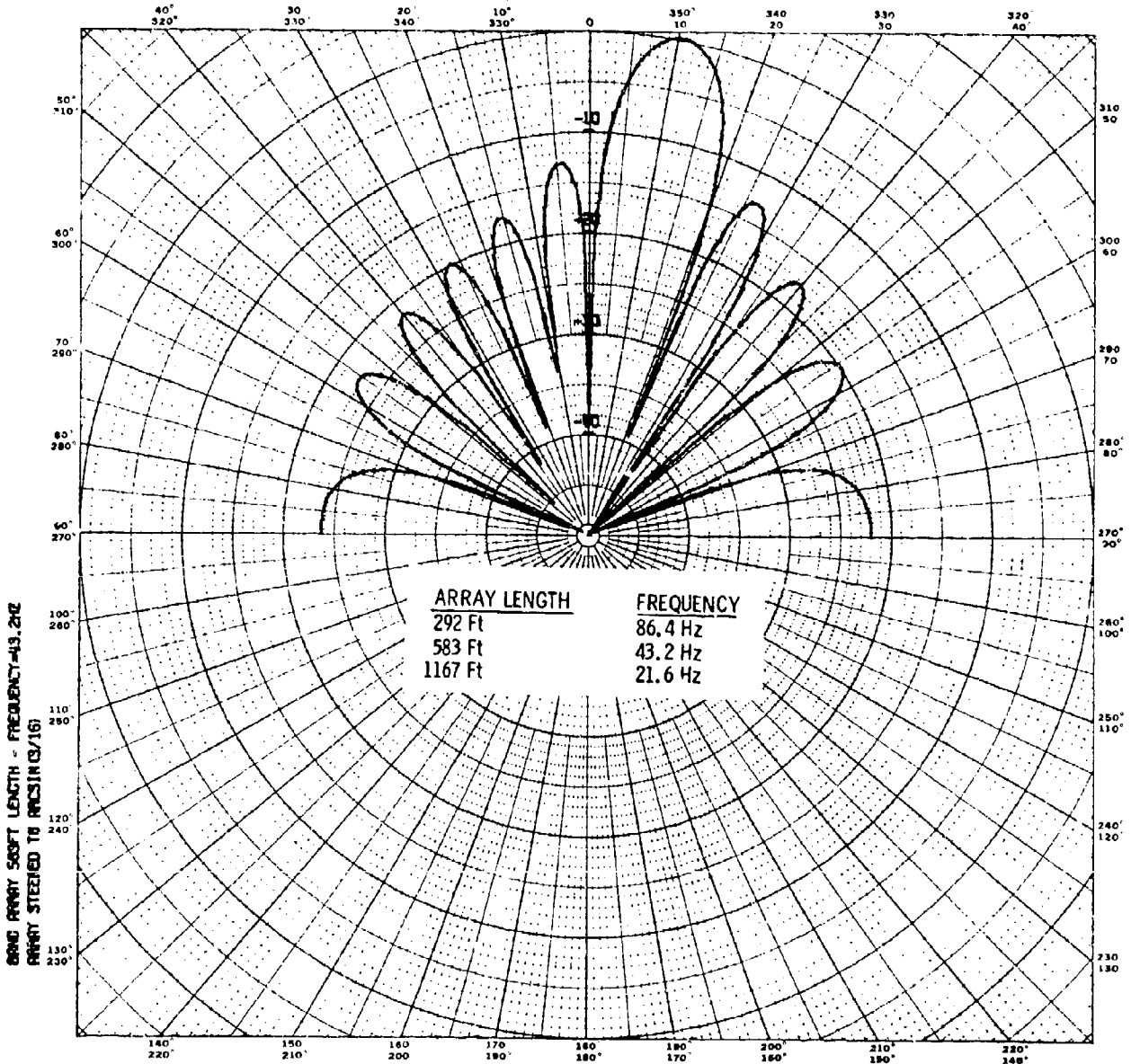


7.2<sup>0</sup> BEAM PATTERN



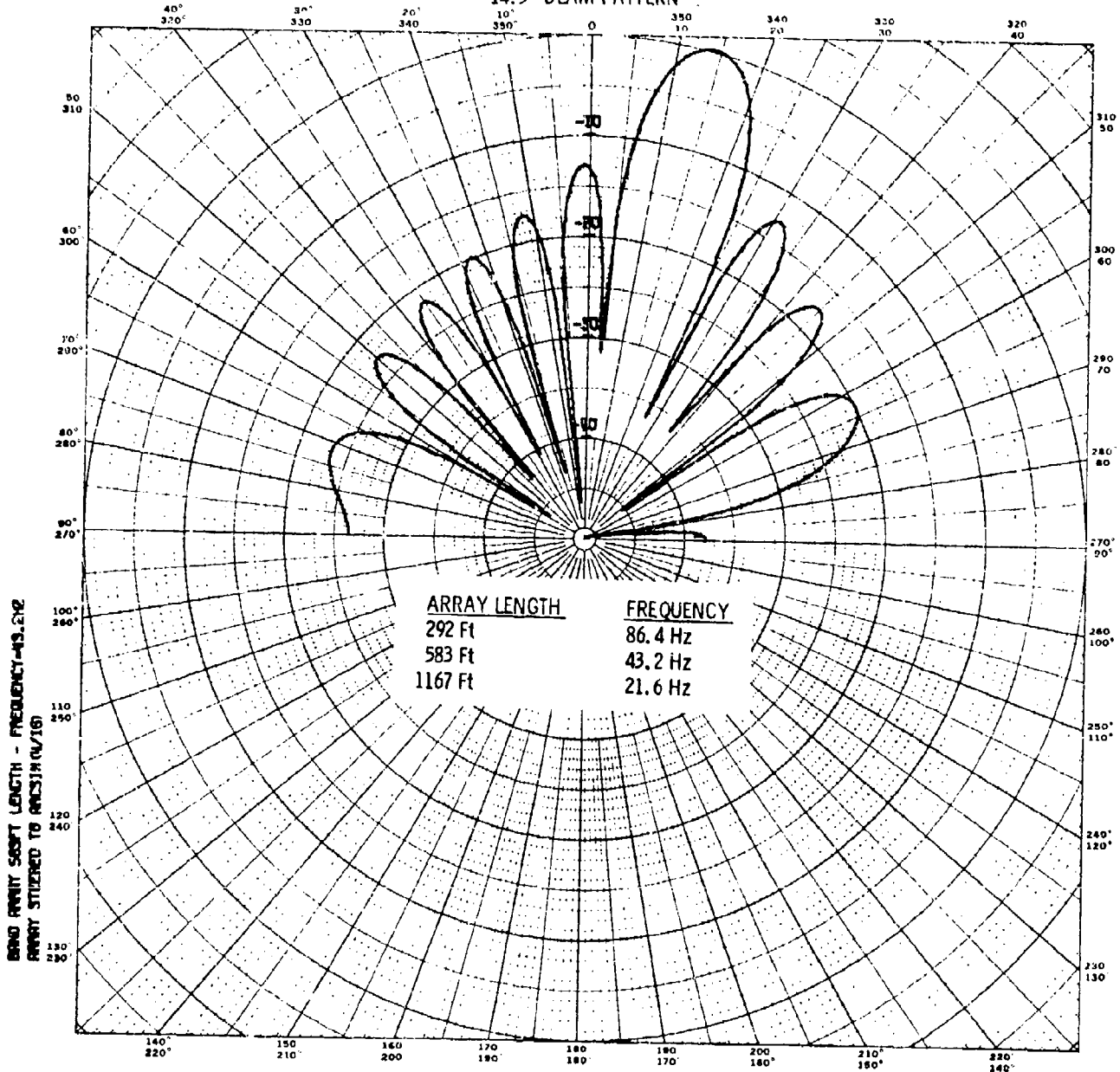
ORND ARRAY SIGHT LENGTH - FREQUENCY-43.2HZ  
ARRAY STEERED TO 180° IN (2/16)

10.8° BEAM PATTERN

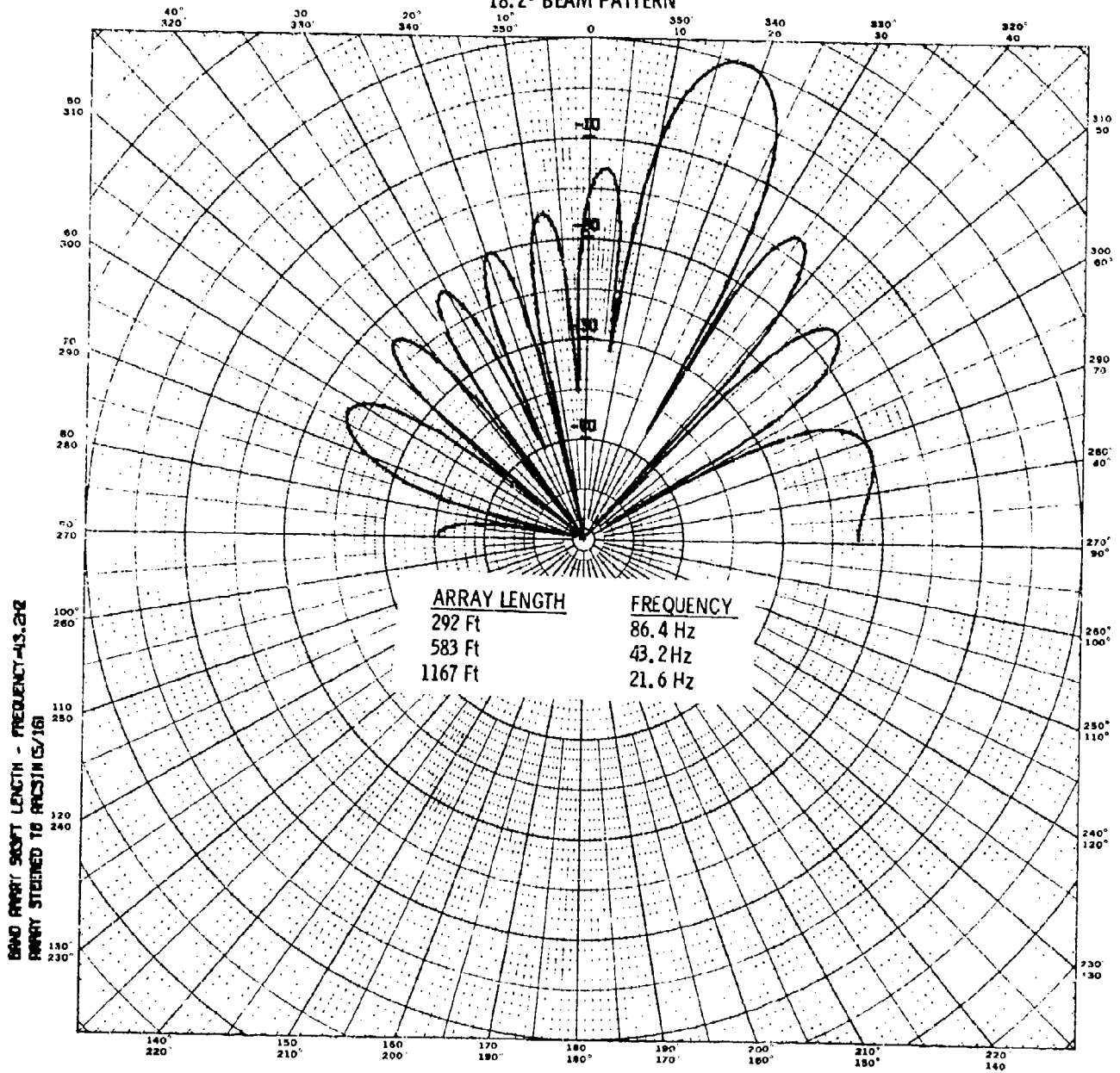


60° 320°  
50° 310°  
40° 300°  
30° 290°  
20° 280°  
10° 270°  
0 260°  
10° 250°  
20° 240°  
30° 230°  
40° 220°  
50° 210°  
60° 200°  
70° 190°  
80° 180°  
90° 170°  
100° 160°  
110° 150°  
120° 140°  
130° 130°  
140° 120°  
150° 110°  
160° 100°  
170° 90°  
180° 80°  
190° 70°  
200° 60°  
210° 50°  
220° 40°  
230° 30°  
240° 20°  
250° 10°  
260° 0°  
270° 10°  
280° 20°  
290° 30°  
300° 40°  
310° 50°  
320° 60°

14.5° BEAM PATTERN

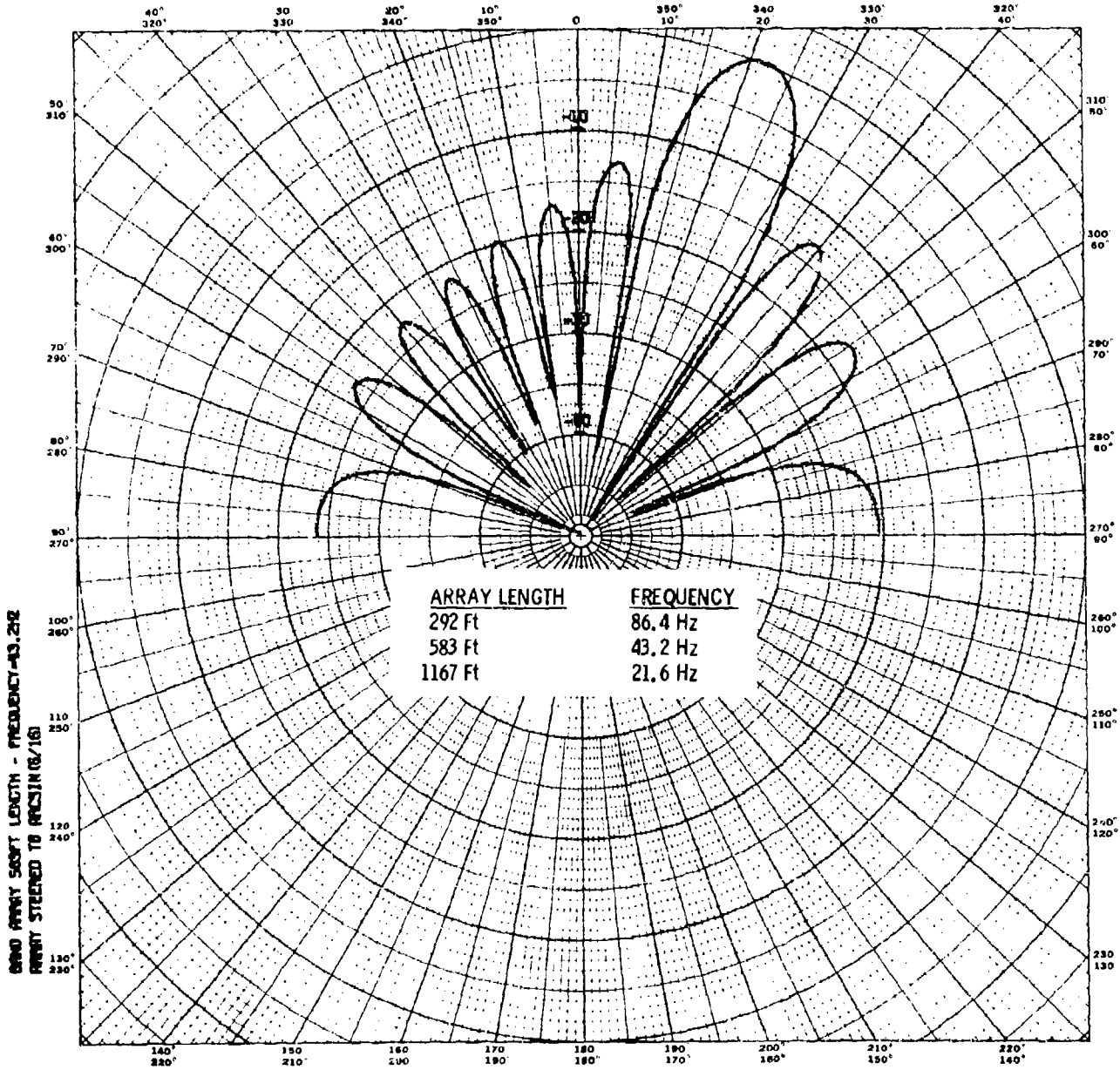


18.2° BEAM PATTERN



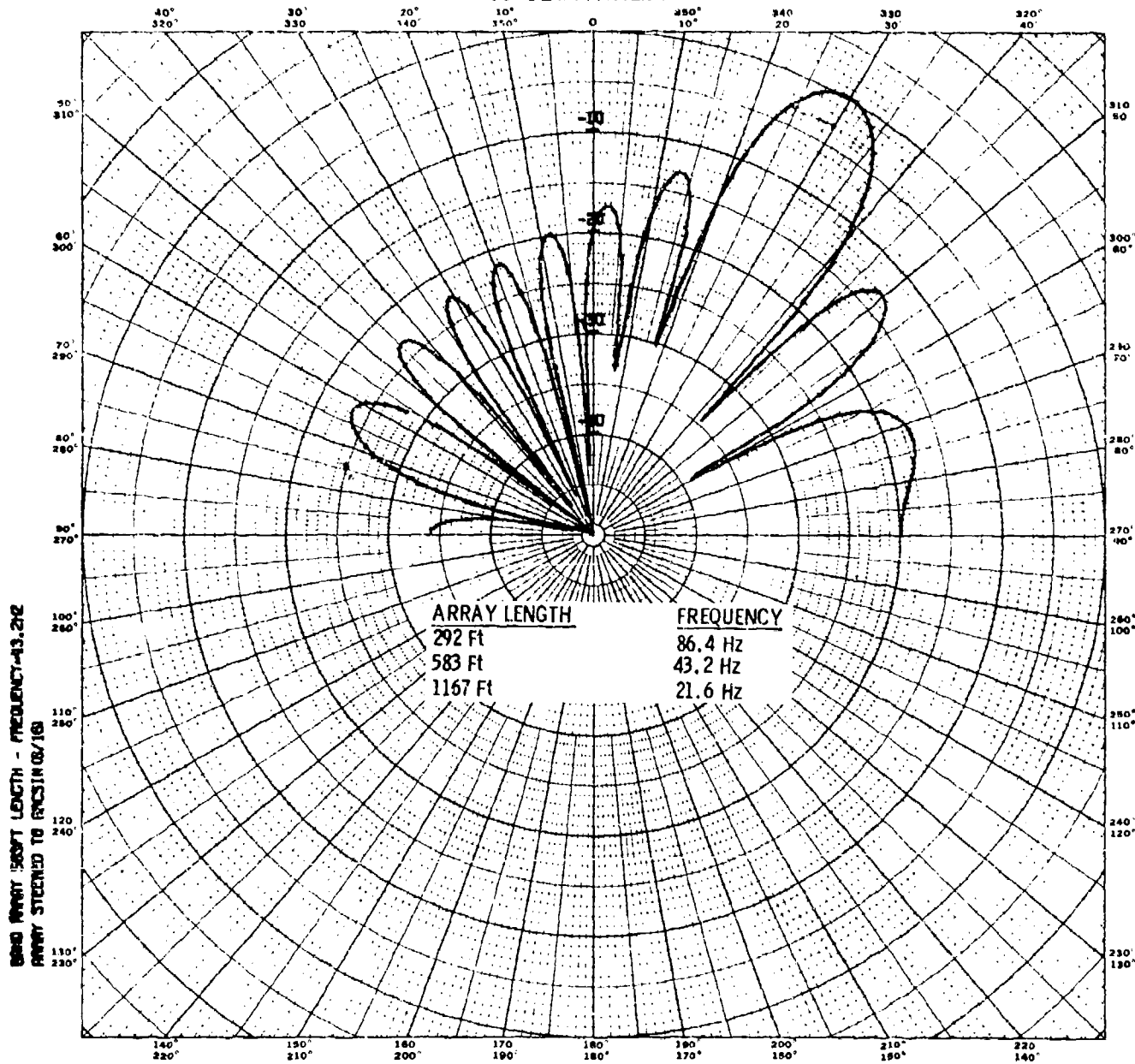
BEAM ARRAY SKETCH LENGTH - FREQUENCY-AS-212  
 ARRAY STEERED TO 180 IN (S/16)

22° BEAM PATTERN



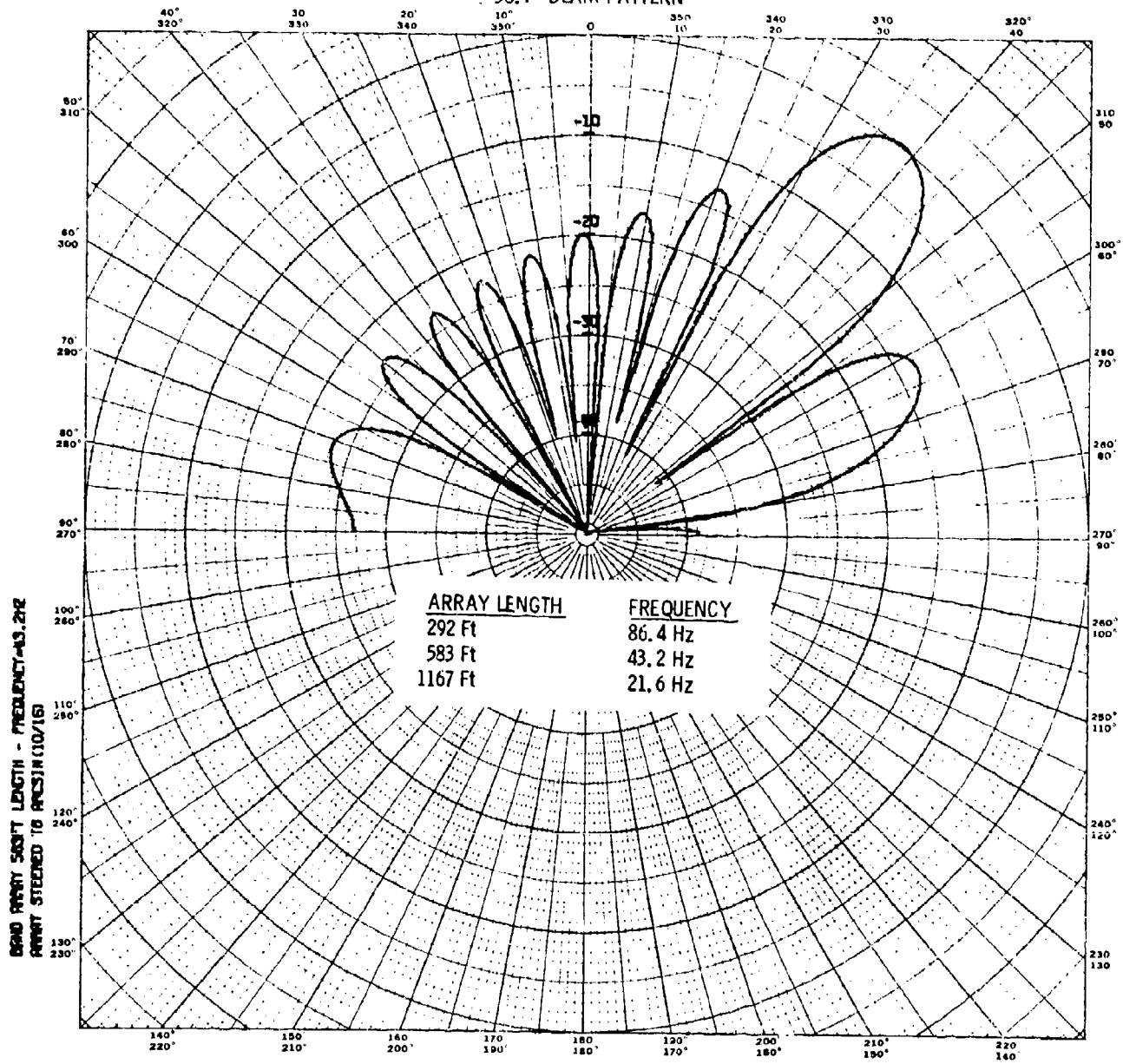


30° BEAM PATTERN

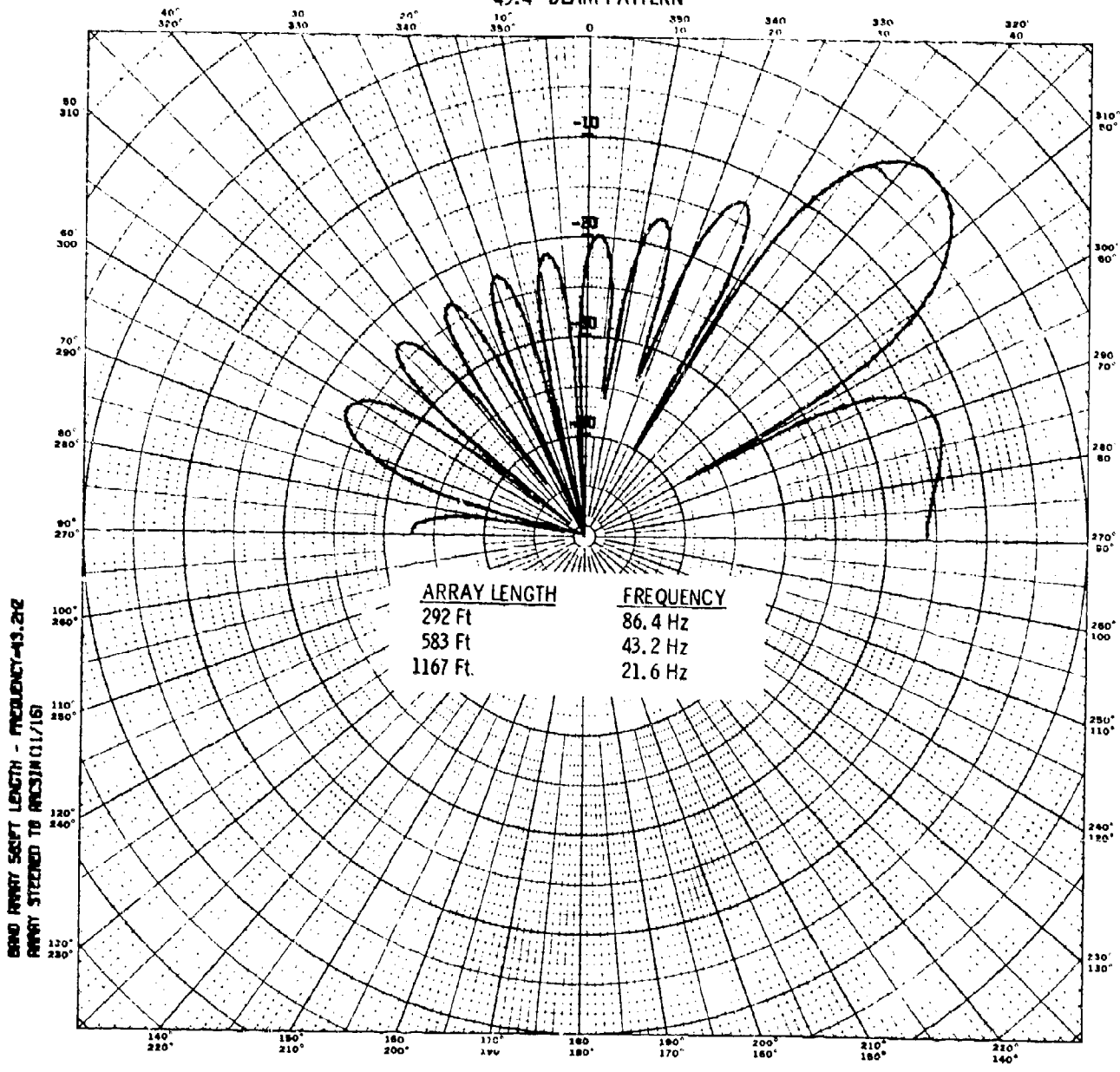




38.7° BEAM PATTERN



43.4° BEAM PATTERN

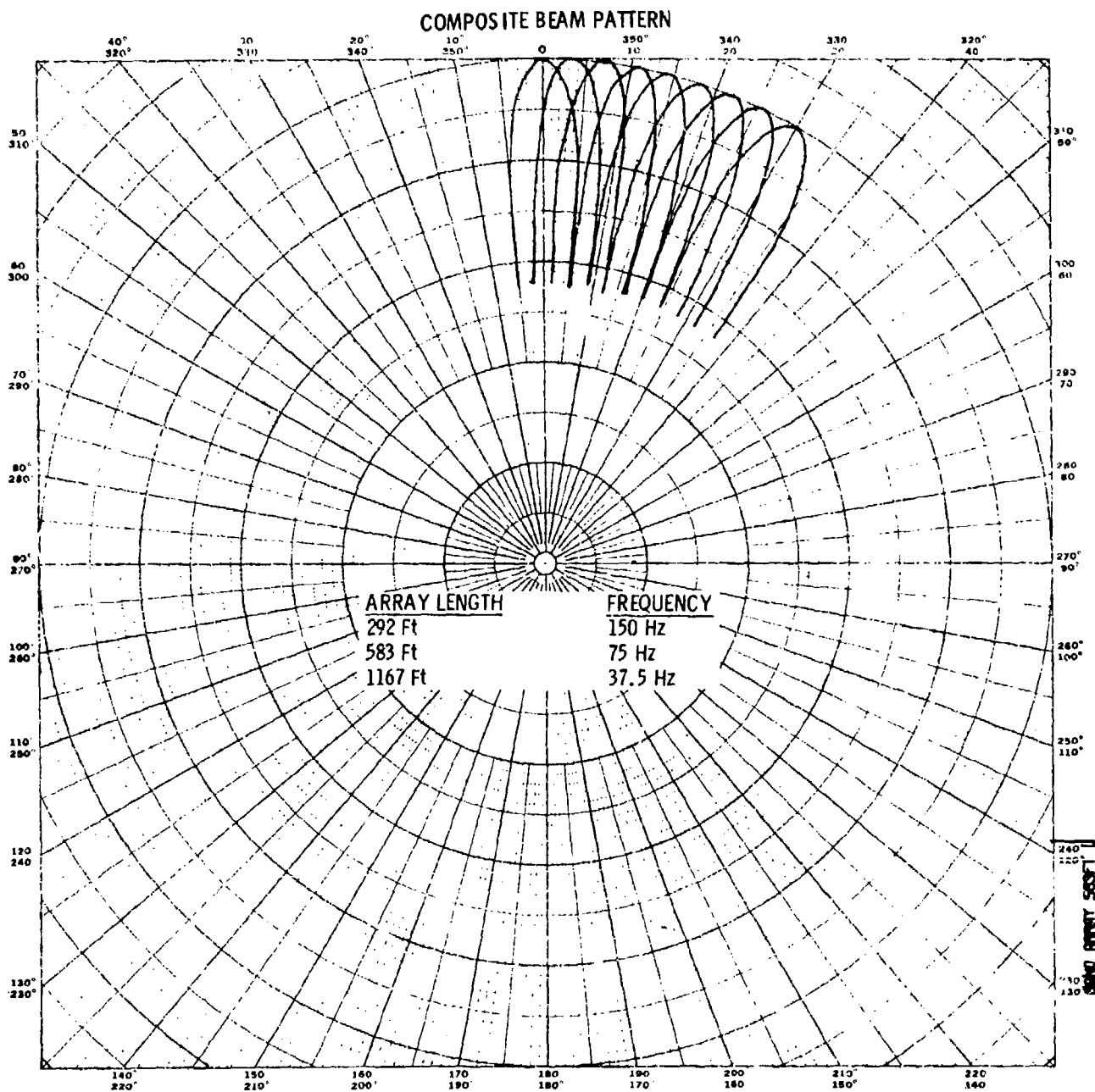


6000 ARRAY SCHEM LENGTH - FREQUENCY-43.242  
 ARRAY STEERED TO 43.4° (11/16)

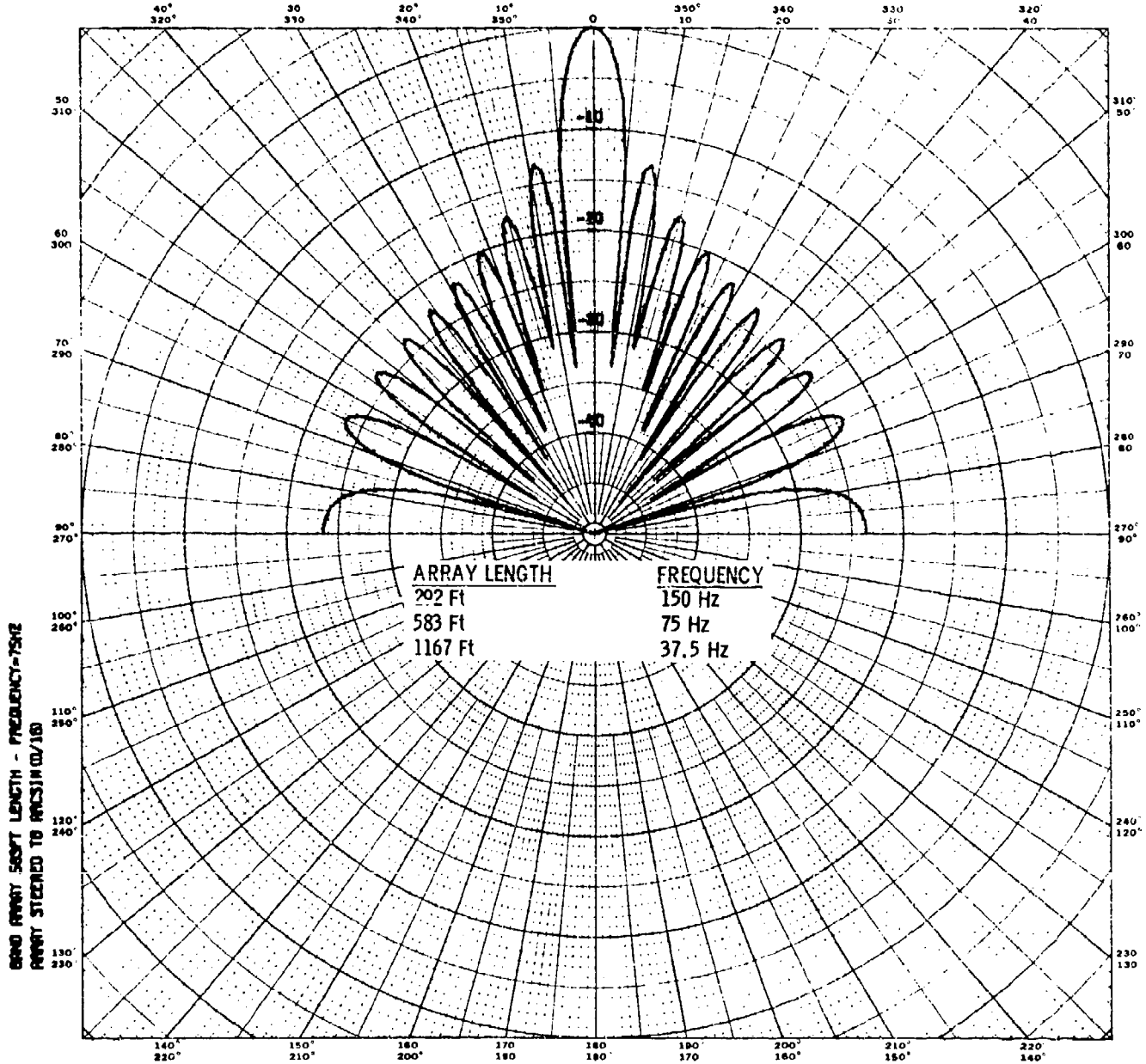


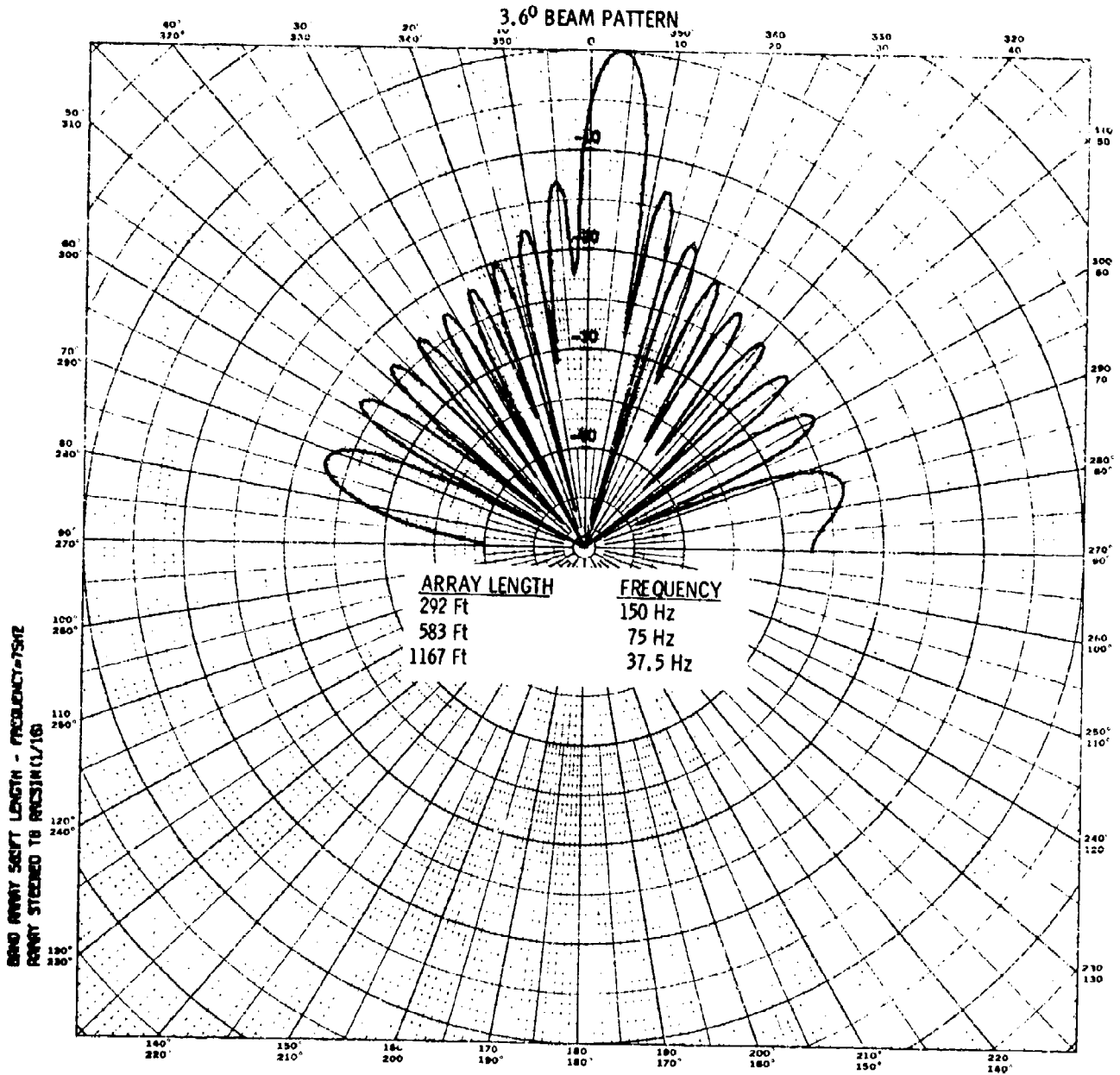


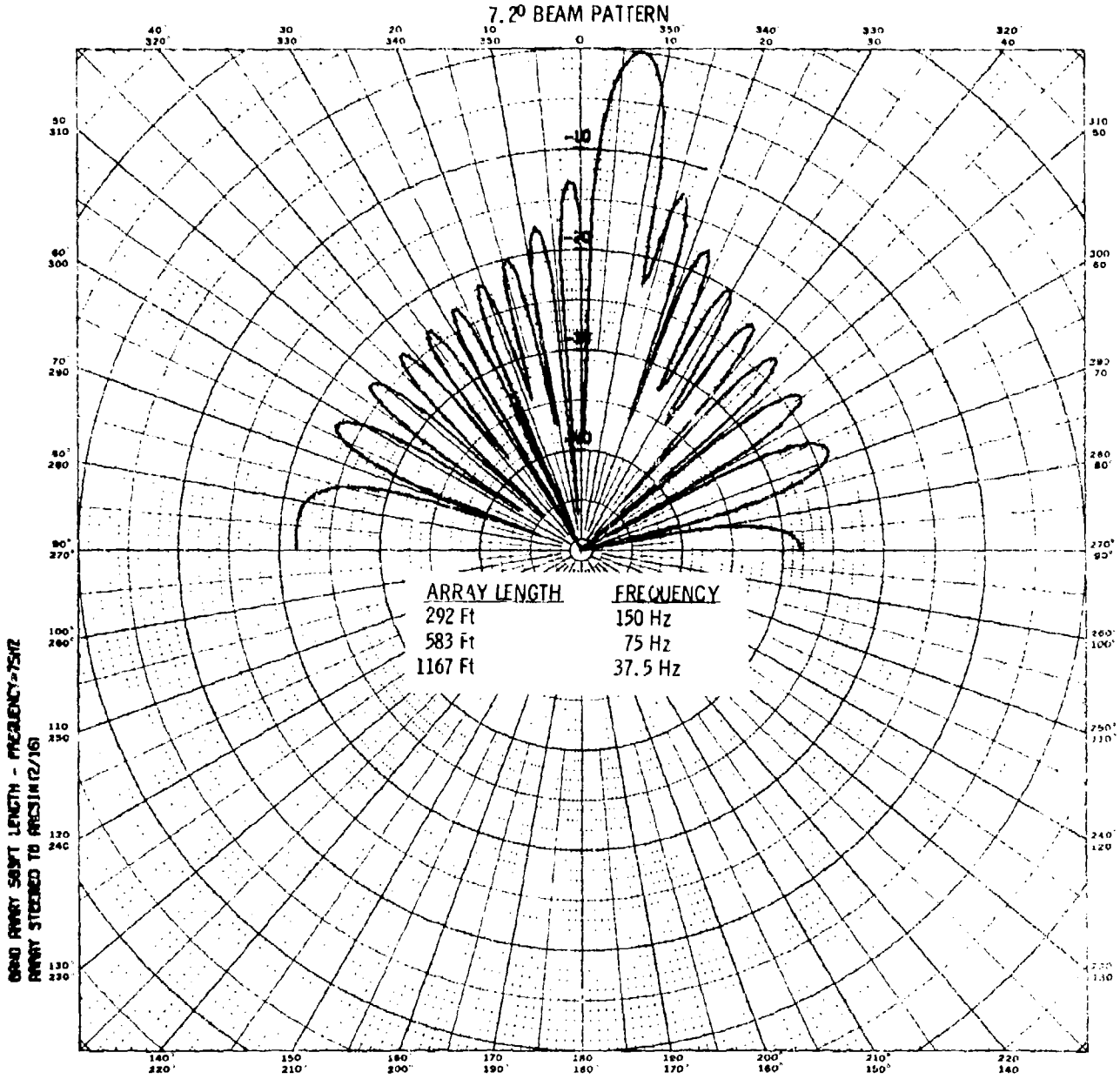




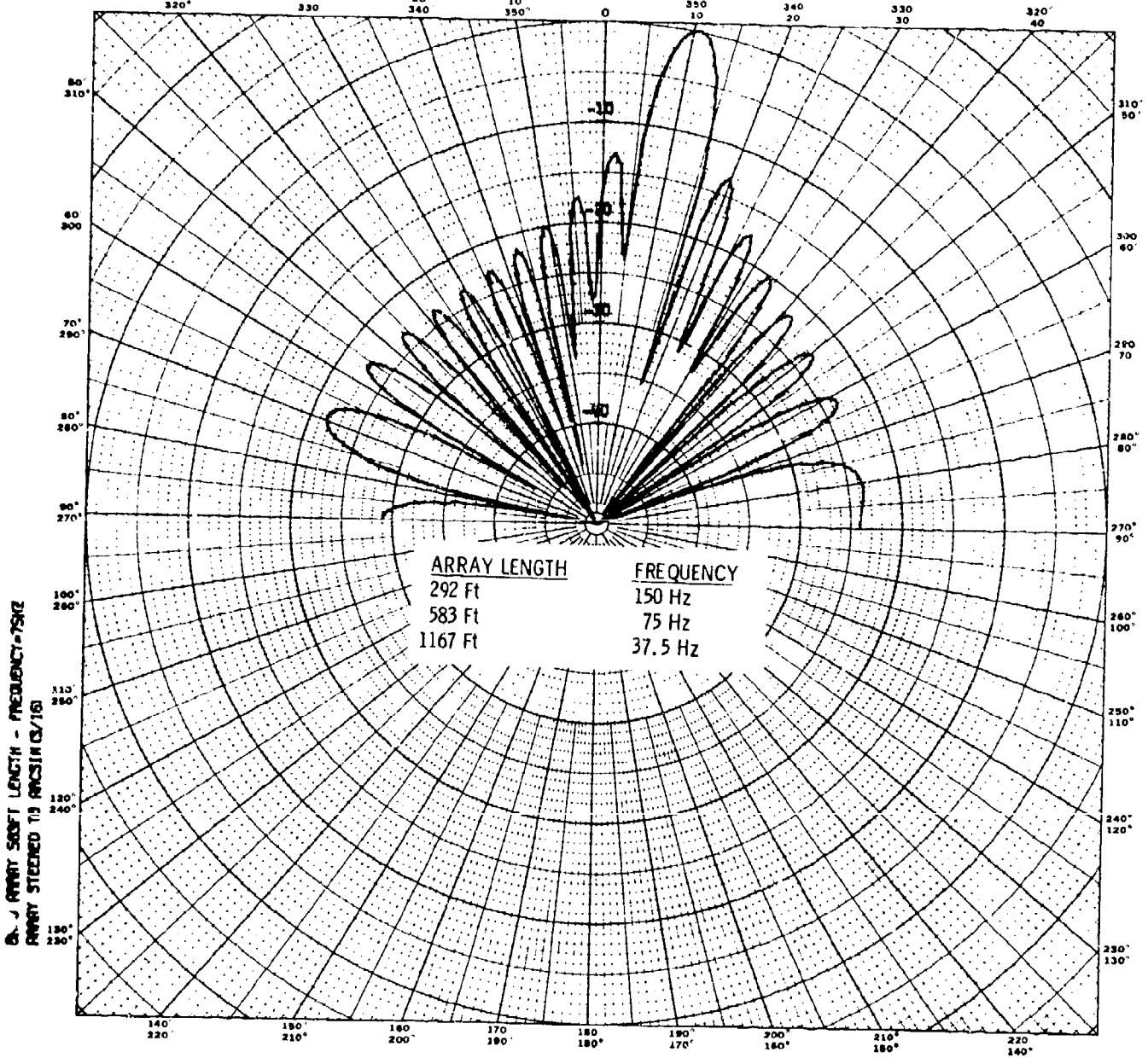
BROADSIDE BEAM PATTERN



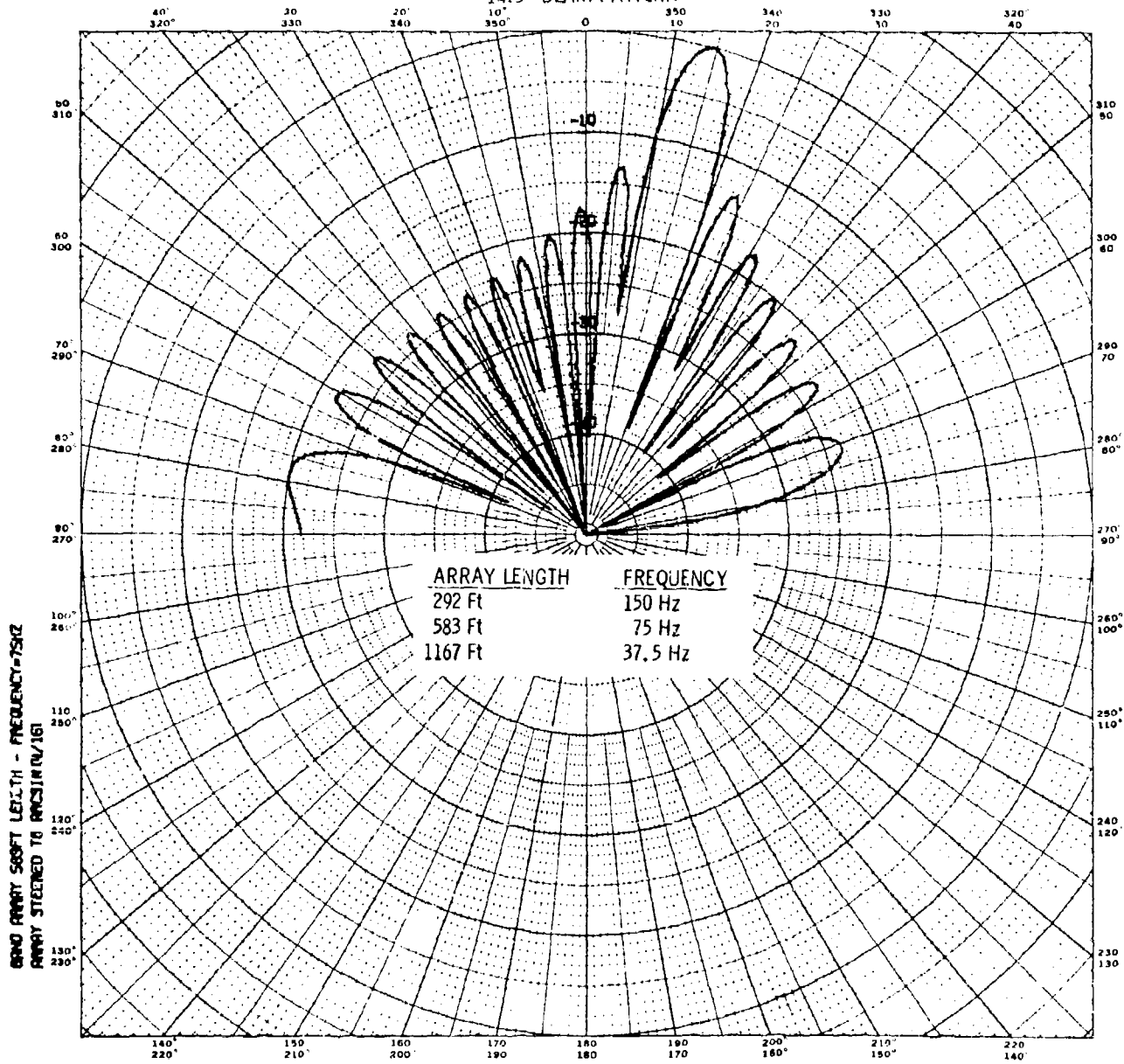


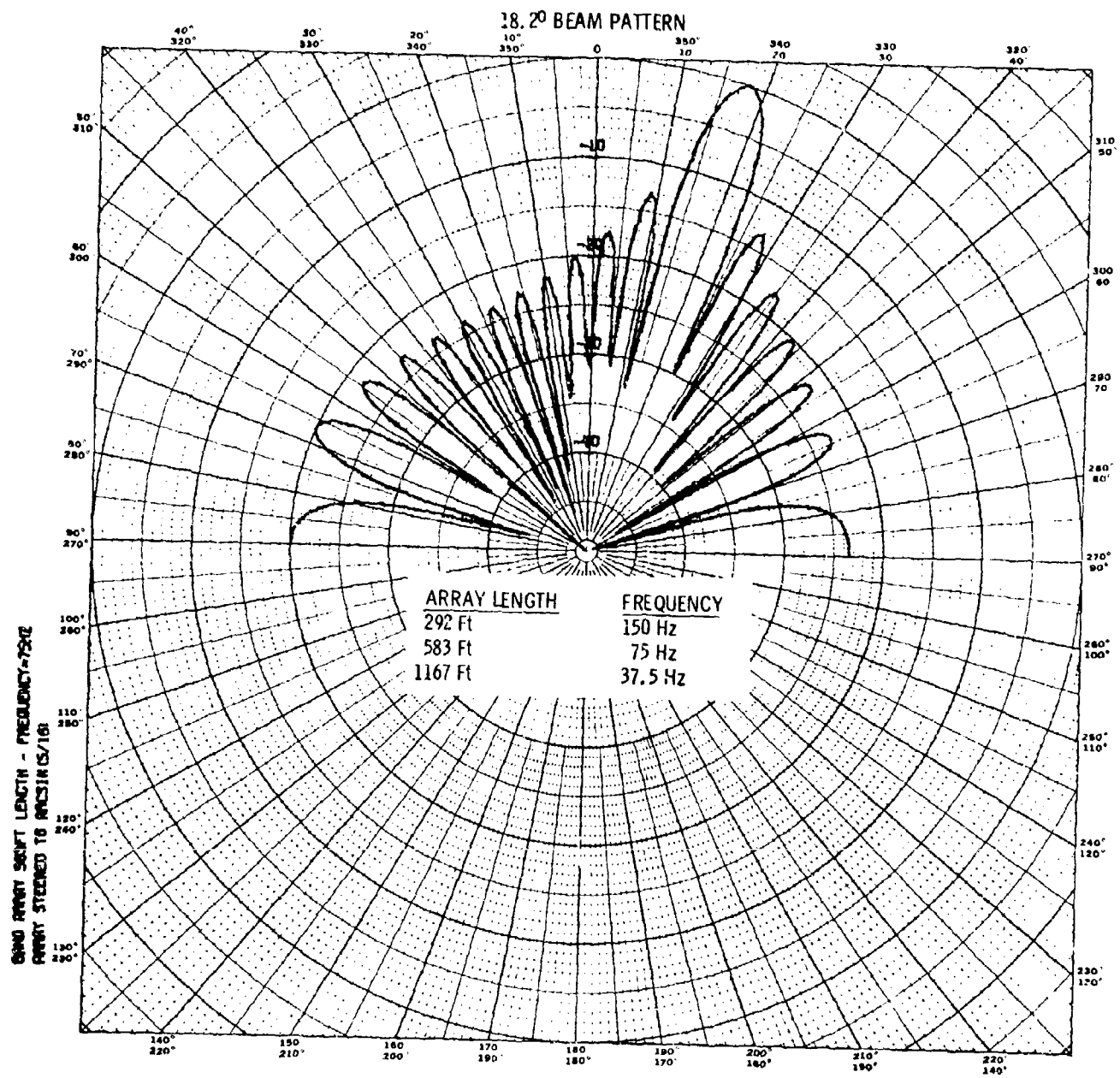


10.8° BEAM PATTERN

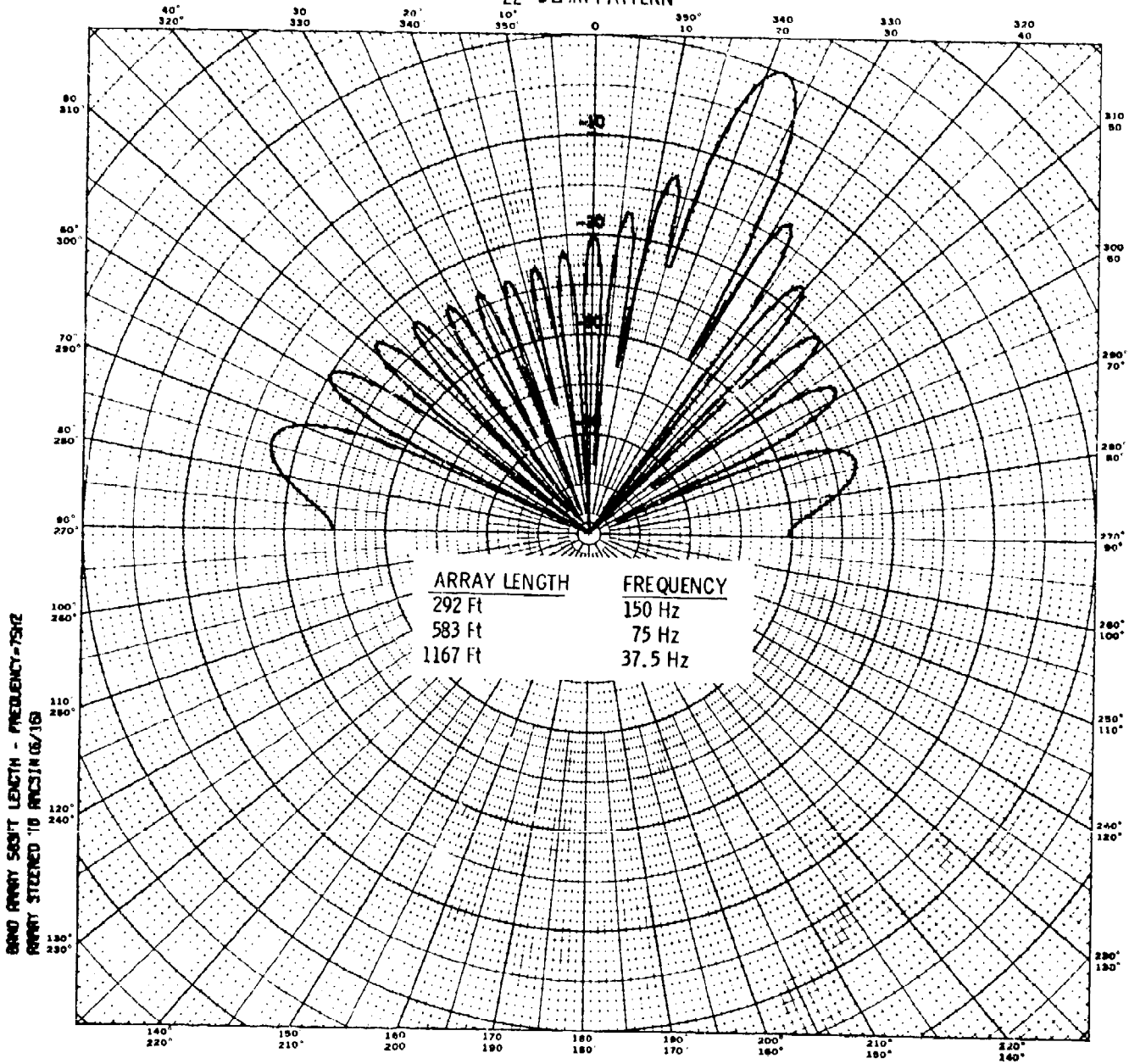


14.5° BEAM PATTERN

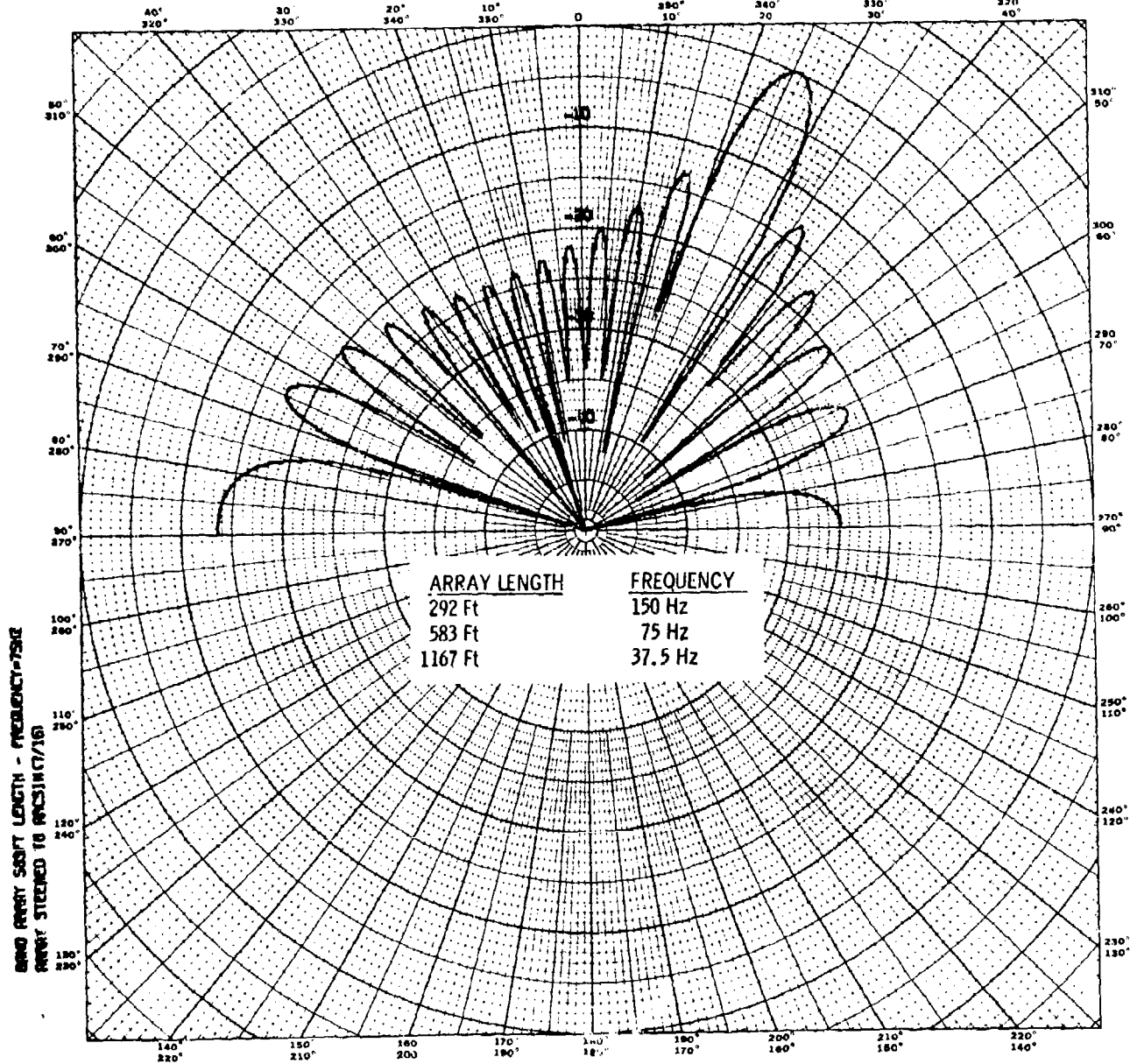


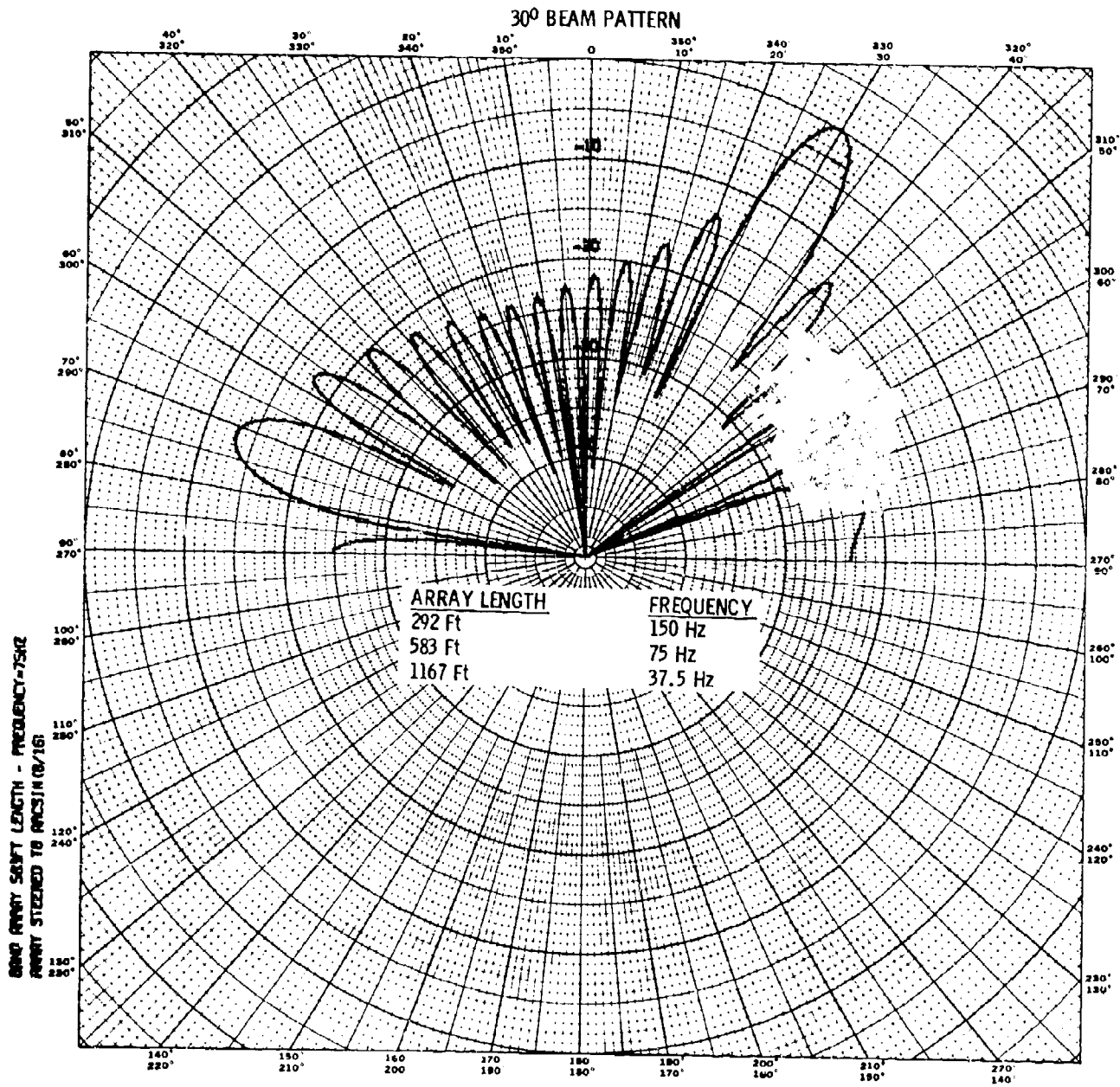


22° BEAM PATTERN

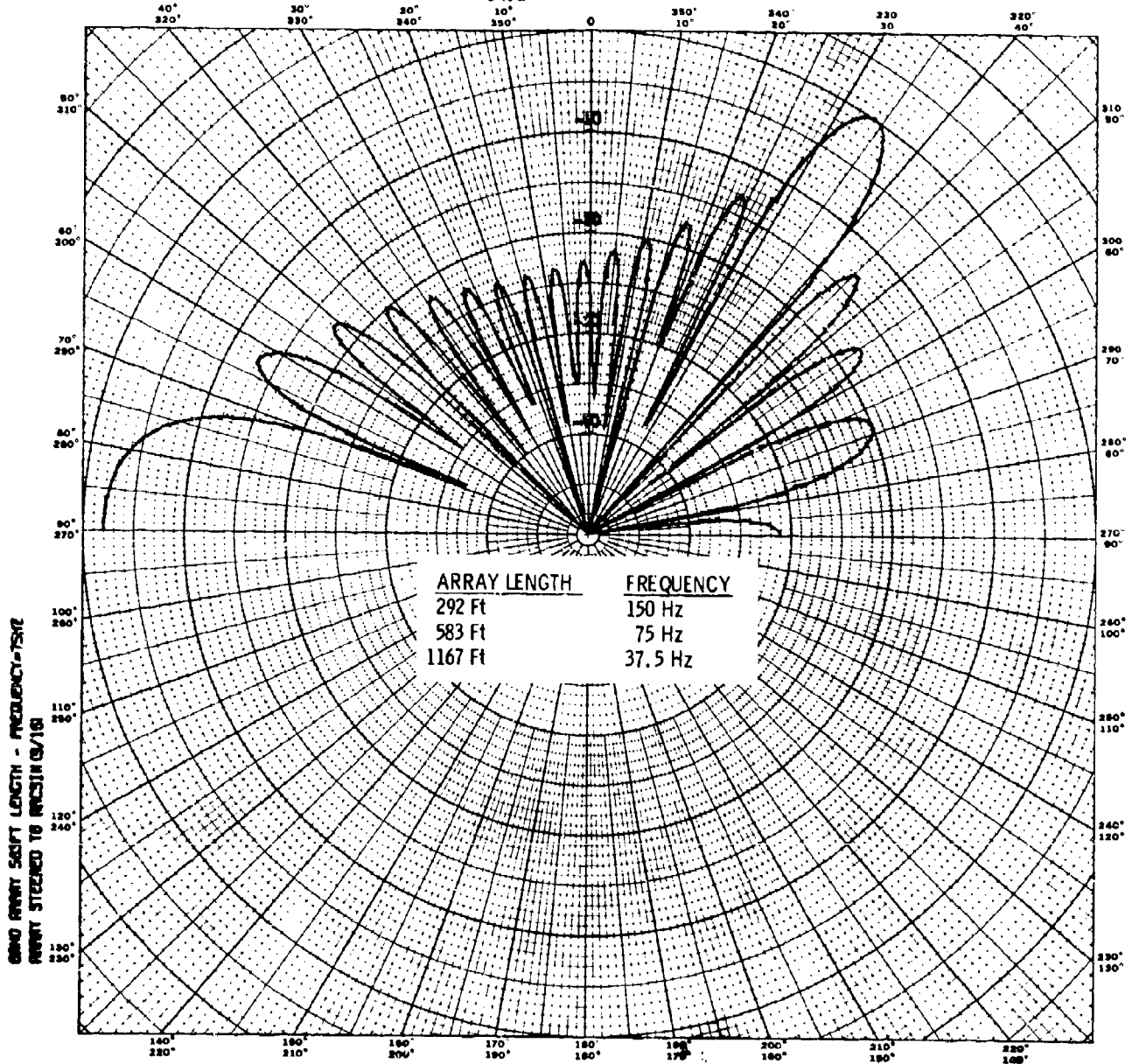


26° BEAM PATTERN

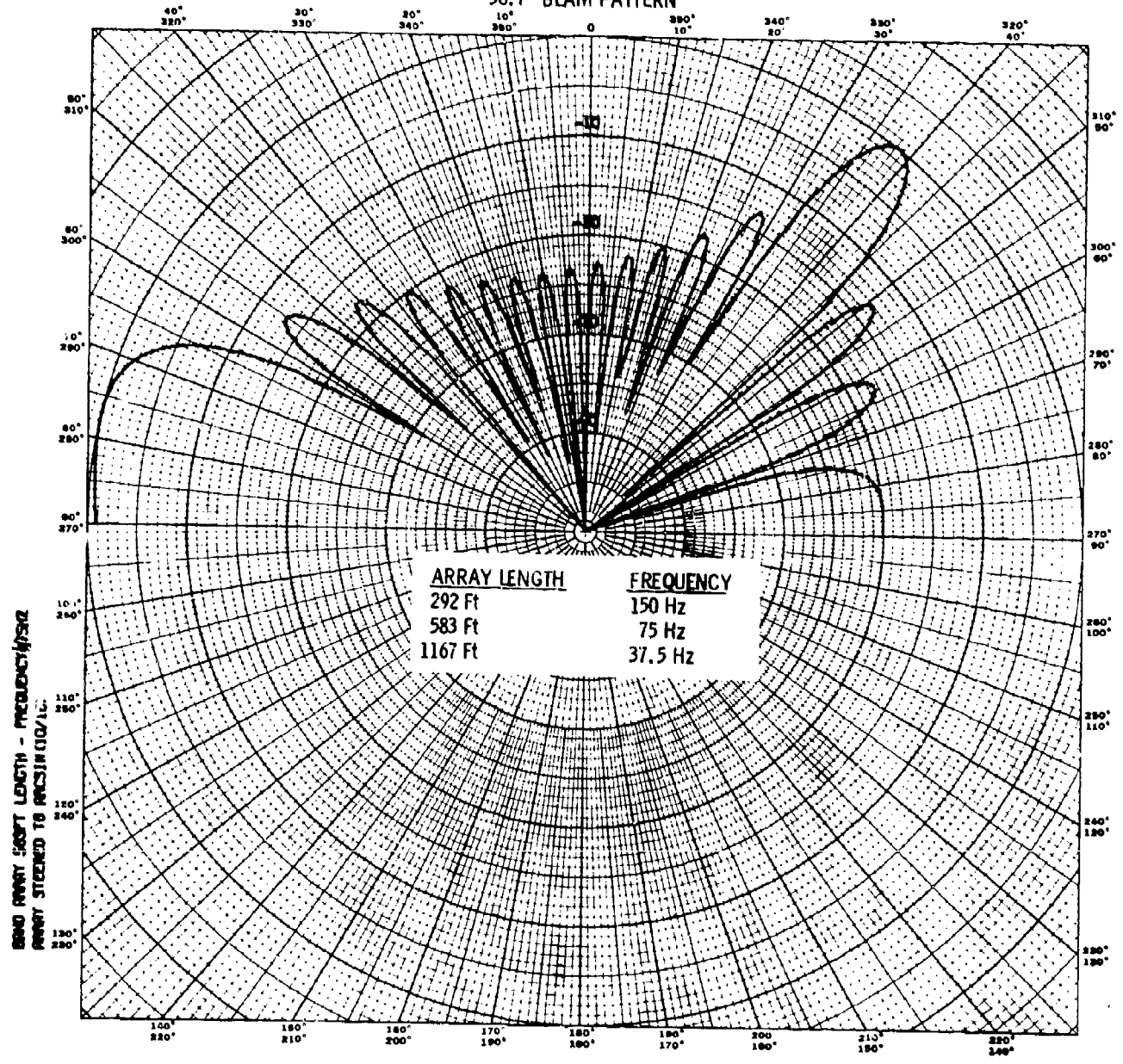




34.2° BEAM PATTERN



38.7° BEAM PATTERN



43.4° BEAM PATTERN

